Międzyuczelniany
Wydział
Biotechnologii
Uniwersytetu Gdańskiego
i Gdańskiego Uniwersytetu
Medycznego

ROZPRAWA DOKTORSKA

*Magister, Maria Camila Tovar Fernandez*

# Pochodzenie peptydów antygenowych szlaku MHC klasy I

## Origin of antigenic peptides in MHC class I pathway

Praca przedst
awiona
Radzie Dyscypliny Nauki Biologiczne Uniwersytetu Gdańskiego
celem uzyskania stopnia doktora
w dziedzinie nauk ścisłych i przyrodniczych
w dyscyplinie nauki biologiczne

Promotor: Dr. Robin Fahraeus
ICCVS
INSERM U1131

GDAŃSK 2

## Abstrakt

Zdolność układu immunologicznego do odróżnienia ‘swojego’ od ‘obcego’ opiera się na prezentacji peptydów antygenowych na cząsteczkach głównego układu zgodności tkankowej klasy I (ang. Major Histocompatibility Complex I, MHC-I). ‘Obce’ peptydy pochodzące z patogenów lub zmutowanych ‘swoich’ białek rozpoznawane są przez cytotoksyczne limfocyty T CD8+, co prowadzi do zniszczenia komórki je prezentującej. Odkrycie, że peptydy pochodzące z intronów są prezentowane na cząsteczkach MHC-I zrodziło pytania o sposób powstawania antygenów dla układu MHC-I. Zrozumienie mechanizmu powstawania tych peptydów pozwoli lepiej pojąć w jaki sposób wirusy i komórki nowotworowe unikają tej ścieżki obrony organizmu. Moja praca doktorska koncentruje się na dwóch mechanizmach powstawania tych peptydów. Po pierwsze, na autofagii jako drodze degradacji białek i po drugie, na produktach pierwszej rundy translacji (ang. Pioneer Translation Products, PTPs) pochodzących z pre-mRNA.

*Pierwszy mechanizm*

Autofagia pełni istotną rolę w utrzymaniu homeostazy komórki i usunięciu z niej zakumulowanych szkodliwych agregatów białkowych, prowadzących do wielu chorób, między innymi chorób neurodegenracyjnych. Odpowiedź immunologiczna wobec komórek niosących takie agregaty pozostaje jeszcze niezbadana i nie ma zbyt wielu dowodów na udział autofagii w produkcji antygenów dla cząsteczek MHC-I.

W celu oceny prezentacji na cząsteczkach MHC-I peptydów pochodzących z autofagii, użylimy limfocytów T CD8+ (OT-1), specyficznie rozpoznających epitop SL8 (SIINFEKL) pochodzący z kurzej owalbuminy (OVA) i prezentowany na mysich cząsteczkach MHC-I (Kb).

Oceniliśmy udział substratów dla procesu autofagii w powstawaniu antygenow MHC-I dzięki fuzji sekwencji owalbumina-SIINFEKL z tworzącą agregaty sekwencją poliglutaminy (PolyQ) oraz z sekwencją białka EBNA1 wirusa Epstein-Barr’a (EBV). Supresja autofagii na drodze knockdownu Atg5 i Atg12 nie wpłynęła na prezentacje peptydów pochodzących z białka EBNA1, ale obniżyła prezentację antygenów pochodzących z samej owalbuminy oraz z produktu fuzji OVA z PolyQ. Co ciekawe, fuzja owalbuminy z sekwencją powtórzeń glicyna-alanina (GAr-OVA; ang. Glycin-Alanin repeats; GAr) pochodzącą z białka EBNA1 i hamującą prezentacje antygenów pochodzących z EBNA1, zahamowała prezentację antygenów pochodzących z

owalbuminy. Wyniki wskazują na zależny od substratu udział autofagii w produkcji antygenów dla cząsteczek MHC-I oraz ilustrują nowy mechanizm unikania przez wirusy prezentacji antygenów powstających na drodze autofagii.

*Drugi mechanizm*

Z biegiem czasu postulat, że peptydy antygenowe w całości pochodzą z degradacji ‘starych’ pełnołańcuchowych białek został zastąpiony nowym, mówiącym, że peptydy antygenowe powstają również z petydów nowo-syntetyzowanych na drodze niekanonicznej, alternatywnej translacji, zachodzącej przed splicingiem mRNA. To tłumaczyłoby prezentację przez cząsteczki MHC-I peptydów pochodzących z intronów. Zgodnie z tym założeniem zaobserwowaliśmy, że sekwencja SIINFEKL wstawiona do drugiego intronu genu β-globiny powoduje proliferację limfocytów T CD8+ OT-1.

Przy użyciu techniki PLA (ang. Proximity ligation assay) zaobserwowaliśmy akumulację peptydów SIINFEKL pochodzących z translacji pre-mRNA po zastosowaniu inhibitora splicingu – isokingentiny. Niedojrzałe mRNA β-globiny przed splicingiem wykryto we frakcji lekkich polisomów, podczas gdy sekwencja β-globiny po splicingu znajduje się we frakcji ciężkiej. Uzyskane wyniki dalej wspierają tezę, że peptydy antygenowe pochodzą z translacji niedojrzałego mRNA (pre-mRNA).

## Abstract

A key component of the immune systems' capacity to distinguish between self and non-self is the presentation of peptides on major histocompatibility complex class I (MHC-I) molecules. Non-self-peptides derived from pathogens or mutated self-proteins are recognized by cytotoxic $CD8^+$ T cells leading to the destruction of the presenting cell. The presentation of intron-derived peptides on MHC-I molecules has raised the question of the origin of antigenic peptides for the MHC-I pathway. A better understanding of the origin of neo-antigens will lead to a better comprehension of viral and cancer immune evasion. For my Ph.D. study, I have focused on two different sources of antigenic peptides. Firstly, autophagy as a protein degradative mechanism, and secondly, pioneer translation products derived from pre-spliced mRNA.

*First mechanism*

Autophagy has an essential role in cellular homeostasis and can help rid the cells of harmful protein aggregates accumulation that can cause several diseases such as neurodegenerative disorders. Immune response towards cells carrying protein aggregates is relatively unknown and there is limited evidence for autophagy processing of antigenic peptides for the MHC class I pathway. To assess MHC-I antigen presentation of autophagy-derived antigenic peptides, we used $CD8^+$ T cells (OT-1) that specifically recognize the chicken ovalbumin (OVA) SL8 epitope (SIINFEKL) presented on the murine Kb MHC-I molecules. We evaluated potential substrates for autophagy processing by the ovalbumin-SIINFEKL sequence fusion to the aggregate-prone polyglutamine (PolyQ) and the Epstein Barr Virus-encoded EBNA1 sequences. Suppressing autophagy by knocking down Atg5 and Atg12 did not affect the presentation of peptides derived from the EBNA1 protein, whereas it reduced the presentation of antigenic peptides derived from OVA, or OVA fused to the aggregate-prone PolyQ sequence. Surprisingly, fusing ovalbumin to the immune-evasive glycine-alanine repeat (GAr) of EBNA1 (GAr-OVA) prevented the presentation of peptides from OVA. These data suggest a substrate-dependent presentation of antigenic peptides for the MHC class I pathway via autophagy and illustrate a novel virus-mediated mechanism for immune evasion of autophagy-dependent antigen presentation.

*Second mechanism*

Over time, the assumption that antigenic peptides are solely derived from the degradation of “old” full-length proteins has been replaced with the postulation that antigenic peptides are also derived from newly synthesized peptides by a specific non-canonical alternative translation event that occurs before mRNA splicing. This would explain the presence of intron-derived peptides on MHC-I molecules. In support of this, we observed that expressing the SIINFEKL sequence in the second intron of the β-globin gene triggered OT-1 $CD8^+$ T cell proliferation. Using the proximity ligation assay (PLA), we observed an increase in SIINFEKL peptides from pre-spliced mRNAs following treatment with the Isoginkgetin splicing inhibitor. To start the characterization of this alternative translation complex, we used polysome fractionation to identify ribosomes on pre-spliced mRNAs. The pre-spliced β-Globin mRNA is found on light polysomes, as opposed to the spliced β-Globin mRNA that is present in the heavy polysomal fractions. The data further supports the notion that antigenic peptides are derived from the translation of pre-spliced mRNAs.

## INDEX



## PART 1



## PART 2

# General Introduction

Specific or adaptative immune response recognizes and responds to two different kinds of antigens. B cells synthesize and release antibodies that recognize antigens in their native state. In contrast, T cells have a T cell receptor (TCR) that recognizes short fragments of antigenic peptide chain products from intracellular proteolysis. TCR engages antigenic peptides bound with a major histocompatibility complex (MHC) molecule on the antigen-presenting cells (APCs)[1–3].

T cells can either express CD4 or CD8 molecules on their surface which creates two different functional classes of T cells: cytotoxic (CD8) and helper T cells (CD4)[2,4,5]. $CD8^+$Tcells recognize antigenic peptides in association with MHC class I (MHC-I) molecules, whereas $CD4^+$ T cells recognize peptides bound to MHC class II (MHC-II) molecules[3,6].

## I. The major histocompatibility complex (MHC)

The MHC molecules are transmembrane glycoproteins encoded in the large group of genes known as MHC[2]. In this conserved region, there are not only MHC molecules but also other products essential for MHC function. In many species, the MHC encodes different MHC-I and MHC-II molecules possibly generated by gene duplication[3].

The MHC molecule is located on chromosome 6 in humans and on chromosome 17 in the mouse. In humans, the genes coding MHC are called human leukocyte antigen (HLA) and in mouse are known as H-2 genes. There are three different classes of genes either for humans or mice. The genes coding for the heavy chain of class I are HLA-A, B, and C in humans and for mice, they are named H-2K, H-2D, and H-2L. Each of the human or mouse genes are organized in 7 or 8 exons coding for different domains: α1, α2, and α3 for the heavy chain. The light chain or β2m is coded by a gene found outside the HLA or H-2 locus, specifically in chromosome 15 for humans and in chromosome 2 for mice. While genes coding for both chains of class II are HLA-DN, DM, and DO in humans and H-2Aα, H-2Eβ, and H-2Eα in mice[7].

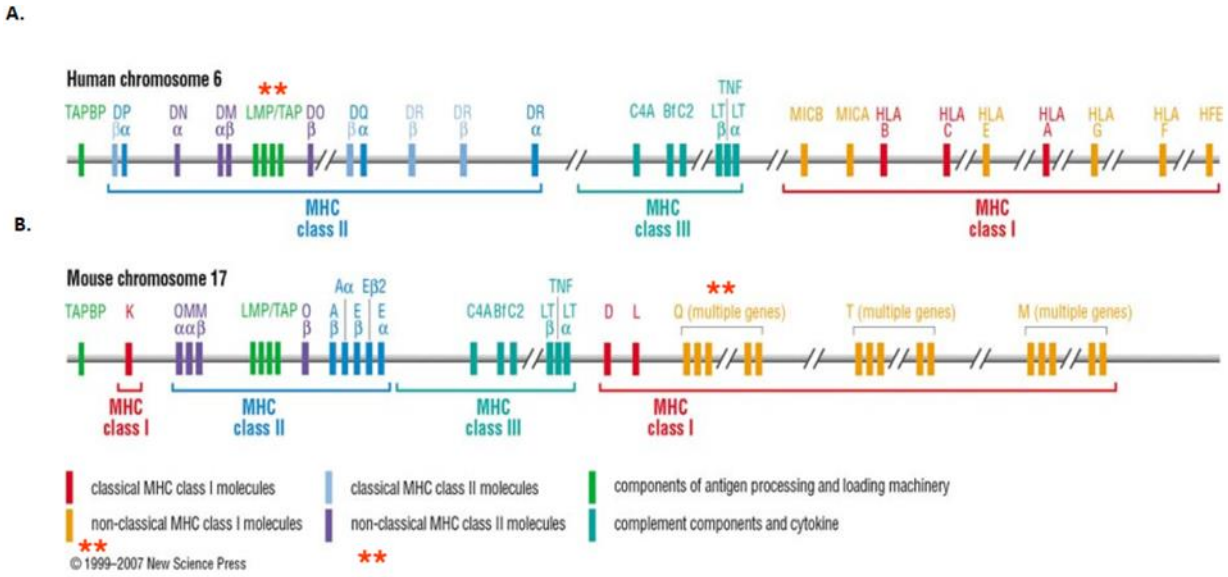


**Figure 1. Schematic representation of MHC genes organization in A.** mouse and **B.** Human[7,8](Image taken from Defranco et al 2007)[9].

- The MHC molecule structure

The MHC-I and MHC-II genes are very polymorphic and have one domain with a high amino acid variation that interacts with peptides, allowing different MHC molecules to bind a broad range of peptides. The peptide binding structure is a groove formed by α-helices and β-sheets chains. For MHC-I molecules, the groove is formed by the N-terminal region of the heavy chain (α) composed of two of the three extracellular subunits α1 and α2. On the contrary for the MHC-II molecules, the groove is formed by the juxtaposition of the N-terminal region of two MHC-encoded α-and β-chains most precisely α1 and β1 subunits. For both molecules, there is also a non-polymorphic domain that resembles Immunoglobulin constant region domains. For MHC-I, the α3 subunit of the heavy chain and the light chain β2 microglobulin (β2m). For MHC-II, the α2 and β2 subunits. The MHC-I heavy chain and the MHC-II α and β- subunits are glycoproteins embedded in the cellular membrane having a short part exposed to the cytosol lumen[3,8,10,11].

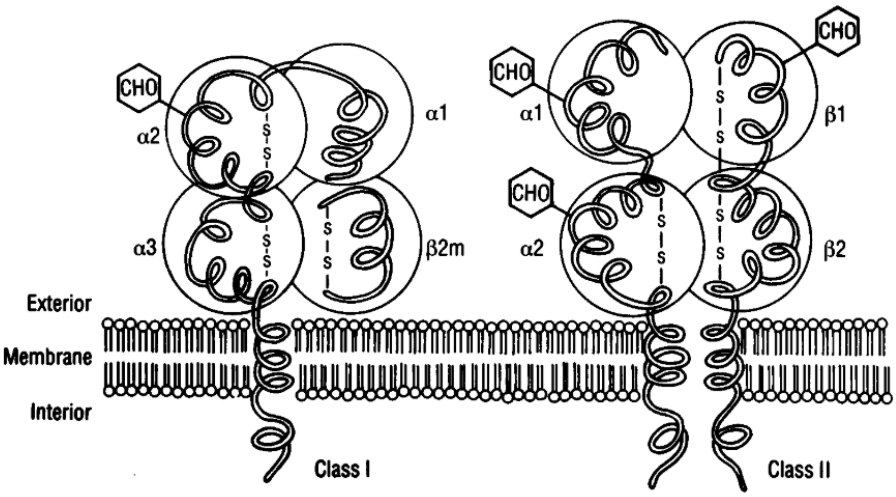


**Figure 2. The MHC class molecules.** The MHC molecule is composed of glycoproteins chains linked with disulfuric bonds and carboxylic extremes on the extracellular domain. Class I and II differs. MHC-I molecule has a light chain ($\beta_2$m) not embedded in the cell membrane, whereas the MHC-II molecule has α and β chains embedded in the cell membrane[8,10](Image taken from Bethesda et al 2002)[11].

## II. Processing and MHC-I presentation of endogenous antigens

The antigens presented on MHC-I can be of endogenous origin including cellular or viral antigens or from an exogenous source for example phagocyted bacterial proteins[1,3,6].

- Source of antigenic peptides

Cytosolic proteins from the host or viral gene products are synthesized in the cell following the translation process. The Eukaryotic translation begins when the small subunit of the ribosome (the 40S) binds the initiator tRNA carrying Methionine (Met-tRNA) and the eukaryotic initiation factors (eIF). The stable form eIF2-GDP changes to eIF2-GTP activated form leading to the binding to Met-tRNA that forms the ternary complex (TC). The TC binds to the 40s with eIF5, eIF3, eIF1, and eIF1A to compose a larger 43S preinitiation complex (PIC). Next, eIF4F binds at the 5' 7-methylguanosine cap (m7G cap) and the poly(A) binding protein (PABP) at the 3' poly (A) tail to activate mRNAs. IF4F compromises a complex formed by eIF4E, eIF4G, and eIF4A. eIF4G has binding sites to eIF4E, PABP, and RNA that generate a closed-loop circularized. eIF4A unwinds mRNA secondary structures and facilitates the 43S PIC recruitment at the m7G cap. eIFs1 and 1A mediate the bound of the single-stranded mRNA to the

40S subunit. The 43S PIC starts the scanning along the mRNA from the m7G cap, in a 3' direction, searching for an AUG initiation codon suitable to make an mRNA codon-tRNA anticodon interaction. Once the tRNA finds the initiation codon, eIF2 suffers a conformation change recruiting eIF5B that mediates the joining of the large subunit (the 60S). Next, the release of eIF5B and eIF1A allows the formation of an 80s ribosome attached to an mRNA with Met-tRNA bound to the AUG codon and starts the elongation phase of protein synthesis. In this stage, the different tRNAs carrying a specific amino acid bind sequentially to complementary codons in the mRNA. Each amino acid binds the growing polypeptide chain in the c-termini through a cycle of four sequential stages. The ribosome moves from codon to codon until reaches the stop codon. At this point, a releasing factor binds to the ribosome and ends the translation releasing the polypeptide[12–14].

Proteins that are at the end of their functional lives are processed by the proteasome generating short peptides used as antigenic peptides for the MHC class I pathway.

- The proteasome

In general, the first step in endogenous antigen processing is the production of peptide fragments by the proteasome[3,6].

Classical proteasome 26S is composed of one catalytic core 20S flanked by two 19S regulatory caps. Both parts are subdivided into different protein complexes. The 20S core is a complex cylinder composed of 28 different subunits organized in four rings of seven subunits each. The two inner rings of the 20s core are composed of proteolytic subunits named β1, β2, and β5, which form the catalytic chamber. On special occasions such as interferon induction, this core changes, and it is displayed by three alternative catalytic subunits called LMP2 (β1i), MECL-1 (β2i), and LMP7 (β5i) that interestingly are encoded in the MHC genome region. As a result, the proteasome can be configured in two different forms the constitutive proteasome and the Immunoproteasome. The immunoproteasome configuration can produce peptides with carboxy-terminal residues that bind with high affinity to the binding groove of the MHC-I molecule[2,15,16].

The 19s cap, bound to both ends of the 20S core, recognizes polyubiquitinated substrates and unfolds the protein to allow the entrance of the substrate to the catalytic

core of the proteasome where it is processed and short peptides that are then released into the cytosol[2,17].

The catalytic core 20S can also be associated with different families of regulators such as 11S complexes and PA200/Blm10. Interestingly, one regulator of the 11S family called PA28αβ (proteasome activator 28) has been implicated in the degradation of unfolded proteins and many studies have implicated this regulator in the production of MHC class I ligands. Many researchers have found that IFN-γ induces the assembling of PA28, composed of two proteins A28α and PA28β, to the 20S proteasome core. This special binding has been related to function as an accelerator of the antigenic peptide production[17,18].

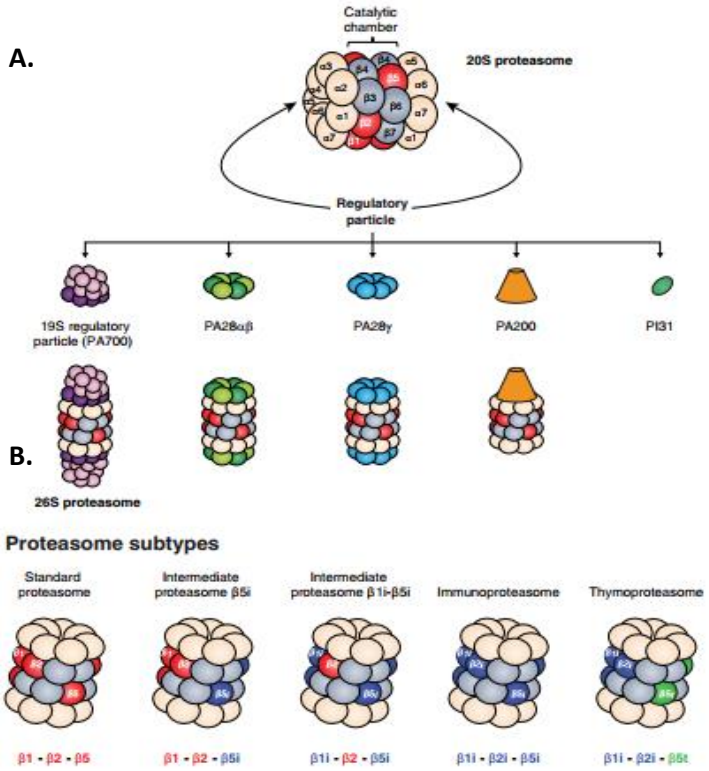


**Figure 3. Structure and composition of proteasomes. A.** The 20s proteasome has a cylindrical form and it is composed of four rings (α subunits and β subunits). The α subunits are located on the extremes and are the gates to the entrance of the protein to the degradation core. The α subunits can be associated with different regulators. **B.** Proteasome subtypes, these five types of proteasomes differ in their catalytic sites. The standard proteasome includes the catalytic subunits $\beta_1$, $\beta_2$, and $\beta_5$, while the immunoproteasome has a different conformation induced by IFN-y. The immunoproteasome is composed of catalytic sites $\beta_{1i}$, $\beta_{2i}$, $\beta_{5i}$ [18,19](Image taken from Vigneron et al 2017)[20].

- Cytosolic aminopeptidases

Recently, studies have uncovered that many aminopeptidases tackle cytoplasmic peptides after proteasome degradation. A degradation mechanism that could explain the short half-live of a peptide of about 6 to 10 seconds and the limited peptide presentation of the MHC-I molecule compared with the high number of peptides produced from the whole proteome by the proteasome. This array of cytosolic aminopeptidases is composed of Tripeptidyl peptidase II (TPPII) and Neurolysin that cleaves large peptide fragments; Thimet oligopeptidase (TOP) that cleaves 8-15 amino acids; LAP removes hydrophobic or aromatic amino acids; PSA that cleaves small peptides and is specific for PolyQ-peptides and Bleomycin hydrolase that also targets small peptides among others[6].

- Peptide binding to MHC-I molecules

Peptides generated in the cytoplasm are translocated in an active ATP-dependent way into the Endoplasmic Reticulum (ER) by the protein translocator TAP (Transporter associated with antigen processing), a heterodimer composed of TAP1/TAP2 proteins encoded by genes in the MHC[3,6]. TAP transport begins when ATP and/or ADP and peptides bind independently to the TAP complex in the cytoplasm. The peptide bond to the heterodimer leads to a conformational change of the TAP complex. This structural rearrangement induces the ATP hydrolysis and translocation of the peptide to the ER lumen[21].

Within the ER, newly synthesized MHC-I molecules are retained until they bind a peptide. The folding and assembly of the MHC-I molecule depends first on the MHC-I α heavy chain associated with the light chain β2m and then on the peptide. This process involves different proteins with chaperone functions. It starts when the synthesized MHC-I α chain enters the ER and binds to the chaperone protein calnexin, which retains the MHC-I molecule in a partially folded state. Then, the β2m binds to the α chain, leading to the calnexin dissociation and the binding to the peptide-loading complex (PLC). This PLC is composed of chaperone-like calreticulin, the tapasin that forms a wall between the MHC-I molecule and TAP, blocking the bounding of any peptide, and a third component the ERp57, a thiol oxidoreductase that has a role in breaking this complex, that allows the encounter of the peptide with the MHC-I molecule. Sometimes peptides too long to bind MHC-I molecule can still be transported into the ER, when this happens, an aminopeptidase called ER aminopeptidase

associated with antigen processing (ERAAP) trims the peptide amino termini in the ER lumen. The binding of a peptide to the semi folded MHC-I molecule induces the releases from the PLC and the full folding of the MHC-I molecule. Then, the MHC-I molecule/peptide can now leave the ER and be transported to the cell surface. Importantly, not all peptides that entered the ER will bind to the MHC-I molecule. Recent findings have identified a transporter ATP-dependent complex the endoplasmic reticulum-associated degradation (ERAD) that can translocate back into the cytoplasm of the non-bound peptides[6,8,22,23].

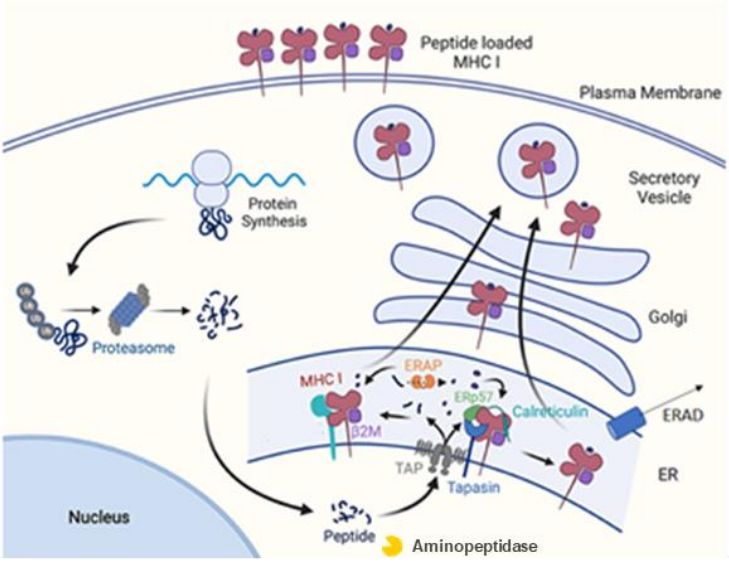


**Figure 4. The MHC class I antigen presentation pathway.** Intracellular proteins are processed by the proteasome and cleaved by the cytosolic aminopeptidases. The peptide products are then translocated to the ER. Within the ER the peptide is further trimmed, if necessary, by the ERAAP. Next, the peptide binds the MHC-I molecule mediated by the PLC complex composed of Tapasin, Calreticulin, and ERP57. The unbound peptides in the ER are extracted by ERAD. Following MHC-I molecule binding to the peptide, they are sent to the cell surface to activate $CD8^+$ T cells[6,24](Image adapted from Dhatchinamoorthy et al 2017)[25].

### III. Processing and MHC-II presentation of exogenous antigens

- Vacuolar pathway

Professional-APCs, such as macrophages, dendritic cells, and B cells, internalized exogenous proteins and degrade them by lysosomal proteolysis. Endocytosis occurs when extracellular proteins and plasma membrane cell components are fully internalized into the cell. Endocytosed proteins enter a vesicular pathway, where it is transported progressively through more acidic and proteolytically active compartments referred to as early endosomes, late endosomes, and lysosomes. When a

professional-APCs internalized exogenous particles, it is designated as phagocytosis. External proteins phagocyted follows a similar path to the vesicular pathway, finishing in phagolysosomes that are formed by the fusion of phagosomes and lysosomes. Phagolysosomes and lysosomes contain a pH of 4,5 and hydrolytic enzymes like cathepsins that reduce the peptides to a length of 13 to 18 amino acids. Depending on the peptide length, short peptides products can be recycled and used for new protein synthesis, whereas large peptides can be a source for MHC-II binding[3,26–28].

- Peptide binding to MHC-II molecules

The MHC-II molecules present these peptides derived from exogenous proteins through a process that involves several stages. First, the MHC-II molecule, composed of α-and β-chains, is assembled in the ER and bound to the invariant chain (Ii). The resulting complex MHC-II/Ii is then transported to a late endosomal compartment called the MHC-II compartment (MIIC). Inside MIIC, Ii is digested, resulting in a residual class II-linked Ii peptide (CLIP) located in the peptide-binding groove of the MHC-II. Next, the HLA-DM molecule mediates the exchange between CLIP and the specific peptide derived from the protein degraded in the vacuolar pathway. After, the MHC-II molecule/antigenic peptide complex leaves the MIIC and goes to the plasma membrane, where it will present its peptide to $CD4^+$ T cells[6].

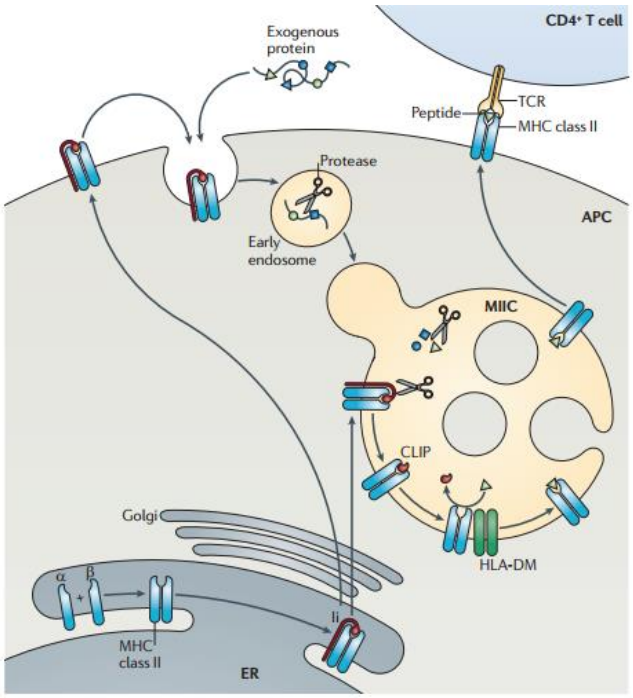


**Figure 5. The MHC class II antigen presentation pathway.** The MHC-II molecule assembles in the ER, where it binds to the invariant chain (Ii). The Exogenous peptides and the Ii-MHC-II

molecule enter the MHC-II compartment (MIIC), where the peptide binds to the MHC-II molecule. Then, the antigenic peptide bound to the MHC-II molecule is transported to the plasma membrane[5,24] (Image taken from Neefjes et al 2011)[6].

## IV. Cross-presentation

However, MHC-I and MHC-II molecules can bind peptides from endogenous and exogenous antigens. For example, MHC-II binds' peptides derived from endogenous plasma membrane receptors that are degraded in the lysosome. In addition, MHC-I molecules can bind peptides derived from exogenous proteins internalized by phagocytosis. This process is denominated cross-presentation[3].

Dendritic cells are exceptional professional-APCs. Specific types of dendritic cells are very efficient in mediating cross-presentation, which is critical for the activation of naïve $CD8^+$ T cells to a broader range of peptides[29,30].

When exogenous antigens are engulfed by dendritic cells. The internalized antigen goes to an endocytic compartment and is processed through two different pathways. In the cytosolic pathway, antigens relocate from the phagosome to the cytosol, where they are going to be folded properly by the hsp90 and degraded by the proteasome. Then, the derived peptides, are transported to the ER by TAP. These peptides can be further trimmed by the ERAAP and loaded into the MHC-I molecule. The other possibility is the vacuolar pathway; however, the processing mechanism remains unclear. The main hypothesis suggests that antigens remain in the phagosome. They are then degraded by proteases like Cathepsin S and the insulin-regulated aminopeptidase (IRAP). An alternative hypothesis claims that the antigens that escape the phagosome, are degraded by the proteasome, relocated to the phagosome, and are again trimmed by IRAP. The peptides produced during these two processes encounter in both cases recycled MHC-I molecules from the plasma membrane in the phagosome, which leads to the loading and the subsequent antigen presentation[30].

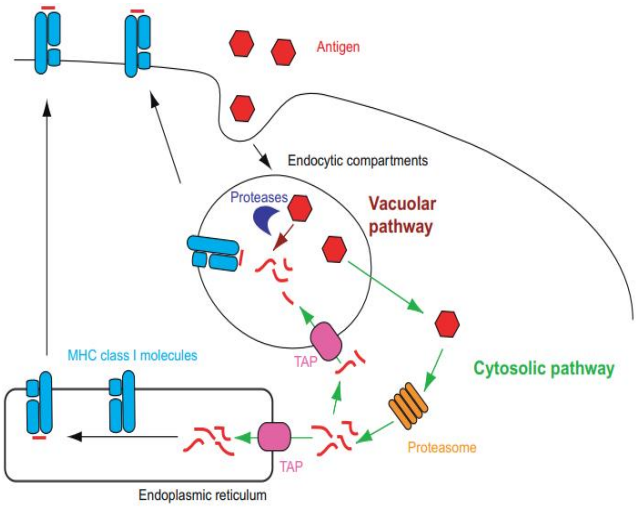


**Figure 6. Cross-presentation.** Exogenous antigens internalized by the dendritic cells can be processed and associated with the MHC-I molecule in the vacuolar pathway or the cytosolic pathway[5,29](Image taken from Segura E. et al 2015)[30].

Until this section, I have introduced the general aspects of antigen presentation. Next, I will divide my Ph.D. dissertation into two parts to better present and discuss the two main approaches that I developed during my Ph.D. to study the origin of antigenic peptides in the MHC class I pathway.

- In the first part, I am going to focus on autophagy and its role in the generation of peptide substrates for the MHC class I pathway.

- In the second part, I am going to focus on the study of the translation machinery responsible for the production of MHC-I antigenic peptides coming from pre-spliced mRNA.

# Introduction – PART 1

In the adaptive immune response, the autophagy pathway is essential for thymus selection, lymphocyte development, immune homeostasis, and antigen presentation[31].

Current studies propose that autophagy is tightly involved in antigen processing for MHC presentation, in which peptide products are used in the activation of T cells. However, there is not much evidence associating MHC-I presentation with the processing of antigenic peptides by autophagy[32]. In this section, I'll describe first the autophagy pathway, second recent studies demonstrating autophagy processing of antigenic peptides presented on MHC-I molecules, and third potential autophagy substrates used for antigenic peptides production on the MHC class I pathway.

## V. The Autophagy pathway

Autophagy is a key degradative process of endogenous cytoplasmic proteins that occurs in response to different forms of stress such as nutrient deprivation, growth factor depletion, infection, or hypoxia. Autophagy plays a critical role in the supply of nutrients during fasting or other types of stress. But it was later revealed that under basal conditions, autophagy has a selectivity for specific cargos to get rid of damaged organelles, such as mitochondria or harmful aggregation-prone proteins[33,34].

There are three classes of autophagy:

1. Microautophagy: In this mechanism, the lysosome engulfs cytoplasmic components by inward invagination.
2. Chaperone-mediated autophagy: In this mechanism, substrates proteins associated with chaperones enter directly into the lysosome without the need for membrane reorganization.
3. Macroautophagy: In this mechanism, endogenous proteins are taken by an organelle called autophagosome and delivered to lysosomes.

Macroautophagy is the major type and the most extensively studied compared to the other two types and more importantly the center of our study. Thus, we will refer to macroautophagy simply as autophagy[35] in this manuscript.

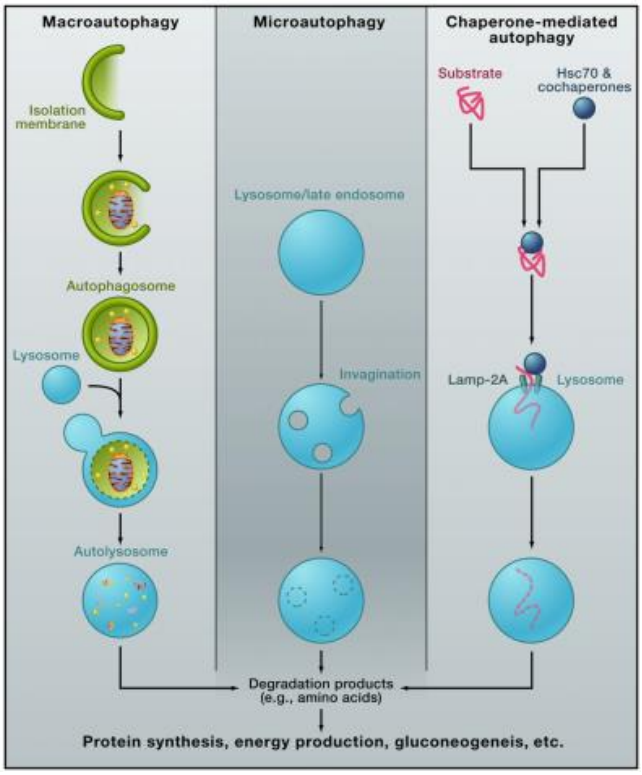


**Figure 7. Different classes of autophagy.** Macroautophagy: the insolation membrane takes a portion of the cytoplasm to form an autophagosome. The autophagosome fuse with the lysosome and the cargo is degraded in the lysosome. Microautophagy: cytoplasm is directly engulfed in the lysosome. Chaperone-mediated autophagy: Hsc70 recognizes KFERQ-like pentapeptide in the substrate proteins. Then, the cargo is translocated to the lysosome through Lamp-2A[36](Image taken from Mizushima et al 2011)[35].

## The autophagy mechanism

The mechanism of autophagy involves many different actors; thus, I am going to explain this process shortly, giving the main points of this pathway, and then I will provide a more detailed explanation of each stage.

Main stages of autophagy mechanism:

The activation of autophagy leads to the recruitment of autophagy-related genes (ATG) and different types of enzymes as kinases to a specific site close to the ER called the phagophore assembly site (PAS). The interaction of all these proteins triggers the nucleation of an isolated membrane that forms a cup-shaped structure called the phagophore. Then, this phagophore will continue expanding, taking with it a portion of the cytosol, until it seals the membrane. A new double-membrane vesicle is then formed termed the autophagosome carrying inside an engulfed material the autophagic cargo. The autophagosome will maturate clearing the ATGs surrounding it

and will move through the microtubules to reach the lysosome. Finally, the autophagosome will fuse the lysosomal membrane to form an autolysosome. Inside this autolysosome, the autophagosome will be transformed into a single membrane autophagic body, which is followed by its degradation[33].

Detailed autophagy mechanism:

- Phagophore formation

Even though other triggering signals exist, amino acid deprivation is the classical activation signal of autophagy. This deprivation will inhibit the master cell growth regulator serine/threonine kinase mTOR, but only one of the two different complexes, mTORC1. In a normal cellular state, mTORC1 is bound to Unc-51-like kinase 1 (ULK1) in a phosphorylated form, upon starvation, mTORC1-ULK sites are dephosphorylated and trigger the release of ULK1. ULK1 then is autophosphorylated, followed by the phosphorylation of ATG13, RB1-inducible coiled-coil protein 1 (FIP200), and ATG101. The formation of this complex triggers the nucleation of the phagophore by phosphorylating components of the classical III PI3K (PI3KC3) complex (composed of class III PI3K, vacuolar protein sorting 34 (VPS34), Beclin 1, ATG14, activating molecule in Beclin 1-regulated autophagy protein 1 (AMBRA1) and general vesicular transport factor (p115)). As a result, it will activate local phosphatidylinositol-3-phosphate (PI3P) production and the formation of a characteristic ER structure identified as the omegasome. PI3P then recruits WD repeat domain phosphoinositide-interacting proteins (WIP2) and zinc-finger FYVE domain-containing protein 1 (DFCP1). This membrane core will be elongated with the delivery of several membranes by vesicles containing ATG9. However, this source only is a part of the lipid bilayer, the rest of the membrane, still, is unknown[33,34].

- Phagophore expansion

WIP2 then attracts and binds ATG16L1, triggering the recruitment of Atg12~Atg5 and the lipid form of LC3. The Atg12~Atg5 and LC3 complexes are the product of two ubiquitin-like conjugation systems. The conjugation of Atg12~Atg5 occurs when Atg12 is activated by Atg7 (E1 ubiquitin-like conjugating system) and then associated with Atg5 by Atg10 (E2 ubiquitin-like conjugating system). LC3 complex then is cleaved by the Atg4 protease, resulting in an exposure of a glycine residue located in the C-terminus. When autophagy is activated, the LC3 terminus is conjugated to the polar

head of phosphatidylethanolamine (PE) a component of the phospholipid bilayer. A reaction can only occur in presence of Atg7, Atg3, and Atg12-Atg5:Atg16L complex. The LC3 associated with PE is the characteristic LC3-II marker as an autophagy activator and is located in the outer as the inner side of the autophagosome membrane, while LC3-I under normal conditions is located only in the cytosolic part. The conjugation system between Atg7, Atg3, and Atg12-Atg5:Atg16L complex and the lipidic LC3 promotes the phagophore expansion, mediates the cargo selective recruitment as they interact with the cargo receptors, and closure of the autophagosome membrane. The human LC3 family is composed of three members, LC3A-C and its homologs GATE-16, GABARAP1, 3, and Atg8L[33,34].

- Autophagosome Maturation and Lysosomal fusion

Once the autophagosome is formed it starts to maturate through the release of the Atg12-Atg5:Atg16L complex and the cleavage of LC3-PE by the Atg4 protease. To fuse with the lysosomal organelles, the mature autophagosome recruits microtubule-based kinases motors in charge of lysosomal delivery and proteins implicated in the fusion with the lysosome, which includes diverse proteins from the SNARE family. For example, on the autophagosome side, Syntaxin 17 (STX17) and the synaptosomal-associated protein 29 (SNAP 29) are recruited. While on the lysosome side, it recruits some proteins such as the vesicle-associated membrane protein 8 (VAMP8) to assist in the autophagosome delivery. Nevertheless, the fusion mechanism between the autophagosome and the lysosome is still not fully understood[33,34].

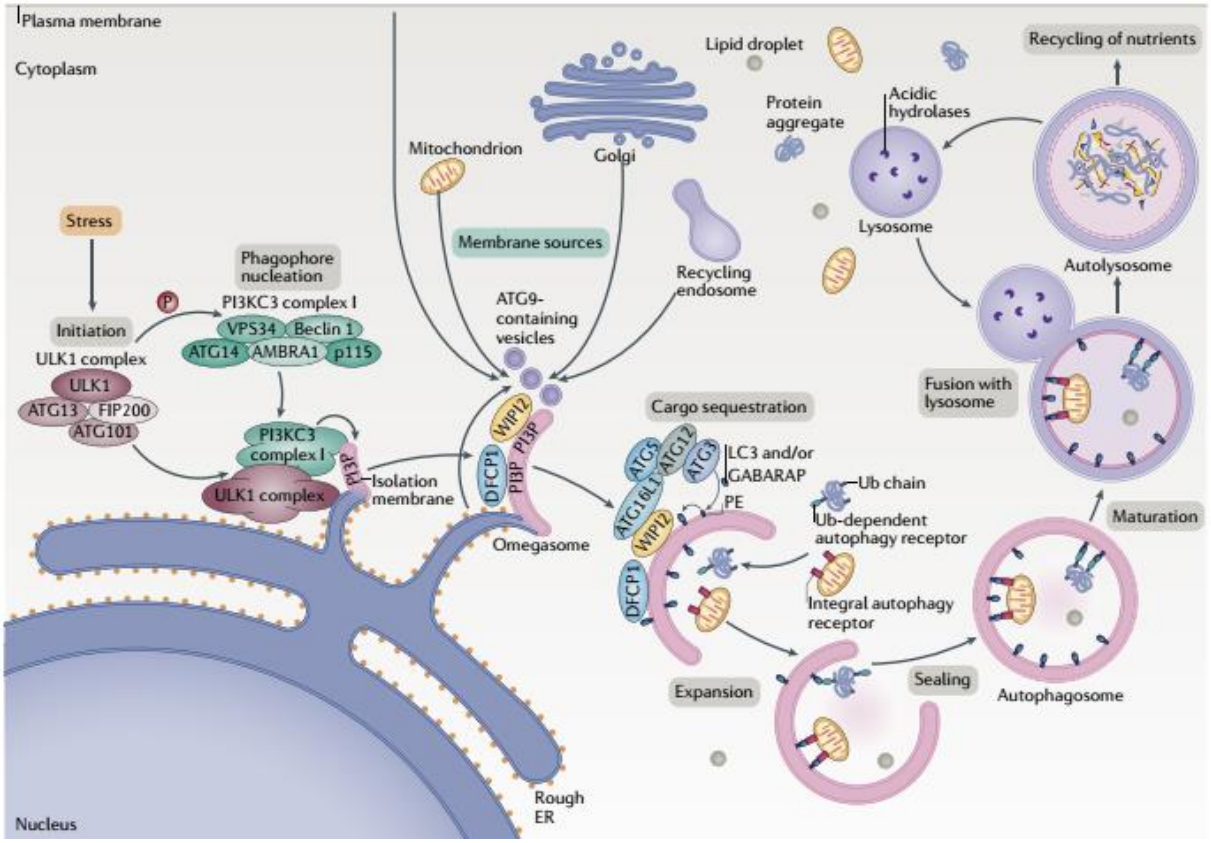


**Figure 8. Autophagy mechanism.** Activation of autophagy starts, for example, with starvation or protein aggregates. This stress leads the Unc-51-like kinase 1 (ULK1) complex to phosphorylate the class III PI3K (PI3KC3) complex I, triggering phagophore nucleation. The P115 component of the PI3KC3 complex I induce the production of phosphatidylinositol-3-phosphate (PI3P), elongating the ER membrane to a structure called omegasome. Next, PI3P attracts effectors proteins such as WD repeat domain phosphoinositide-interacting proteins (WIPIs; here WIPI2) and zinc-finger FYVE domain-containing protein 1 (DFCP1). WIPI2 then binds to ATG16L1 and consequently leads to the recruitment of Atg12~Atg5. Those bindings enhance the Atg3 mediated conjugation with the microtubule-associated protein light chain 3 (LC3) proteins and γ-aminobutyric acid receptor-associated proteins (GABARAPs) to the membrane-resident phosphatidylethanolamine (PE) that allowed the cargo sequestration and then its expansion. The sealing of the phagophore forms an autophagosome with a double membrane bilayer that next maturate and fuses with the lysosome[34,37](Image taken from Dikic et al 2018)[33].

### V.A Intracellular quality control by selective autophagy

Under nutrient-rich conditions the contribution of autophagy was unclear but new studies have revealed that autophagy can function as a quality-control system of different cytoplasmic components and help in cell homeostasis. This quality control is made mostly through a selective autophagy mechanism, which uses ligand receptors and scaffold proteins. In recent years it has been a considerable number of studies

demonstrating the existence of different receptors and scaffold proteins dependent on the cargo nature[35].

For example, the ubiquitination of substrates is a traditional “eat me signal” in the recognition and degradation by selective autophagy. There are three mammalian ubiquitin cargo receptors the SQSTM1, NRB1 and OPTN found in autophagosomes that allow the entrance of different cargos ubiquitinated. The discovery of autophagy selectivity through ubiquitination signaling revealed that ubiquitination was not only a signal of proteasome degradation but also an autophagy signal. However, we still do not know how both systems are harmonized in the cell. The scientific community has proposed that autophagy could degrade big cargos that are not able to be destroyed by the proteasome or maybe the different length and nature of the ubiquitin chains decide the degradative destiny for such cargos[38].

In this context, I am going to outline some cargos displaying ubiquitin labeling that can be recognized by specific receptors expressed in the autophagosome membranes.

- Aggregates clearance by autophagy

Aggregation-prone proteins like Amyloid-β, Huntingtin (HTT), and SNCA (synuclein alpha) has been demonstrated to be autophagy substrates. So far, it is known that the aggrephagy mechanism is triggered only by ubiquitin. This tagging is recognized by four different receptors TOLLIP, SQSTM1, NRB1, and OPTN. Moreover, recent data have observed that the nucleocytoplasmic shuttling protein WDFY3 can bind the Atg5 protein, the SQSTM1 receptor, and LC3, serving as a scaffold protein. Interestingly, this study has also revealed that WDYF3 depletion blocked the clearance of aggregated polyQ proteins[38,39].

- Intracellular pathogens clearance by autophagy

Clearance of intracellular pathogens such as viruses, bacteria, and fungi via autophagy is denominated, Xenophagy. New studies have uncovered bacterial proteins from *Salmonella typhimurium* that were ubiquitinated and recognized by the autophagosome cargo receptors SQSTM1 and OPTN. Moreover, the expression of these receptors has been associated with a growth restriction of intracellular pathogenic bacteria such as *S. Typhimurium*, *M. Tuberculosis*, mutant *S. Flexneri*, and mutant *L. Monocytogenes*[38,40].

Interestingly, new findings have determined that some intracellular pathogens contain LC3 Interaction Motif (LIR) to trick the host autophagy machinery. For example, the influenza A virus (IAV) Matrix 2 (M2) ion channel protein blocks autophagosome-lysosome fusion and recruits LC3 to the plasma membrane through the LIR motif present on the cytoplasmic tail of the M2 protein. A recent publication examined the presence of counteracting LC3 LIR sequences in databases containing more than 16000 viral sequences. The authors found several interesting candidates with a potential role similar to LIR sequences. For example, a potential LIR was identified in the HIV-1 protein Nef, which has been previously described as an inhibitor of autophagosome maturation. This LIR candidate seems to colocalize with LC3 and BECN1 to avoid autophagy degradation[40].

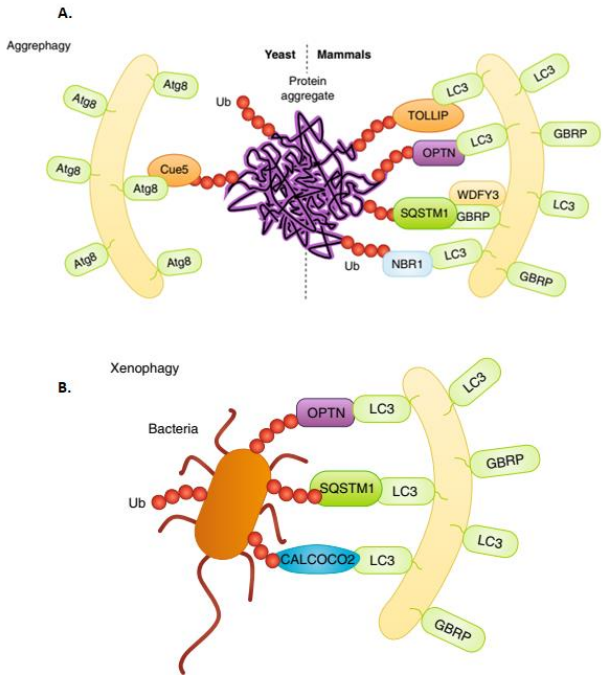


**Figure 9.** Aggrephagy and xenophagy. **A.** In yeast and mammals, protein aggregates are ubiquitinated and then recognized by specific receptors. In mammals, ubiquitin is recognized by TOLLIP, SQSTM1, NBR1, and OPTN. They are linked to LC3/GABARAP in the autophagosome, allowing the entrance of the protein aggregate. In yeast the receptor is Cue5. **B.** Intracellular pathogens such as bacteria are ubiquitinated and recognized by receptors embedded in the autophagosome membrane such as SQSTM1, OPTN, CALCOCO2, and NBR1[39](Image taken from Gatica et al 2018)[38].

## VI. Autophagy and MHC-I presentation

The most accepted autophagy participation in the antigen presentation is through the MHC class II pathway. Traditionally, scientists have thought that only exogenous antigens engulfed by professional-APCs activate $CD4^+$ T cells. However, data also

suggested that intracellular sources such as a viral, tumor, or other self-proteins are presented by MHC-II molecules via autophagy [32,41–43]. Moreover, new studies have uncovered that dendritic cells, depending on the source of the antigenic peptide, can cross-present and activate $CD8^+$ T cells via autophagy[44,45].

However, little evidence exists that points to autophagy as a processing mechanism of antigenic peptides in the MHC class I pathway. There is more available evidence showing indeed the opposite. For example, Schmid and colleagues fused the LC3 sequence to a viral epitope that induced an increase in MHC-II presentation and evaluated this same LC3-viral epitope in the MHC class I pathway. Strikingly, they did not see any increase in the MHC-I presentation as in the MHC-II presentation response [46]. Nevertheless, some evidence reveals that autophagy can contribute to MHC-I antigen presentation. English L. and colleagues have shown that macrophages, infected with herpes simplex virus type 1 (HSV-1) in an advanced stage of infection displayed autophagy processing of HSV-1 antigenic peptides for the MHC class I pathway. Furthermore, they observed that the autophagosomes activated where originated from the nuclear envelope and that these antigenic peptides were further processed by the proteasome [47]. Similarly, another study has used dendritic cells infected with the herpes simplex virus lacking the protein 34.5 (ICP34.5), which has been shown to suppress autophagy, resulting in an efficient stimulation of $CD8^+$ T cells and low viral protein abundance. Interestingly the last study employs nonprofessional-APCs[48]. Tey and colleagues infected fibroblasts deficient or not in TAP expression with the adenovirus encoding the UL138 transgene and submitted them to autophagy or proteasome inhibitors. They have seen that autophagy inhibition decreased antigen presentation of $CD8^+$ T cells specific for Pul138 only in fibroblasts deficient in TAP. These studies revealed that the role of autophagy in the MHC class I pathway is still poorly understood[49].

Autophagy has not been related much to antigen processing in the MHC class I pathway, instead, it has been implicated in the localization of the MHC-I molecules on the cell surface. Dendritic cells deficient in Atg5, Atg7 or Vps34 induce an increase in MHC class I surface levels compared with wild-type dendritic cells. Thus, autophagy mediates also the endocytosis of the MHC-I molecules on the cell surface[50,51].

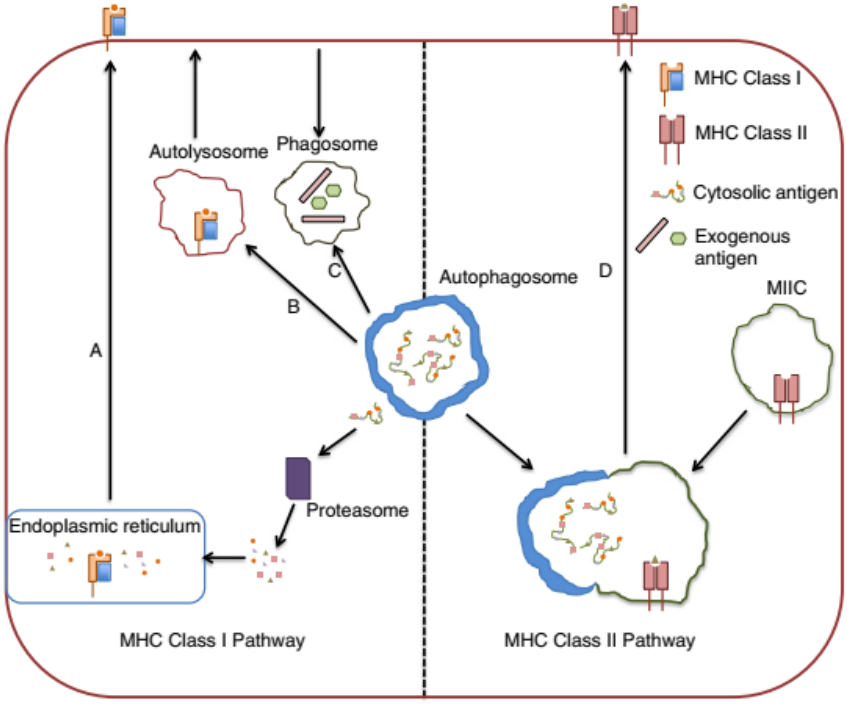


**Figure 10. Autophagy and antigen presentation pathways. A.** Following autophagosome engulfment, the antigen is released and enters the proteasome to be processed, followed by the binding to the MHC-I molecule in the ER and the display of this antigenic peptide/MHC-I molecule to $CD8^+$ T cells. However, some studies claim that are proteasome-independent. **B.** MHC-I molecules may also be loaded in lysosomes before transport to the cell surface. **C.** In cross-presentation phagosomes can encounter autophagosomes carrying extracellular antigens that can then take the MHC class I pathway. **D.** For the MHC class II pathway, it is well accepted that autophagosomes fuse MHC class II compartments to display $CD4^+$ T cell response from endogenous antigens[31,52] (Image taken from Puleston et al 2014)[32].

## VII. Autophagy substrates

Throughout this section, we have described the autophagy pathway and how this degradation pathway can be related to the MHC class I pathway. Various approaches have determined that autophagy can degrade long-lived proteins, aggregate-prone proteins, and proteins derived from pathogens among others. Interestingly, cells take advantage of this mechanism to process these proteins and used the antigenic peptides to activate the immune system. Thus, recovering organism homeostasis by the clearance of infected or damaged cells.

The link between autophagy and antigenic peptides generation for the MHC class I pathway is still poorly understood. According to the available evidence, this association seems to be substrate-dependent. In this Ph.D. study, we have focused on two different kinds of substrates. An aggregate-prone protein and a viral protein.

## VII.A Protein aggregation

Protein aggregates are oligomeric complexes formed by non-native components and interactions among their structure that leads to trapped intermediates related to protein folding or assembly. They tend to be insoluble and stable under physiological conditions. They can as well be observed with a structured morphology or being amorphous. Aggregation occurs when there is partial unfolding, caused by oxidative, thermal, or viral stress, or when there is an alteration in the protein's primary structure, caused by mutation, RNA modification, or translational misincorporation[53,54].

Initially, it was thought that protein aggregation was disorganized and random. Further analysis in bacteria has observed that defective proteins slowly started to polymerize and formed seeded foci that deposit all these defective proteins. This resulted in a protein aggregate deposit called inclusion bodies. However, in mammalian cells is more complicated than that, because some studies have found that cells used the microtubule machinery for the sequestration of protein aggregates within the cytoplasm. They have shown that the depolymerization of microtubules did not disperse the aggresomes conformation but instead blocked aggresome formation. Or in another study, Garcia-Mata has observed, using video time-lapse microscopy, the small protein aggregates delivered to the aggresomes. With these findings, they proposed a new theory suggesting that aggresomes or inclusion bodies are formed after the delivery of protein aggregates by the microtubule machinery[53].

- Poly-glutamine (Poly-Q) aggregates

Consecutive expansion of the trinucleotide CAG repeats encoding polyglutamine (PolyQ) is found in more than 60 human proteins. Recent studies have found that PolyQ domains contribute to the maintenance of protein interactions. The PolyQ, when is expressed in the coiled-coil region will expand to facilitate the interaction with another coiled-coil region in another protein[55]. It is believed that the continued expansion of PolyQ will trigger misleading interactions and result in pathological effects such as aggregation. PolyQ diseases such as Spinocerebellar Ataxia, Dentatorubral Pallidoluysian atrophy, Spinobulbar muscular atrophy, and Huntington's have been related to different causes, but all of them have in common that each pathogenic protein in each disease has more than 40 CAG repeats[56]. Previous studies have related autophagy as a mechanism of quality control of these abnormal PolyQ proteins. For example, it has been shown that autophagy inhibition by 3-MA drug induces the

accumulation of N-termini Huntingtin protein bearing different long of PolyQ sequences[57].

### VII.B The Epstein-Barr virus-encoded EBNA1

The Epstein-Barr virus (EBV) belongs to the herpesvirus family. Most world's population is EBV infected, between 90 to 95%, with no apparent illness. However, sometimes EBV infection can cause diseases such as infectious mononucleosis (IM) characterized by an excessive immune response[58–60].

The EBV infects B lymphocytes and some epithelial cells. Infection of B cells with EBV has been associated with the development of different lymphoproliferative disorders such as Burkitt's lymphoma, Hodgkin lymphomas, and other related lymphomas in immunocompromised patients[58–61].

Among the proteins coded by this virus, the EBV nuclear antigen 1 (EBNA1) has been found in the majority of all tumors positive for EBV[62].

#### EBNA1 escapes immune surveillance

Even though EBNA1 protein is always expressed, it manages to escape immune surveillance. This is due to the low antigen presentation of EBNA1-derived peptides on MHC-I molecules. Several studies have related the domain glycine-alanine repeat (GAr) of EBNA1 with the absence of $CD8^+$ T cells response. For example, one study has observed that individual $CD8^+$ T cells clones from EBV seropositive donors had antigen-specific cytotoxicity in cells expressing EBNA1 lacking GAr but not in cells expressing endogenously the full-length[62,63]. In another study, Levitskaya and colleagues observed that the fusion of the GAr domain to another EBV protein (EBNA4) also inhibited antigen presentation to $CD8^+$ T cells[62,64].

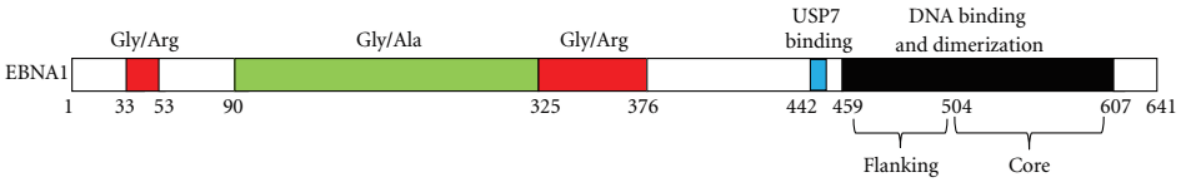


**Figure 11. EBNA1 protein sequence arrangement.** Amino acids numbers are shown below[65] (Image taken from Frappier et al 2012)[62].

Two years after the same group tried to explain how the GAr inhibits EBNA1 antigen presentation on the MHC class I pathway. They evaluated antigenic peptide production by proteasome degradation through ATP addition of cells either expressing EBNA4,

GAr fused to EBNA4 and EBNA1. Upon ATP addition protein levels decrease only in EBNA4 but not in EBNA1 or GAr fused to EBNA4. Claiming with this result that GAr inhibits proteasome function[66]. However, other studies demonstrated that the GAr on its own does not explain the low EBNA1 turnover in cells[67].

These observations did not explain GAr association with the MHC-I antigen presentation. Years later, research developed in our lab found that the GAr mediates suppression of antigenic peptides for the MHC class I pathway by inhibiting EBNA1 mRNA translation *in cis*[68].

The GAr domain of EBNA1

- Translation inhibition

Research carried out in the lab has shown that GAr peptide length and the position of GAr fusion to ovalbumin controlled synthesis and antigenic peptides production[69]. Kinetic pulse-chase experiments and analysis of the ribosomal profile of GAr-ovalbumin expressing cells revealed that GAr targets the initiation step of translation[69]. This result was then confirmed when they introduced a sequence known to allow alternative cap-independent mechanisms of mRNA translation, the *c-myc* IRES, in the 5' UTR of the GAr-ovalbumin. They observed that GAr-ovalbumin fused to *c-myc* IRES increased protein levels and antigen presentation, suggesting that the GAr inhibition mechanism targets only some translation initiation mechanisms[70].

Proteins binding RNA structures affect gene expression. Among the secondary structures, G-quadruplex (G4) are non-canonical nucleic acid structures formed by the stacking of several G-quartets. These structures are planar arrangements of four guanines connected by Hoogsten hydrogen bonds. When these RNA G4 structures are found in the 5' UTR of the mRNA has been associated with translation suppression[71–73].

GAr domain in EBNA1 encodes a guanine-rich sequence that forms G4 structures. Research studying G4 structures formed by GAr has demonstrated that destabilizing the RNA G4, through mutation insertion or using oligos in vitro, prevented inhibition of antigen presentation and increased mRNA translation[74,75].

Further studies uncovered that the multifunctional protein Nucleolin interacts with the GAr-encoding G4 RNA structures and that this interaction mediates the repression of

translation and antigen presentation. Nucleolin overexpression enhanced GAr mediated inhibition of EBNA1 protein expression and treatment with a G4 ligand competitor of Nucleolin, PhenDC3, prevented Nucleolin binding and reversed the GAr inhibition of translation and antigen presentation[76].

- GAr prone to form aggregates

It is reported that EBNA1 exists as an aggregate. Luka and colleagues observed protein aggregation of EBNA1 during the purification of this protein from human lymphoid cell lines[77]. Another study states that EBNA1 has a similar coding sequence to the silk protein. This study proposed that EBNA1 protein might have some β-sheets structure as the silk protein, but also aggregation structure due to the irregular periodicity of the GAr copolymer domain[78].

- EBNA1 is presented in MHC-II molecule via autophagy

Previously the available evidence about EBNA1 antigen presentation suggested that only extracellular peptides could be presented to $CD4^+$ T cells. However, Munz C. demonstrated that the nuclear EBNA1 derive peptides can also be presented in the MHC-II molecule and activated $CD4^+$ T cells via autophagy. They observed that upon lysosomal inhibition, EBNA1 protein was accumulated in autophagosomes and more interestingly it decreases the MHC-II antigen presentation[79].

# VIII. Aim of Ph.D. study – PART 1

Initially, autophagy was thought to be an unspecific degradative process, however, over time scientists have uncovered the selectivity of this pathway. Among the different intracellular constituents, aggregates are specifically degraded by autophagy. Currently, a growing body of studies is interested to know the different functionalities of autophagy in the steady-state of cells, and antigen presentation is one of them.

There is little evidence of autophagy processing in the MHC class I pathway and is unknown the role of the immune system to target and destroy aggregate-carrying cells.

The first part of my Ph.D. aimed to evaluate MHC class I antigenic peptides production from autophagy processing of different types of substrates.

- The EBNA1 viral protein is characterized by the GAr domain conferring an aggregate-prone protein conformation and to be autophagy processed, via Atg5/12, to produce antigenic peptides for the MHC class II pathway.
- Ovalbumin protein fused to aggregate-prone glutamine repetitions (OVA-PolyQ).

# IX. Material and Methods – PART 1

*Plasmids*

The pCDNA3-EBNA1, pCDNA3-EBNA1ΔGAr, pCDNA3-Ovalbumin (OVA), pCDNA3-GAr-OVA, pCDNA3-*c-myc* GAr-OVA, GFP and GAr GFP constructs were obtained as described previously[70,80] respectively.

*c-myc* EBNA1 and *c-myc* EBNA1ΔGAr were generated by amplification of full-length human *c-myc* by polymerase chain reaction (PCR), using a 5' sense primer containing a HindIII site 5' AAT**AAGCTT**CCACTGCTTACTGGCTTATCG 3' and a 3' antisense primer 5' TAA**AAGCTT**CGGCCGTTACTAGTGGATCC 3' containing another HindIII site. The fragment was cloned into the 5'UTR digested pCDNA3-EBNA1 and EBNA1ΔGAr constructs.

The OVA Poly 125 glutamine (Q) construct was made by digestion of OVA construct with EcoRI and XbaI enzyme and introducing 125 glutamine repetition sequence contained in a vector already mentioned previously[81].

*Cell culture and Transfection*

H1299 cells (Human non-small cell lung carcinoma) were cultured in RPMI-1640, supplemented with 10% fetal bovine serum (FBS), 2mM L-glutamine, and 1% Penicillin- Streptomycin and mouse cell atlas (MCA-205) cells were cultured in RPMI-1640, supplemented with 10% fetal bovine serum (FBS), 2mM L-glutamine, 1% non-essential amino acids, 1% sodium pyruvate and 1% Penicillin-Streptomycin. For antigen presentation, western blot, and qRT-PCR experiments, cells were cultured in 6 wells plates ($8x10^4$ cells/well) at 37˚C with 5% $CO_2$. The day after seeding and Atg5/12 siRNA induction, transfections were performed using 3 µl of Gene Juice reagent according to the manufacturer's protocol (Merck Bioscience). Cells were co-transfected with 0.5 µg of murine MHC class I molecule Kb and 1 µg of EBNA1, EBNA1ΔGAr, GAr-OVA, and PolyQ-OVA cDNA carrying the SIINFEKL (SL8) epitope coding sequences in its open reading frame (ORF). In all antigen presentation assays, 1 µg of an OVA cDNA was used as positive control and the same quantity for the empty vector as a negative control.

*siRNA against Atg5/12*

The day after seeding, cells were transfected with Human siRNAs or Murine siRNAs at 20 pM using Jet Prime reagent (Polyplus) following the manufacturer's instructions.

The knock down of these proteins was evaluated by Real-time PCR (qRT-PCR) and Western Blot at the end of 72 hours of incubation and 120 hours.

Human siRNAs used were: two siRNAs against Atg12 (SI02655289 and SI04335513, Qiagen) and three siRNAs against Atg5 (SI02655310, SI02633946, and SI00069251, Qiagen).

Murine siRNAs used were: two siRNAs against Atg12 (SI00900319|S0 and SI00900333|S0, Qiagen) and three siRNAs against Atg5 (SI02696806|S0, SI02720186|S0, and SI02745435|S0, Qiagen).

*Autophagy drug modulator treatment*

The day after seeding, cells were treated with Chloroquine at [30µM] for 36 hours. The autophagy inhibition was evaluated by Western Blot assessing LC3-II accumulation.

*Proteasome drug modulator treatment*

The day after seeding, cells were treated with Epoxomycin at [20µM] for 6 hours. The proteasome inhibition was evaluated by Western Blot assessing P21 accumulation.

*Antigen Presentation assay: OT1 $CD8^+$ T cells proliferation*

To determine the levels of antigen presentation, we used $CD8^+$ T cells that express specific receptors to the OVA epitope, SIINFEKL, recognized by H-2 Kb. These $CD8^+$ T cells were purified from OT1 transgenic mice expressing a transgenic TCR specific for SIINFEKL-Kb. Spleen and lymph nodes from OT1 transgenic mice were passed through a 70 µm cell strainer and red blood cells were lysed with ACK buffer treatment for 5 minutes. After several washes with PBS-FBS 5%, $CD8^+$ T cells were negatively selected using a $CD8^+$ T cell isolation kit (MACS Miltenyi Biotec) according to the manufacturer's instructions. Afterward, the $CD8^+$ T cells were stained with CellTrace™ Violet at 5µM for 10 minutes (Thermo Fisher Scientific, USA) according to the manufacturer's protocol.

Two days after transfection, H1299 cells used as presenting cells were briefly washed with PBS, trypsinized, resuspended in splenocytes medium (RPMI-1640), supplemented with 10% (FBS), 4mM L-glutamine, 1% Penicillin-Streptomycin, 0.05 mM 2-Mercaptoethanol, and 5 mM HEPES) and seeded in 48 wells plates ($1.25x10^5$) cells per well. Except for the antigen presentation upon proteasome inhibition, H1299

cells were fixated with 0.1% v/v glutaraldehyde during 20 s and 0.2 M of glycine was used to block fixation. Then, cells were washed three times with PBS and seeded also in 48 wells plates ($1.25x10^5$) in Splenocytes medium. Then, $5x10^5$ CellTrace™ labelled T-cells were added per well and the co-cultures were incubated at 37°C with 5% $CO_2$. The levels of antigen presentation were deduced from the percentage of T-cell proliferation verified by flow cytometry.

*Flow Cytometry analysis: OT1 $CD8^+$ T cells proliferation*

After 3 days, cells were harvested, stained with anti-mouse CD45.2-PE-Cy7 (BD Pharmingen), fixable viability dye eFluor® 506 (eBioscience, USA), and analyzed on a CANTO II flow cytometer (BD Biosciences, USA). Cells were gated for live CD45.2+ cells ($4x10^5$ events collected) and data were analyzed using FlowJo software version 8 (Tree Star). The percentage of live $CD8^+$ T cells in each generation was calculated using the FlowJo proliferation platform and this value was considered for statistical analysis.

*Antigen Presentation assay: Direct measurement in the presenting cells*

H1299 cells co-expressing murine MHC I Kb and the constructs mentioned above were submitted to Chloroquine treatment. Then, cells were harvested and stained with APC anti-mouse H-2 Kb bound to SIINFEKL Antibody (Biolegend) and Fixable viability 506 (eBioscience, USA). These cells were analyzed on a CANTO II flow cytometer (BD Biosciences, USA) and were gated for live cells. Data were analyzed using FlowJo software version 8 (Tree Star).

*Direct measurement of MHC I Kb* and HLA-ABC

MCA-205 and H1299 cells were submitted to murine or human Atg5/12 siRNA transfection. Then, cells were harvested and stained. MCA-205 cells with anti-mouse H-2 Kb Antibody (Biolegend) and FITC anti-mouse IgG2a Antibody (Biolegend); H1299 cells with HLA-ABC FITC antibody (Invitrogen). Both cell types were also stained with Fixable viability 780 (eBioscience, USA). These cells were analyzed on a CANTO II flow cytometer (BD Biosciences, USA) and were gated for live cells. Data were analyzed using FlowJo software version 8 (Tree Star).

*RNA extraction, RT-PCR and qRT-PCR*

At 72 hours post siRNA Atg5/12 transfection, H1299 cells were washed with PBS, and RNA was purified using the RNeasy Plus Mini Kit (Qiagen) following the manufacturer's protocol. cDNA synthesis was carried out using M-MLV reverse transcriptase and oligo(dT) primers (Invitrogen). For qRT-PCR, the StepOne (Applied BioSystems) real-time PCR system was used, and the reactions were performed with the Perfecta SYBR green Fast mix ROX (Quanta) using specific primer pairs for human Atg5 (Forward: 5' GCTGCAGATGGACAGTTGCA 3'and Reverse: 3' TGTTCACTCAGCCACTGCAG 5'), human Atg12 (Forward: 5' ATGACTAGCCGGGAACACCA 3' and Reverse : 3' CACGCCTGAGACTTGCAGTA 5'), murine Atg5 (Forward: 5'TGTGCTTCGAGATGTGTGGTT 3'and Reverse: 3' GGTCCCCTTTGCACACTTACA 5') and murine Atg12 (Forward: 5'GCCATCTCACCAGCCCAATA 3' and Reverse: 3'CATGCCTGGGATTTGCAGT 5').

*LC3-GFP induction*

To confirm the blockage of autophagosome formation by Atg5 and Atg12 siRNA, we performed epifluorescence microscopy. For this, we seeded 1.5 x $10^4$ H1299 cells in a 24 well plate over a sterile 22x22mm coverslip. Then, cells were transfected with 20 pM of siRNA against Atg5/12 and 0.1 µg of an LC3-GFP construct at 24 and 48 hours after seeding, respectively. After 72 hours of culture, cells were treated with a starvation buffer described elsewhere[82] (140 mM NaCl, 1 mM CaCl2, 1 mM MgCl2, 5 mM glucose, and 20 mM Hepes, pH 7.4) for 2 hours and a complete RPMI-1640 medium was used for the negative control cells. Images were taken at 63x using the Axio Imager D2 microscope. All images were analyzed in Fiji software and the number of green dots was calculated as previously described[73].

*Western Blot*

Cells were trypsinised and the obtained pellets were resuspended with 50 µl of lysis buffer (20 mM HEPES KOH, 50mM β-Glycerol phosphate, 1mM EDTA, 1mM EGTA, 0.5mM Na3VO4, 100 mM KCL, 10% Glycerol and 1% Triton x-100, protease inhibitor cocktail Roche). Total lysates were obtained after the mechanic hitting and freezing at -80°C for at least 2 h. After, samples were centrifuged at 13 000 RCF for 10 min at 4°C, and supernatants were collected. Samples were quantified using Bradford Reagent (BioRad) and 50 µg of protein were separated on 4-12% SDS-PAGE gels (Thermo Fisher Scientific) and transferred to nitrocellulose blotting membranes (Pall

Corporation). After saturation of membranes with TBS- 0.5% Tween containing 5% non-fat milk, membranes were overnight incubated with anti-EBNA1 (16216-1-AP Abnova), anti-Atg12 (R&D systems), anti-chicken egg albumin (C6534 Sigma), anti-LC3B (L75443 Sigma), anti-GFP (11814460001 Roche), anti-P21 (cell signaling) and anti-actin (AC-15 Sigma) antibodies. After washing with TBS-Tween, bound antibodies were detected using a rabbit anti-mouse (Dako) or a mouse anti-rabbit (Dako) secondary antibody conjugated to horseradish peroxidase (1:1000; 1 h at room temperature). Immunocomplexes were then revealed with ECL (Thermo Scientific) and imaged using a MyECL Imager (Thermo Scientific).

*Immunofluorescence*

H1299 cells were seeded as described for LC3-GFP induction experiments and transfected with 0.8 µg of EBNA1, EBNA1ΔGAr, GAr-OVA, EBNA1 *c-myc*, EBNA1ΔGAr *c-myc*, GAr-OVA *c-myc*, OVA, PolyQ-OVA or empty vector. Samples were fixed with 4% paraformaldehyde and permeabilized with 0.4% Triton x-100 0.05% CHAPS PBS. Afterward, cells were blocked with 3% Bovine serum albumin (BSA) Saponin 0.1% PBS for 1 hour and then incubated with mouse anti-EBNA1 (16216-1-AP Abnova) or rabbit anti-egg albumin (C6534 Sigma) for 1 hour at room temperature. After two washes with PBS, samples were incubated with an anti-mouse Alexa 488 or anti-rabbit Alexa 647 antibodies for 1 hour at room temperature. Next, samples were washed with PBS, stained with DAPI, and mounted with a fluorescence mounting media (Dako). Samples were examined in an LSM 800 confocal laser microscope (Carl Zeiss MicroImaging GmbH, Jena, Germany) and images were treated using the Fiji software.

*Statistics*

Data were analyzed by two-tailed unpaired Student's t-test or One sample T-test using GraphPad Prism 6 for Windows (GraphPad Software). Data shown are mean ± sd. of minimum three independent experiments. *P < 0.0332; **P < 0.0021; ***P < 0.0002; ****P < 0.0001; 0,1234 ns, not significant.

# X. Results - PART 1

Transfection efficiency

The research developed during this Ph.D. is based on transient lipid transfection of different cDNA constructs or siRNA. I have tested the transfection efficiency of the Gene Juice reagent into H1299 cells. Two different GFP cDNA constructs were transfected at [1µg] and 48 hours later harvested cells were quantified by flow cytometry. We observed that percentage of GFP expressing cells in both transfections was between 31% to 48% (**Fig. 12**). Furthermore, no cell toxicity was observed (data not shown) why this approach was chosen.

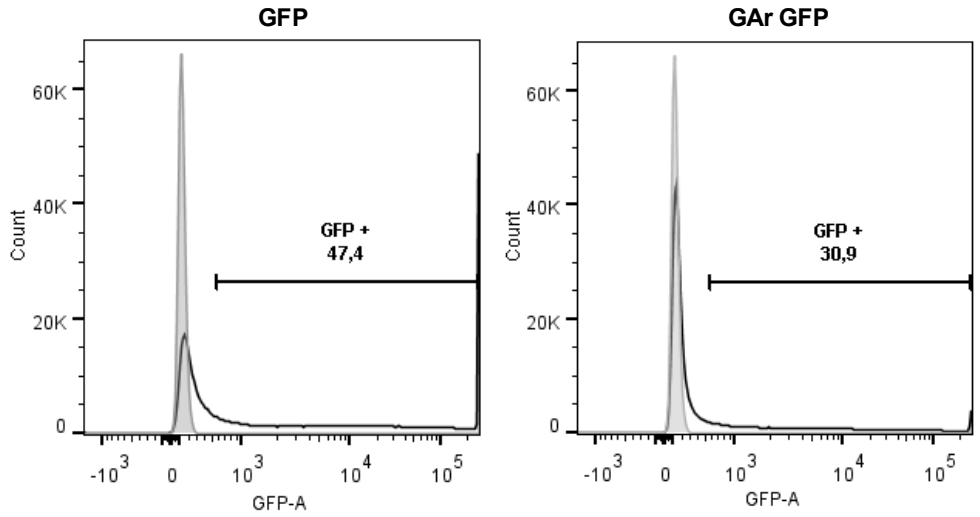


**Figure 12.** *Quantification of transfection efficiency is around 31 to 50%*. H1299 cells were transfected with 1ug of GFP or GAr GFP cDNA constructs. After 48 hours cells were harvested and quantified by Flow Cytometry. Gray histogram shows cells expressing empty vectors (not fluorescent cells) and open histograms of the corresponding cDNA constructs.

Knocking down Atg5 and Atg12 blocks autophagy in H1299 cells

To evaluate the role of autophagy in antigen presentation to the MHC class I pathway, we knocked down the expression of Atg5 and Atg12 using specific siRNAs. These proteins are crucial for the conjugation system that allows the formation of autophagosomes and their downregulation is reported to block the autophagy pathway[79,83,84]. The efficiency of siRNA treatments was confirmed by the downregulation of Atg5/12 mRNA (**Fig. 13A**) and protein levels (**Fig. 13B, upper lane**). siRNA treatments resulted in a decreased ratio of LC3 II-I (**Fig. 13B, middle lane**) and suppressed autophagy flux following serum starvation (**Fig. 13C, upper part**). Of note, LC3-GFP protein levels did not change under serum starvation (**Fig. 13C, bottom**

**part**). Together, these data show that the siRNA against Atg5/12 interferes with the autophagy pathway in H1299 cells.

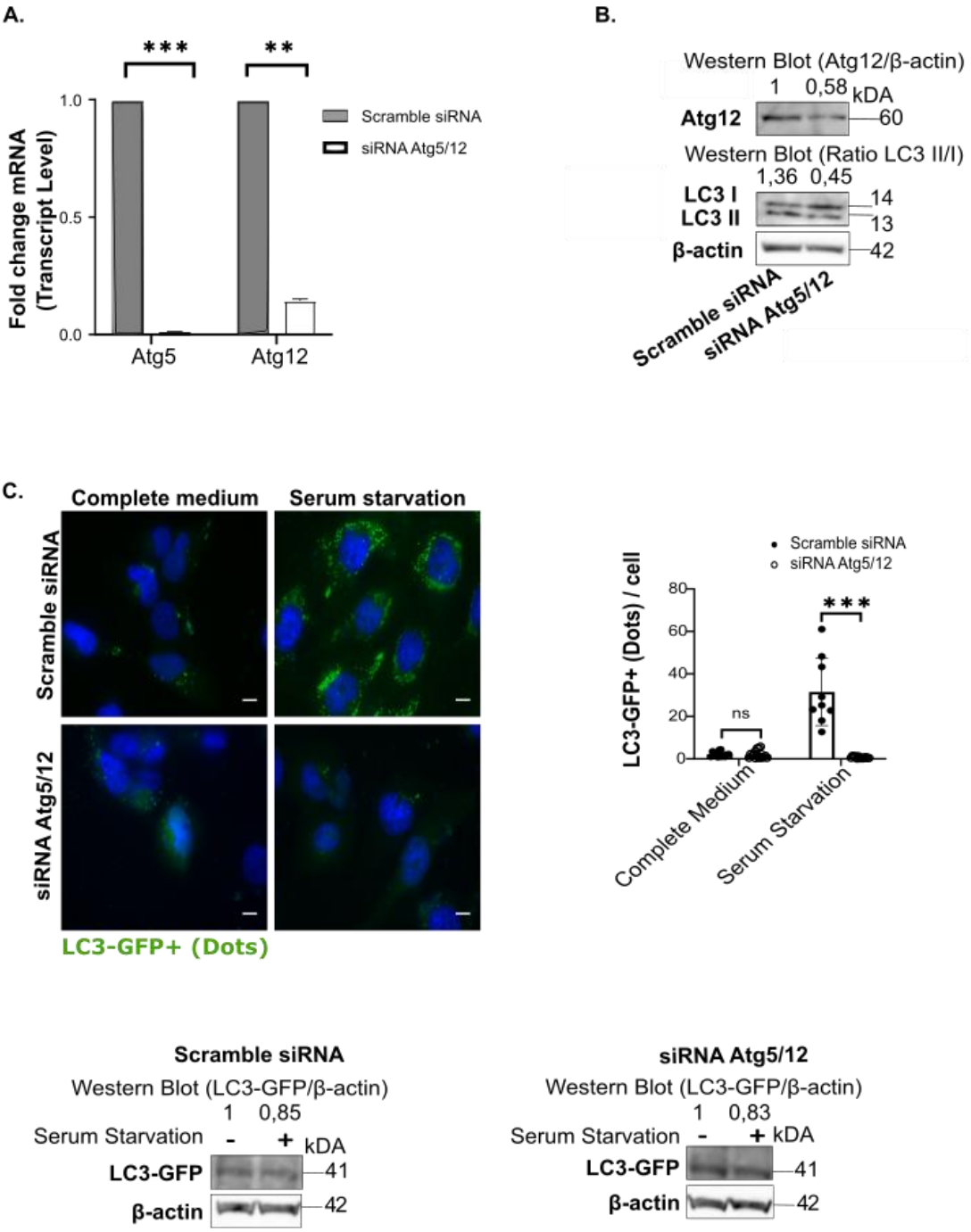


**Figure 13.** *Autophagy Inhibition*. **A.** The Atg5/12 mRNA levels were confirmed using RT-qPCR seventy-two hours following transfection of [20 pM] human siRNA against Atg5/12 or scramble siRNA **B.** Western Blots depicts the expression of Atg12, LC3 I, and LC3 II. Values above the bands show the densitometry analysis normalized against β-actin and the fold change compared with the scramble siRNA. Autophagy suppression was estimated by the ratio between LC3 II and LC3 I **C.** H1299 cells were transfected with a plasmid encoding LC3-GFP 24 hours after treatment with siRNAs as in A. 48 hours later, cells were treated without serum for two hours, and then fixed. One representative image is shown from the three independent

experiments performed. LC3-GFP fluorescence was observed as green dots, indicating autophagosome formation. The number of GFP dots was quantified (top right graph). LC3-GFP expression was determined by Western Blot (bottom panels). Values above the bands show the densitometry analysis of bands normalized with β-actin and the fold change comparing the complete medium with the serum starvation treatment. Significant values were calculated using Multiple paired groups T-test. ***P < 0.0002; **P < 0.0021; 0,1234 ns, not significant. White scale bars denote 10 μm.

Atg5 and Atg12 knock down does not affect MHC class I cell surface expression

Previous studies have found that dendritic cells impaired autophagy via siRNA knock down of Atg5 and Atg7 proteins increased MHC class I cell surface localization. Loi and colleagues uncovered that these two proteins mediate the endocytosis of the MHC I molecule from the cell surface and its later degradation through autophagy[51].

To further pursue our antigen presentation research, first, we needed to evaluate the influence of Atg5/12 knock down on MHC class I cell surface localization. Our research in the MHC class I pathway has been based on the use of the SIINFEKL (SL8) immune epitope from chicken ovalbumin. This peptide is specifically recognized by $CD8^+$ T-cells derived from transgenic OT-1 mice in the context of the murine (Kb) MHC class I molecule. We have transfected murine MHC-I (Kb) into human H1299 cells. Transfected cells were subjected to autophagy inhibition through Atg5/12 siRNA treatment. Later, these presenting cells were co-cultured with OT1 $CD8^+$ T cells and free SL8 peptide [1μg/ml]. The relative level of antigen presentation was estimated by OT-1 CD8+ T-cells proliferation using flow cytometry in response to the free SL8 bound to MHC-I (Kb) on the surface of the APCs. We observed no effect in OT-1 $CD8^+$ T cells proliferation upon Atg5/12 knock down compared to the scrambled control cells, showing that Atg5/12 down-regulation does not affect the MHC class I pathway per se (**Figure 14A**). Moreover, we analyzed the changes in the membrane localization of endogenous MHC-I (Kb) molecules in murine MCA-205 cells or MHC-I (HLA-ABC) molecules in human H1299 cells and we observed no difference in MHC class I cell surface localization (**Figure 14B, left panels**). Of note, murine Atg5/12 knock down showed the same marked downregulation as the Human Atg5/12 siRNA (**Figure 14B, right graphs**).

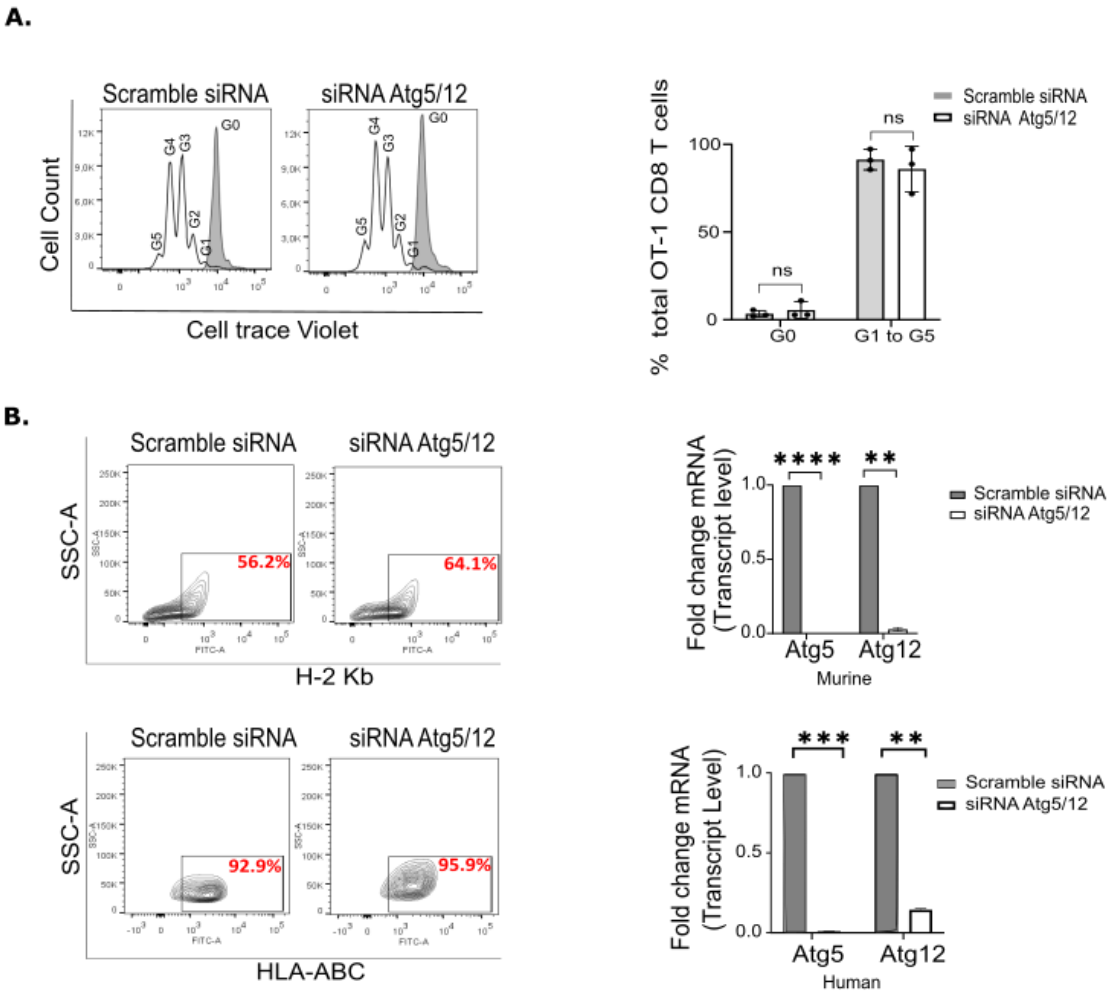


**Figure 14.** Presentation of exogenous SL8 peptide and membrane location of MHC Class I molecule is not affected by Atg5/12 knock down. **A.** H1299 cells co-expressing murine MHC-I (Kb) were transfected with human siRNA Atg5/12 [20 pM] or scramble siRNA for 72 hours. Next, three days after these presenting cells were co-incubated with OT-1 $CD8^+$ T cells labeled with Cell-trace violet and free SL8 peptide [1ug/ml]. The levels of OT-1 $CD8^+$ T cells proliferation were analyzed by Flow Cytometry. Open peaks in the histogram represent the proliferating populations and grey peaks denote unstimulated populations (Empty Vector transfected cells) (Left panel). The percentage of total OT1 $CD8^+$ T cells was calculated using the number of cells in each generation generated by the modeling of the Proliferation tool in Flow Jo software. The graph shows the sum of the percentage of cells from generation 1 to 5 compared with the percentage of non-divided cells (generation 0) from 3 independent experiments. **B.** MCA-205 and H1299 cells were transfected with murine/human siRNA Atg5/12 [20 pM] or scramble siRNA respectively for 72 hours. HLA-ABC FITC or H-2 Kb FITC antibodies were used to measure MHC class I molecules in live cells by Flow Cytometry. Murine or human Atg5/12 siRNA knock down was confirmed by qRT-PCR. Significant values were calculated using Multiple paired groups T-test. **P < 0.0021; ***P < 0.0002; ****P < 0.0001; 0,1234 ns, not significant.

Preventing autophagy reduces MHC class I antigen presentation independently of protein aggregate formation

Autophagy can degrade harmful cytosolic proteins, including aggregates[33,38,39]. We tested the capability of this pathway to process protein substrates for the MHC-I pathway. We used a chicken OVA construct whose secretion is blocked by the deletion of the first 50 amino acids[85]. This construct enabled us to study the antigen presentation via the MHC-I pathway using OT-1 $CD8^+$ T cells. We also fused a poly-glutamine repetition (PolyQ), known to cause aggregates and to be processed by autophagy[86–88], to OVA (**Fig. 15A**). Immunohistochemistry assays using anti-OVA antibodies showed that PolyQ-OVA forms approximately 10 aggregates per cell (white arrowheads) while OVA was uniformly stained throughout the cells and no visible aggregate was detected (**Fig. 15B**). Expression of the reporter constructs was not significantly affected by siRNA against ATG5/12 (**Fig. 15C and annexes suppl. Fig. 1**). We did not detect any accumulation of PolyQ-OVA upon ATG5/12 knock down, presumably because the PolyQ-OVA is not only present in the aggregate conformation (**Fig. 15B**) due to the limited time (24 hours) of expression. To test the role of autophagy in the processing of antigenic peptide substrates for the MHC class I pathway, we co-expressed the indicated SL8-carrying constructs together with the (Kb) MHC cDNA in human H1299 cells. Transfected cells were subject to autophagy inhibition through Atg5/12 siRNA treatment and antigen presentation was evaluated by co-culture with OT1 $CD8^+$ T-cells. The relative level of antigen presentation was estimated by OT1 $CD8^+$ T-cells proliferation using flow cytometry. For every assay, we confirmed suppression of autophagy by, in parallel estimating the LC3 I/II ratio (Fig. 13B and data not shown). We observed that under Atg5/12 knock down, OVA and PolyQ-OVA showed a higher percentage of cells in the non-proliferating OT1 $CD8^+$ T cell population (G0) and a corresponding decrease in the proliferating population (G1 to G5), indicating a reduction of antigen presentation (**Fig.15D**). The percentage of OT1 $CD8^+$ T cells in each generation is shown in (**Annexes suppl. Fig. 2)**. Despite being uniformly expressed and showing no apparent formation of aggregates, it was surprising to see that knocking down Atg5/12 affected the presentation of antigenic peptides from OVA as much as from PolyQ-OVA.

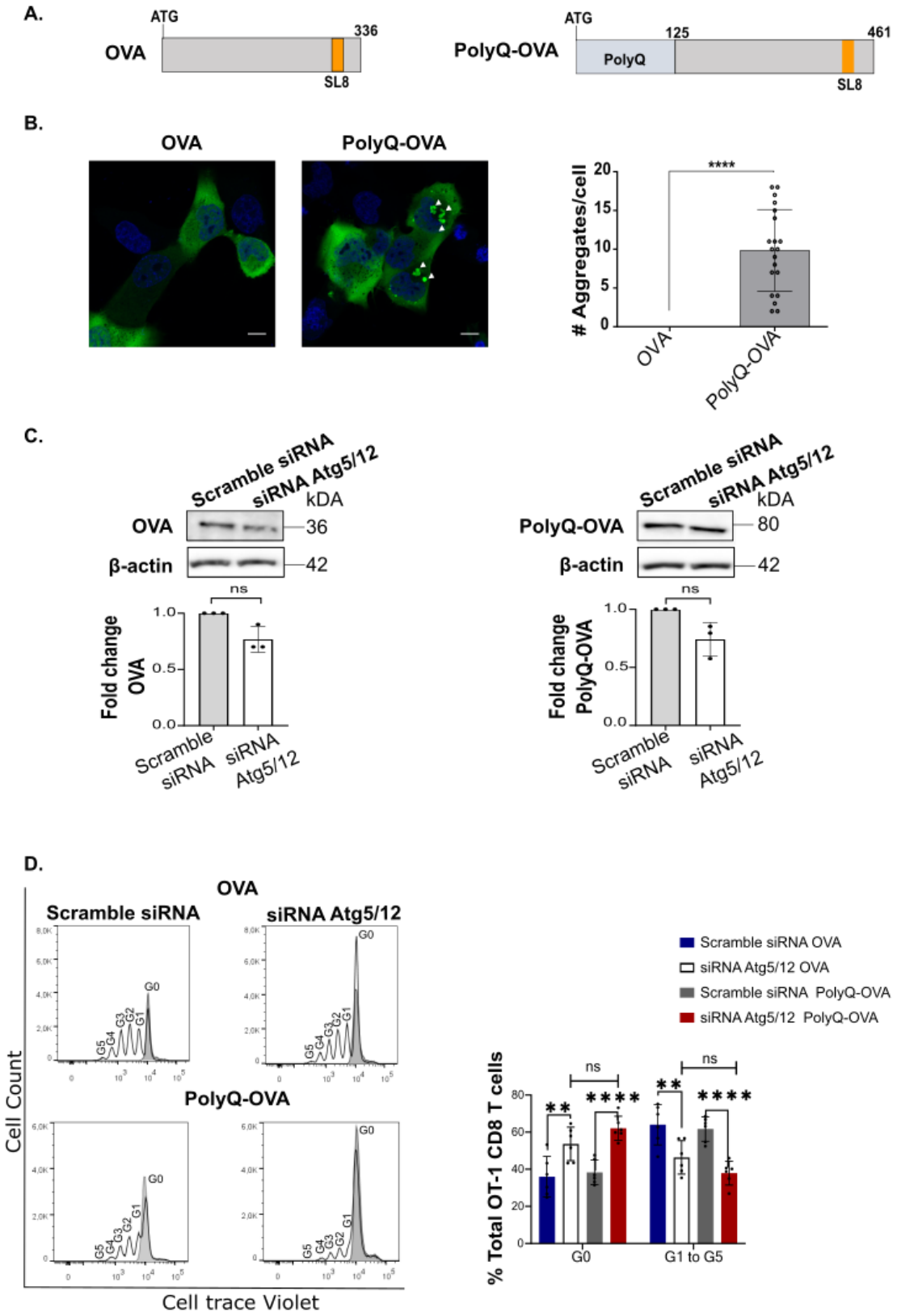


**Figure 15**. *Autophagy affects antigen presentation of Ovalbumin and Ovalbumin fused to the polyglutamine peptide* **A.** Cartoon illustrating chicken ovalbumin (OVA) sequence with the location of the immune peptide SL8 and the glutamine repeat (PolyQ) **B.** Representative immunofluorescence image of OVA and PolyQ-OVA. White arrow heads indicate an

aggregation pattern. The graph shows the average number of aggregates observed **C.** Western Blot represents the effect of 72 hours of Atg5/12 human siRNA transfection on OVA and PolyQ-OVA expression. The graphs below show the densitometry analysis, normalized against β-actin and expressed in fold change compared with the scramble siRNA **D.** H1299 were transfected with human siRNA Atg5/12 [20 pM] or scrambled siRNA. 24 hours later they were transfected with murine MHC-I (Kb) and indicated constructs. After 48 hours they were incubated with OT-1 CD8+ T cells labeled with cell-trace violet for 3 days. OT-1 CD8+ T cell proliferation was analyzed by Flow Cytometry. A higher rate of proliferation indicates more antigen presentation. Open peaks in the histogram represent the proliferating populations and grey peaks denote unstimulated populations (Empty Vector transfected cells) (left panel). The graph shows the sum of the percentage of cells from generation 1 to 5 compared with the percentage of non-dividing cells (generation 0) from 6 independent experiments (right graph). Significant values were calculated using Multiple paired groups T-test. *P < 0.0332; **P < 0.0021; ***P < 0.0002; ****P < 0.0001; 0,1234 ns, not significant. White scale bars denote 10 μm.

Proteasome affects the presentation of Ovalbumin derive antigenic peptides

The proteasome is known to be one of the main processing mechanisms that produce antigenic peptides in the MHC class I canonical pathway [6]. As the proteasome can be another possible degradation machinery besides autophagy, we evaluated antigen presentation of OVA-derived peptides under proteasome function inhibition. H1299 cells co-expressing MHC-I (Kb) and OVA were treated with or without Epoxomycin (Epoxo.) for 6 hours. Next, harvested cells were fixed and co-culture with OT-1 $CD8^+$ T cells. The levels of OT-1 $CD8^+$ T cell proliferation were analyzed by Flow Cytometry. We demonstrated that OT-1 $CD8^+$ T cells proliferation was significantly decreased in response to OVA antigenic peptide presentation upon Epoxo. treatment compared with DMSO (**Figure 16A**). In parallel, we observed an increase in the OVA protein levels during proteasome inhibition by western blot (**Figure 16B**). We also confirmed proteasome inhibition, as the specific proteasome target P21 cell cycle protein [89] was accumulated with this drug treatment (**Figure 16B**). This is in line with previous studies stating that OVA-derived antigenic peptides are degraded by the proteasome[90,91]. The autophagy pathway, as well as the proteasome, could both tackle OVA protein because OVA is very susceptible to polyubiquitination and this tag signal is recognized by both mechanisms[38,92].

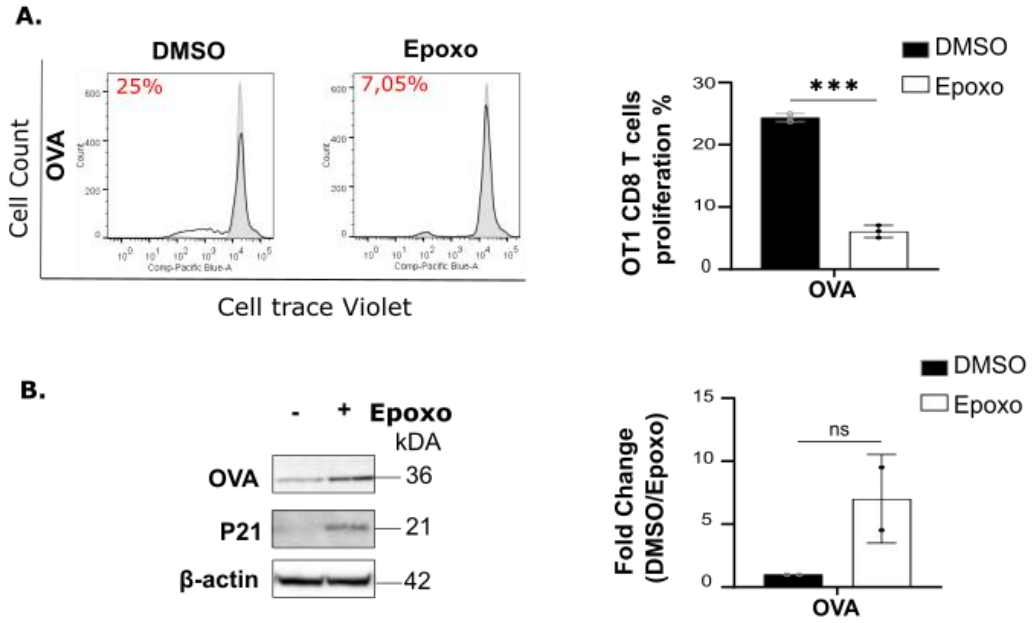


**Figure 16.** *Proteasome also affects the presentation of Ovalbumin derives antigenic peptides.* **A.** H1299 cells co-expressing MHC-I (Kb) and OVA were treated with Epoxomycin (Epoxo.) [20 µM] or without (DMSO) for 6 hours. Then, these cells were fixated and co-culture with OT-1 CD8+ T cells labeled with Cell-trace violet for 3 days. The levels of OT-1 CD8+ T cells proliferation percentage were analyzed by Flow Cytometry. A higher rate of proliferation indicates more antigen presentation. Open peaks in the histogram represent the proliferating populations and grey peaks denote unstimulated populations (Empty Vector transfected cells) (left panel). The graph shows three independent experiments **B.** Western Blot showing OVA expression upon [20 µM] Epoxo. treatment for 6 hours. P21 protein accumulation confirmed proteasome inhibition during Epoxo treatment. The graph shows the densitometry analysis, normalized against β-actin and expressed in fold change compared with DMSO. Significant values were calculated using Multiple paired groups T-test. ***P < 0.0002; 0,1234 ns, not significant.

## MHC class I-restricted presentation of peptides derived from EBNA1 is not affected by the suppression of autophagy

The Epstein-Barr virus-encoded EBNA1 protein has been reported to be an aggregate-prone protein due to its long repeat of non-polar gly-ala residues (GAr) [77,78]. Since EBNA1-derived antigenic peptides are processed for the MHC class II pathway via autophagy [79] [33,38,39], we wanted to know if EBNA1-derived peptides can also be presented for the MHC class I pathway through autophagy. We inserted the antigenic SL8 peptide into the EBNA1 open reading frame (ORF), or in an EBNA1 depleted of the GAr-domain (EBNA1ΔGAr). We also used a construct carrying the GAr-domain fused to OVA cDNA (GAr-OVA) (**Fig. 17A**). To test if EBNA1 shows the same aggregation pattern observed for PolyQ-OVA, we performed immunohistochemistry

assays. However, we observed no obvious aggregates of EBNA1, EBNA1ΔGAr, or GAr-OVA and no differences in subcellular localization with, or without, the GAr (**Fig.17B**). The GAr mediates suppression of antigenic peptides for the MHC class I pathway by inhibiting *EBNA1* mRNA translation *in cis* [68]. In agreement with this, we observed a low percentage of $CD8^+$ T cell proliferation in response to SL8 derived from EBNA1 and GAr-OVA, as compared to EBNAΔGAr (**Fig. 17C**) and OVA (**Fig.15D**). Importantly, we observed no significant difference between percentages of OT-1 $CD8^+$ T cells in the undivided (G0) or the proliferating populations (G1 to G5), for any of the tested conditions following Atg5/12 siRNA treatment (**Fig. 17C and annexes suppl. Fig. 2B**). We also showed that Atg5/12 knock down had no significant effect on EBNA1, EBNA1ΔGAr, and GAr-OVA expression (**Fig. 17D and annexes suppl. Fig. 1**). These results support the idea that the autophagy pathway does not provide EBNA1-derived antigenic peptides for the class I pathway and that the fusion of the GAr prevents OVA from being presented via autophagy. Hence, EBNA1 can be processed by autophagy and presented to the class II pathway but not the class I pathway.

<u>Drug inhibition of autophagy does not affect antigen presentation of EBNA1, EBNA1ΔGAr, or GAr-OVA in the MHC class I pathway</u>

To confirm the absence of effect in the autophagy inhibition by Atg5/12 siRNA on EBNA1 derive antigenic peptides presentation, we treated H1299 cells co-expressing MHC I (Kb) and EBNA1, EBNA1ΔGAr, GAr-OVA with Chloroquine (CQ) for 36 hours. We evaluated antigen presentation directly in the presenting cells with the labeling of SL8 H-2 Kb. Cells having SL8 H-2 Kb on the cell surface were measured by Flow Cytometry using the APC anti-mouse H-2Kb bound to the SL8 antibody. We showed that autophagy inhibition with CQ treatment had no effect in presenting antigenic peptides derived from EBNA1, EBNA1ΔGAr, or GAr-OVA (**Fig. 18A**). Next, western blots showed that Chloroquine decreased EBNA1 protein levels and blocked autophagy efficiently, as LC3 II protein levels were accumulated compared with the control condition water (**Fig. 18B**). These observations support the data obtained using siRNA against Atg5/12 and that the GAr sequence prevents OVA from being presented to the class I pathway via autophagy.

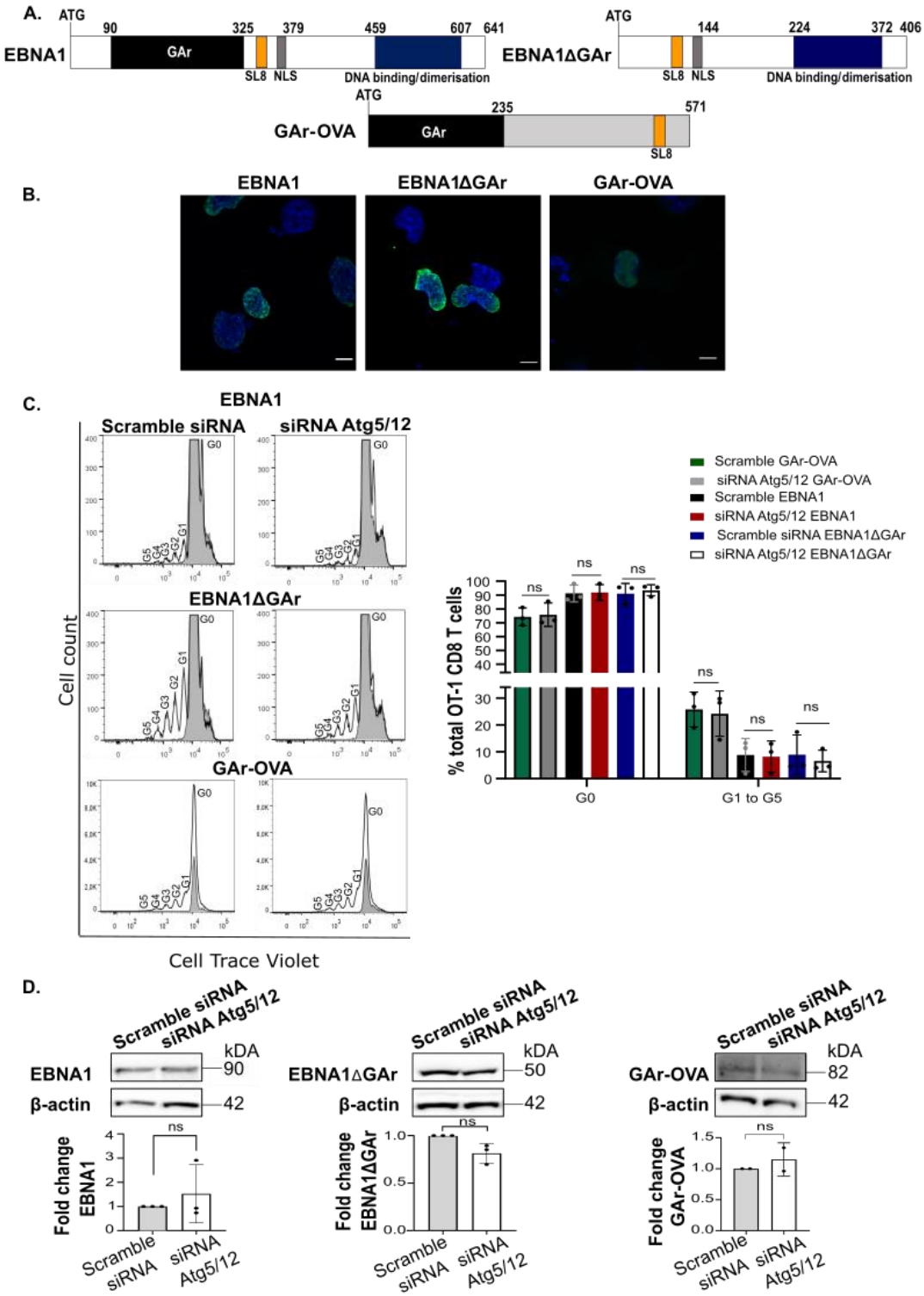


**Figure 17.** *Fusion of the EBNA1-derived gly-ala repeat (GAr) sequence suppresses Atg5/12-dependent antigen presentation*. **A.** Cartoon illustrating different EBNA1 constructs with, or without, the GAr (EBNA1ΔGAr) and GAr fused to Ovalbumin. The location of the nuclear localization signal (NLS), the DNA binding/dimerization sequence in EBNA1, and the SL8 epitope are indicated. **B.** Representative immunofluorescence image of EBNA1, EBNA1ΔGAr, and GAr-OVA. **C.** H1299 cells co-expressing murine MHC-I (Kb) and the indicated constructs were transfected with human siRNA Atg5/12 [20 pM] or scramble siRNA for 72 hours like in figure 17D. The graph shows the percentage of cells from generations 1 to 5 compared with

the percentage of non-divided cells (generation 0) from 3 independent experiments (right graph) **D.** Western Blots show one out of three representative experiments on the effect of autophagy inhibition on EBNA1, EBNA1ΔGAr, and GAr-OVA protein expression levels. The graphs show densitometry analysis normalized against β-actin and expressed in fold change compared with the scramble siRNA. Significant values were calculated using Multiple paired groups T-test. Not significant ns: 0,1234. White scale bars denote 10 µm.

<u>The level of protein expression does not determine MHC class I restricted antigen presentation via the autophagy pathway.</u>

The above results (Fig.15 and Fig.17) were surprising considering that OVA alone, or OVA fused to the PolyQ, presents antigenic peptides in an Atg5/12-dependent fashion, while this antigen presentation pathway is prevented by the fusion of the GAr. We next set out to test if the effect of the GAr on antigen presentation via autophagy is associated with its effect on suppressing mRNA translation *in cis.* For this, we fused the *c-myc* 5'UTR to the 5' of the GAr-OVA (**Fig. 19A**). The presence of the *c-myc* sequence overcomes the translation inhibitory capacity of the GAr and restores protein synthesis without altering the coding sequence [70]. Initially, we confirmed by western blot and immunofluorescence that the insertions of the *c-myc* sequence resulted in the expected increase in expression of GAr-OVA (**Fig. 19B**). When we compared antigen presentation we observed the expected significant increase in presentation from the *c-myc*-carrying GAr-OVA construct, as compared to GAr-OVA alone (**Fig. 19C**).

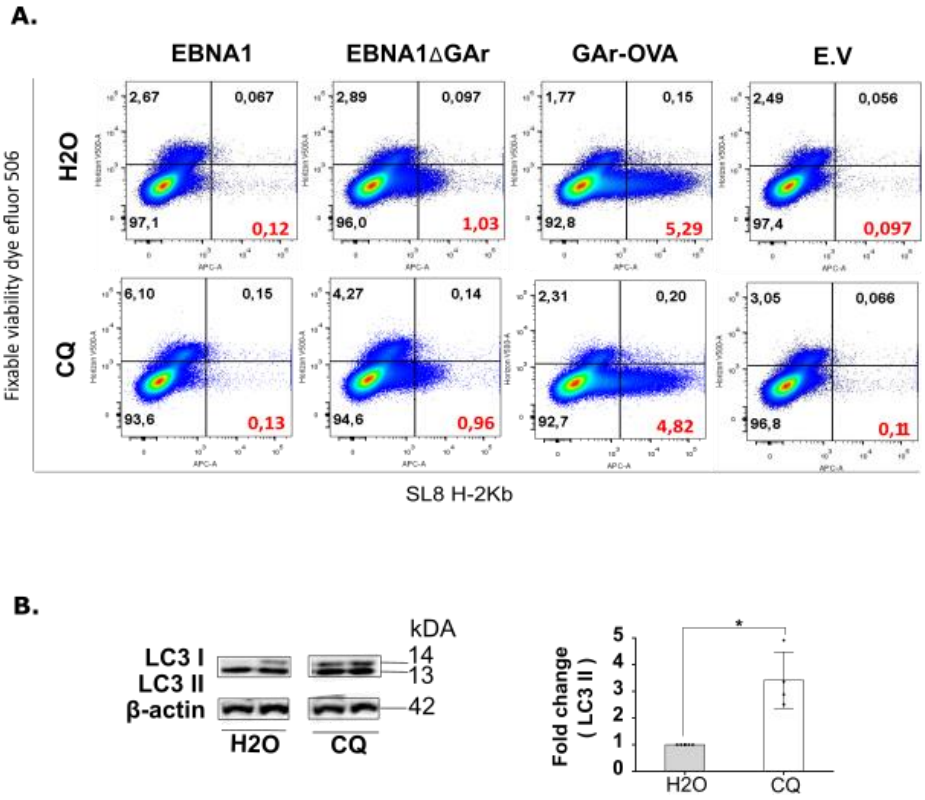


**Figure 18.** *Chloroquine treatment does not affect EBNA1, EBNA1ΔGAr, or GAr-OVA antigen presentation* **A.** H1299 cells co-expressing murine MHC-I (Kb) and EBNA1, EBNA1ΔGAr, GAr-OVA or E.V were treated with Chloroquine [30 μM] during 36 hours. Then, cells were harvested and labeled with SL8 H-2 Kb and fixable viability dye. Cells having SL8 H-2 Kb on the membrane were measured by Flow Cytometry. **B.** Western Blots show the effect of 36 hours of Chloroquine treatment at [30μM] on EBNA1 and EBNA1ΔGAr protein expression. Autophagy inhibition was confirmed by the accumulation of LC3 II. The graphs (Right side) show the densitometry analysis, normalized against β-actin and expressed in fold change compared with water. Significant values were calculated using Multiple paired groups T-test. *P < 0.0032; 0,1234 ns, no significant.

Once we verified that *c-myc* insertion increased GAr-OVA protein synthesis and GAr-dependent antigen presentation, we assessed if an increase in protein levels has an effect on the presentation of substrates to the class I pathway via autophagy. Additionally, to the fusion of *c-myc* 5' UTR to the 5' of the GAr-OVA, we also fused the *c-myc* to the 5' of the EBNA1 and EBNA1ΔGAr (**Fig. 20A**). Western blots showed that the insertion of the *c-myc* sequence resulted in the expected increase in expression of EBNA1 and GAr-OVA but not EBNAΔGAr (**Fig. 20B**). Immunofluorescence showed that *c-myc* insertion did not change the subcellular localization of EBNA1, EBNA1ΔGAr, and GAr-OVA proteins (**Fig. 20C**), and western blots showed that Atg5/12 knock down did not affect the expression of either construct (**Fig. 20D and**

**annexes suppl. Fig.1**). Next, we compared antigen presentation between the different constructs and we observed no significant difference in antigen presentation between *c-myc* carrying constructs following Atg5/12 knock down (**Fig. 20E and annexes suppl. Fig.2**). Taking together these results suggest that the levels of EBNA1 or GAr-Ova protein expression do not affect the autophagy-dependent presentation of antigenic peptides for the MHC class I pathway.

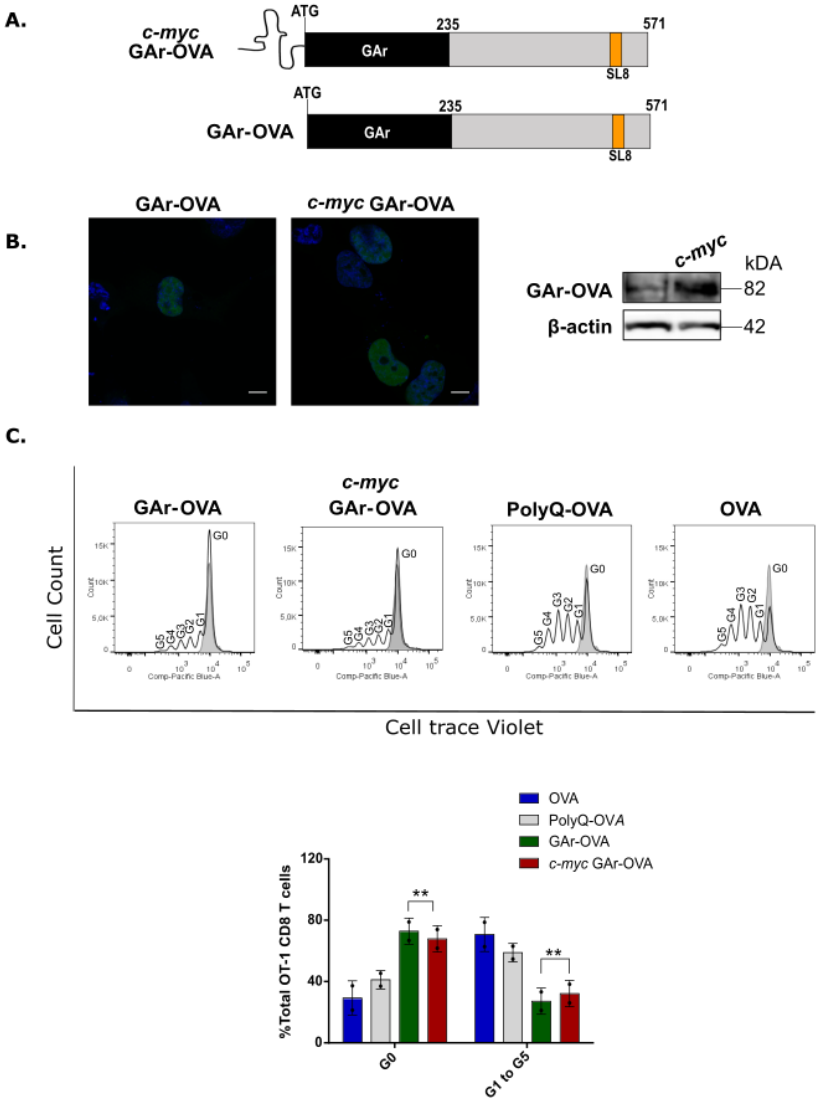


**Figure 19.** *c-myc sequence increases protein expression of GAr-OVA and antigen presentation of GAr-OVA derive antigenic peptides.* **A.** Cartoon illustrating the location of *c-myc* 5' UTR RNA sequence inserted in the 5'UTR of GAr-OVA and the unmodified GAr-OVA sequence. **B.** The *c-myc* fused to the 5' UTR of the GAr-OVA construct overcomes GAr-mediated mRNA translation suppression. Immunofluorescence and Western blot show the differences in protein expression levels. **C.** H1299 cells co-expressing murine MHC-I (Kb) and GAr-OVA, *c-myc* GAr-OVA, PolyQ-OVA, or OVA were co-cultured with OT1-CD8+ T cells for three days. OT1 CD8+ T cells proliferation was measured by Flow Cytometry. The graph shows the percentage of cells from generations 1 to 5 compared with the percentage of non-

divided cells (generation 0) from 2 independent experiments (bottom graphs). Significant values were calculated using Multiple paired groups T-test. *P < 0.0332; **P < 0.0021; 0,1234 ns, no significant.

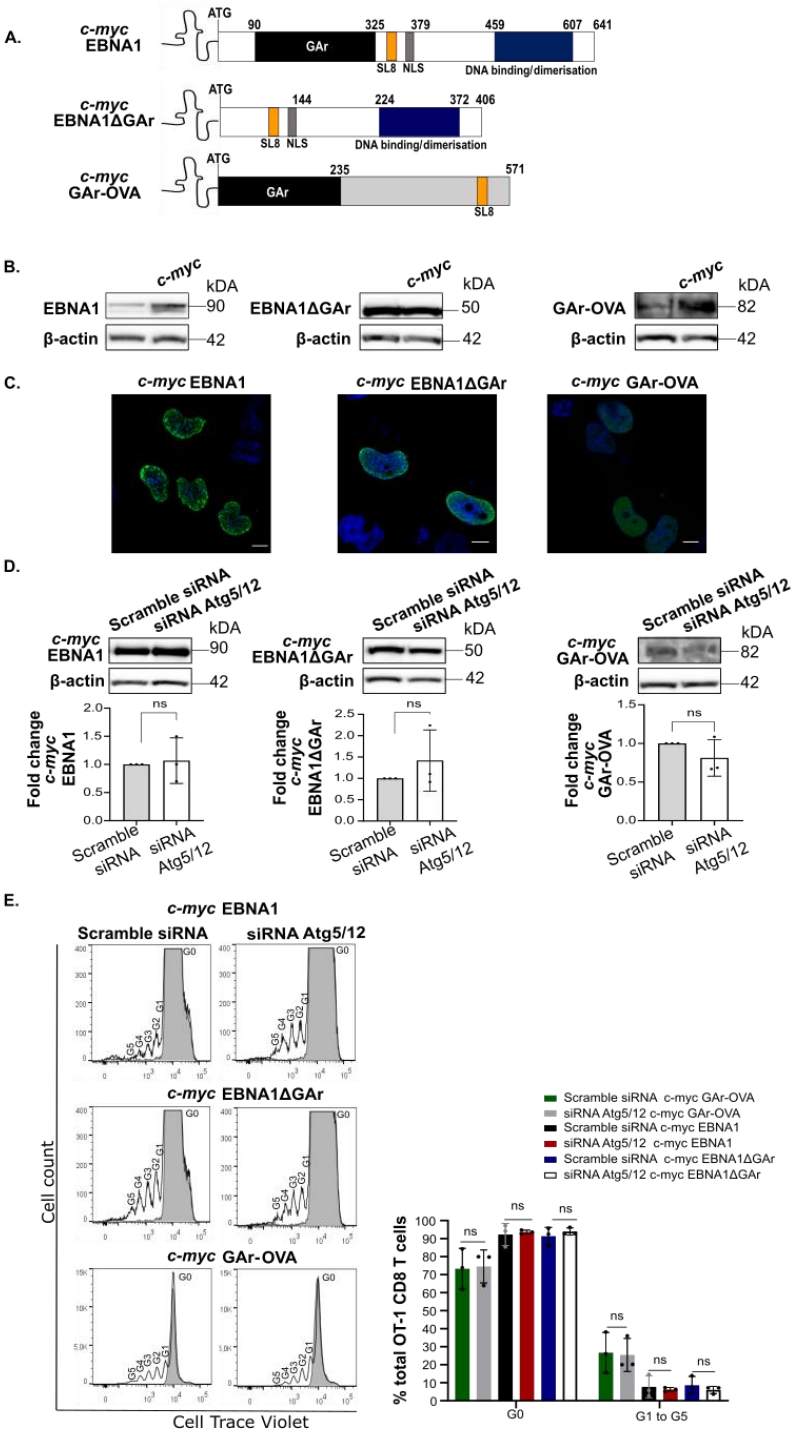


**Figure 20.** *Protein levels do not change autophagy-dependent antigen presentation*. **A.** Cartoon illustrating the location of *c-myc* 5' UTR RNA sequence inserted in the 5'UTR of EBNA1, EBNA1ΔGAr, and GAr-OVA **B.** The *c-myc* fused to the 5' UTR of EBNA1, EBNA1ΔGAr, and GAr-OVA constructs overcome GAr-mediated mRNA translation suppression. Western blots show the differences in protein expression

levels **C.** Representative immunofluorescence of EBNA1, EBNA1ΔGAr, and GAr-OVA constructs carrying the *c-myc*. **D.** Western Blot showing the effect of autophagy inhibition on protein levels of the indicated constructs. The graphs show densitometry analysis, normalized against β-actin for all targeted proteins and expressed in fold change compared with the scramble siRNA. **E.** H1299 cells co-expressing murine MHC-I (Kb) and the indicated constructs following human siRNA Atg5/12 [20 pM] or scramble siRNA treatment for 72 hours. The antigen presentation was estimated as described in figures 5 and 7. The graph shows the percentage of cells from generations 1 to 5 compared with the percentage of non-divided cells (generation 0) from 3 independent experiments (right graph). Significant values were calculated using Multiple paired groups T-test. Not significant ns: 0,1234. White scale bars denote 10 µm.

# XI. Discussion – PART 1

Antigenic peptide substrates processed by autophagy for the MHC class I pathway

Alternative sources of peptides for the MHC class I pathway have been proposed but if, and to what extent, peptides derived from the processing of substrates via the autophagy pathway can be presented to the class I pathway is unknown. We have tested different types of substrates that were potentially good candidates to be presented in the MHC class I pathway via autophagy which gave us a broader idea of the relationship between autophagy and the different kind of peptides.

The SIINFEKL peptide derived from chicken ovalbumin (OVA) has been used as a gold standard method to study antigenic peptides for the direct or cross-presentation MHC class I pathways. Initial studies with OVA used as an antigenic peptide have been focused on proteasome degradation mechanism and little is known about autophagy influence in ovalbumin derived peptide presentation via MHC class I pathway[93,94]. Strikingly, during this Ph.D. study, we observed that OVA-derived peptides were significantly reduced upon autophagy inhibition by Atg5/12 siRNA, without showing any visible aggregates of OVA protein and confirming that it was not related to an effect of siRNA methodology per se in the MHC class I functionality. Importantly, indirect measurement of the free SL8 in the murine H2-Kb transfected molecule in H1299 cells co-culture with OT1-$CD8^+$ T cells did not show any difference during Atg5/12 knock down. Secondly, when we measured endogenous MHC class I (Kb) of murine MCA-205 cells or HLA-ABC molecules in human H1299 cells during Atg5/12 siRNA there was no difference in MHC class I cell surface location under Atg5/12 siRNA compared with the scramble. Furthermore, the presentation of SL8 fused to EBNA1 was not affected by autophagy knock down. Hence, these observations show that Atg5/12 knock down, does not affect the MHC class I pathway per se.

In line with our results, Liu and colleagues implicated OVA as a substrate for autophagy and showed that mice immunized with OVA caused an allergic reaction and induced activation of autophagy accompanied by a relative increase of LC3 II compared to LC3 I in eosinophils cells from lung tissues[95]. Our study shows an autophagy-dependent presentation of OVA for the direct class I pathway, but other studies have associated autophagy with cross-presentation. For example, it was found that the high accumulation of OVA in the phagosome, triggered the cross-presentation of the OVA derive peptides in a TAP-independent manner, partially due to the processing by the cysteine protease cathepsin S in the lumen of the phagophore[96]. Another example is

the study done by Tabachnick and colleagues that demonstrated that polyQ fused to OVA was shown to be presented to the MHC class I pathway following injection into mice[86].

EBNA1 is a viral protein expressed in all Epstein-Barr virus (EBV)-infected cells[62], which bears a repetition disorder called GAr known to cause aggregates[77,78]. EBV needs to ensure that EBNA1-expressing cells are not detected and destroyed by the immune system. It has been previously proved that the GAr sequence has a translation-mediated control in cis on EBNA1 protein expression[68]. Essentially, EBV uses this mechanism to minimize EBNA1 synthesis to evade the MHC class I pathway and $CD8^+$ T cell recognition but keeps sufficient EBNA1 expression to maintain the virus alive[97]. However, although autophagy has been shown to contribute to the processing of EBNA1 for the MHC class II pathway[79], our data suggest that this mechanism is not involved in the production of EBNA1-derived substrates for the MHC class I pathway. This raises the possibility that EBNA1 has evolved a mechanism to evade autophagy-mediated class I- but not class II-restricted antigen presentation. An idea that is supported by the fact that GAr fused to OVA prevents OVA from being presented via autophagy as we have evidenced in this study. This suggests that evasion of autophagy-mediated MHC class I-restricted antigen presentation is another mechanism employed by viruses to remain undetected by the immune system.

By inserting *c-myc* 5' UTR upstream of GAr-carrying constructs we could override its translation inhibitory capacity and show that protein expression levels have little effect on GAr-mediated evasion of antigen presentation via autophagy. This points towards a more selective mechanism for how peptide substrates are presented to the class I pathway by autophagy and have interesting implications for understanding not only the cell biological aspects of how proteins are processed by autophagy, but also in terms of disease. As shown by animal studies, which have suggested that the inflammasome plays a role in Alzheimer's disease, indicating that the immune response can play a role in the etiology of neurological disease associated with protein aggregates[98,99]. It is an interesting possibility that selective autophagy-dependent processing of cellular disease-associated substrates for the MHC I and II pathways could exist. Further studies using more substrates and deeper analysis of autophagy pathways shall confirm, or not, this possibility. Nevertheless, published new data have revealed protein aggregates clearance by autophagy in polyglutamine disorders such as

Hungtington disease[56]. Qin and colleagues showed that autophagy inhibition reduced cell viability and increased Huntingtin protein aggregation[57].

OVA protein did not show any visual sign of aggregate formation but showed an Atg5/12-dependent antigen presentation. Fusion of the PolyQ sequence to OVA resulted in the formation of aggregates but this had a little significant effect on Atg5/12-dependent antigen presentation. Moreover, we were not able to detect aggregates caused by GAr in GAr-OVA or EBNA1 expressing cells, although it is known that the disordered gly-ala domain affects protein folding and unfolding[81]. Nevertheless, our antigen presentation assays indicate that GAr-OVA or EBNA1 are not substrates for autophagy in the MHC class I pathway.

The constructs that we used carry the PolyQ and the GAr sequences in the N-terminus of the OVA reporter construct and even though the GAr is located inside the EBNA1 protein, it is likely that GAr and PolyQ location can affect how substrates are presented to the class I pathway via autophagy. In recent studies in available databases, it was noted that PolyQ appears often at the c-terminus of coiled-coil regions. Schaefer et al 2012 demonstrated that PolyQ serves to increase the length of the coiled-coil to extend to a neighboring coiled-coil region and facilitate its interaction with another protein, causing abnormal interactions and protein aggregation[55]. In our study, PolyQ was fused to the N-termini and did indeed cause aggregates but it cannot be ruled out that the location of the PolyQ within the protein can have an effect on how the substrate is processed by autophagy.

Proteasome as alternative processing machinery

Generally, the proteasome is the principal degradation organelle in the MHC class I pathway. For this reason, we wanted to determine if the degradation of the different antigenic substrates was processed exclusively by autophagy or not.

We observed a significant autophagy dependence of OVA-derived antigenic peptides, but also on the proteasome. Although we are aware that antigen presentation upon proteasome inhibition showed very low levels of OT1 $CD8^+$ T cell proliferation in response to OVA derive antigenic peptides as it is usually observed, because of our fixation strategy. Interestingly, we have observed protein accumulation only during proteasome and not during autophagy inhibition. This result suggests that the majority of OVA full-length protein is degraded by the proteasome and not by the autophagy

pathway. However, OVA-derived antigenic peptide presentation was affected by both pathways. This observation is explained by the fact that OVA protein is highly ubiquitinated[92]. Some work carried out several years ago has found that reducing the ubiquitin-ligation by the inducible inactivation of the E1 enzyme in ts20 cells greatly decreased OVA antigen presentation[92]. Ubiquitination mechanism that serves as targeting signal for degradation either by proteasome or autophagy[90,100].

The challenge of measuring murine H2-Kb directly with antibodies

Our model of antigen presentation was based on human H1299 cells transfected with H2-Kb to be recognized by OT1-CD8+ T cells. To demonstrate that H2-Kb cell surface localization was not affected by the Atg5/12 siRNA, we measured OT-1 CD8+ T cell proliferation by adding the synthetic SL8 peptide to the co-culture. Given that this experiment was an indirect measurement, we tried to estimate the H2-Kb cell surface by Flow Cytometry. However, we observed that H2-Kb transfected into H1299 cells did not give any positive signal (**Annexes supplementary figure 3**). We may hypothesize that the double chain structure of the H2-Kb transfected molecule might have one chain human and the other murine, explaining why the murine anti-H2-Kb does not bind.

As a result, we instead measured endogenous MHC class I membrane localization in the human H1299 and murine MCA-205 cells using anti-HLA ABC and anti-H2-Kb, following Atg5/12 siRNA treatment. We confirmed that cell surface localization of the MHC-I molecule was not affected by the Atg5/12 down-regulation in either species. Of note, MCA-205 cells had a lower H2-Kb positive population (60%) than H1299 cell's HLA-ABC positive population (80%) because the murine antibody only recognizes one class of H-2 the K.

# XII. Concluding Remarks – PART 1

After the discovery of autophagy-related proteins, many studies have found the importance of autophagy in human health. However, there is still plenty of discoveries to be made in the autophagy field. For example, recently it has been proposed that certain types of autophagy can take place without Atg 5/7 intervention in mice[101].

My Ph.D. study aimed to evaluate autophagy (via Atg5/12) as an antigenic peptide processing mechanism for the MHC class I pathway.

This work has proved that autophagy via Atg5/12 can interfere with the availability of antigenic peptide sources for the MHC class I pathway. Demonstrated by the downregulation of OVA-derived peptides in antigen presentation upon Atg5/12 siRNA.

This study suggests that protein aggregation is not a key feature to provide antigenic peptides for the MHC class I pathway via Atg5/12-dependent autophagy. But the fact that we observed substrate-specific processing suggests that other mechanisms select which substrates shall be presented or not, for the class I pathway. It is interesting to point out that EBNA1 is presented to the class II pathway via autophagy

We have shown that autophagy is not involved in the production of EBNA1-derived substrates for the MHC class I pathway and that the GAr sequence prevented OVA from being presented via autophagy. This led us to suggest that EBNA1 has evolved a mechanism to evade autophagy-mediated class I, but not class II, antigen presentation.

Taken together, this study shows a substrate-specific presentation of peptides via autophagy that is selective for the MHC class I pathway. It has interesting implications for viral immune evasion and for inflammatory reactions associated with disease in which cellular proteins are processed by autophagy.

# Introduction – PART 2

## XIII. The classical conception of peptides derived from the degradation of the full-length protein comes into question

The median protein half-life is approximately 46 hours until it reaches obsolescence and is degraded by the proteasome. But this did not fit with observations on the presentation of viral antigenic peptides, which took much less time. Therefore, the scientific community started to challenge the theory that antigenic peptides used for the MHC class I presentation come from the degradation of full-length proteins by the proteasome. Furthermore, if we think carefully, the abundance of the proteome is much higher than the immunopeptidome (repertoire of peptides presented by MHC-I molecules). Each cell expresses approximately $10^4$ to $10^5$ MHC-I molecules on its cell surface. Thus, if all proteome peptides have access to the class I pathway, the sensitivity of detecting viral or tumor neoantigens would be much lower[6,102,103].

These and other observations prompted our group to test to which extent antigenic peptides originate from full-length protein degradation via the proteasome pathway. The method used was based on the NFkB pathway. Activation of NFkB starts with an extracellular stimulation, such as the TNF-α receptor, that results in IkB phosphorylation that triggers ubiquitination and degradation via the proteasome. This causes the release of NFkB and its transfer to the nucleus. Introducing a mutation on IkB prevented phosphorylation and, therefore proteasomal degradation. When an antigenic peptide OVA257-264 (SIINFEKL, SL8) was fused to the wild type IkB or the mutated IkB, it was shown that both constructs synthesized a similar amount of SL8 peptide. When cells were treated with TNF-α, they observed that the wild-type IkB was rapidly degraded and, as expected, there was no effect on the mutant IkB. Importantly, despite the rapid degradation of the wild type IkB, there was no effect on antigen presentation. This shows, that the degradation of full-length protein via the proteasome is not a source for the production of antigenic peptides[104]. Interestingly, using a different approach, they found that transfected capped ovalbumin mRNAs produced full-length proteins up to eight hours after translation, while antigen peptides from the same mRNA were only produced for 2 hours[104]. Other studies by other groups also supported this statement, such as Yewdell et al., who engineered a recombinant vaccinia virus that produced different cytosolic peptides with high affinity to mouse class I H-2K$^b$ and GFP tagged. They showed that those antigenic peptides derived

from the vaccinia virus competed with each other for the MHC class I binding but not with peptides derived from full-length protein[105].

In this context, a growing number of studies have evaluated the relationship between the proteome and the immunopeptidome. Many studies have observed that antigenic peptides were found at a high rate, while the protein source remained low[106,107]. Interestingly, one study compared the MHC-I peptidome with the proteome of the same culture cells, using pulse-chase experiments based on capillary chromatography and Tandem mass spectrometry (MS). They have uncovered that the immunopeptidome and the proteome only have approximately 6% of correlation[108].

There are potentially two theories proposed to explain this poor correlation between the proteome and the immunopeptidome.

1) Peptide splicing by the proteasome as a source of MHC class I antigenic peptides

The first theory suggests that the poor correlation is due to the ligation of two peptides by the 20S core of the proteasome in a mechanism called peptide splicing[20]. In 2004, Hanada et al. observed that $CD8^+$ T cells were specific for a renal carcinoma peptide composed of two fragments distant in the original FGF-5 protein[109]. Later, this finding was supported by another study which found also $CD8^+$T cells activation to non-contiguous fragments of the melanoma differentiation antigen gp100[110]. They have demonstrated that the production of this peptide involves the excision of four amino acids and splicing of the fragments[110]. Furthermore, the authors reproduced the experiment in vitro with isolated proteasomes and observed that splicing occurred by transpeptidation involving an acyl-enzyme intermediate of the proteasome[110]. However, this theory is questioned for two reasons. First, biochemistry assays argue that transpeptidation happens in an aqueous solution and is a reaction very hard to obtain because the water will compete with the peptide substrate. Thus, peptide splicing is very inefficient and unlikely to occur. Second, new studies questioned the bioinformatics employed in these studies[111].

2) Alternative mRNA translation as a source of MHC class I antigenic peptides

The second theory proposed that peptide substrates originate from a specific mRNA translation event. In a major advance in 2013, Croft et al. showed a correlation between

protein synthesis and peptide generation. Demonstrating that antigenic peptides are newly synthesized polypeptides. They used MS selection-reaction monitoring and evaluated eight different peptides. For the early vaccinia virus protein, peptides were detected on the first time point evaluated at 30 minutes. Strikingly, for almost all peptides studied the levels remained the same or declined when the synthesis of different genes was downregulated[112]. Moreover, previous studies have revealed that specific translation mechanisms synthesizing antigenic peptides differ from the canonical translation. There are alternative translation processes that potentially have an important role in the generation of antigenic peptides. For example, some studies have observed an alternative translation mechanism that synthetizes polypeptides with a very short half-live [102,103]. These observations could explain why there is a production of viral antigenic peptides before the expression of the viral protein in the host cell [102,103]. In a 2015 study, Laumont and colleagues searched MHC class I antigenic peptides on the six-frame translation of the B-cells transcriptome. To determine antigenic peptides derived from non-canonical reading frames, they performed high-throughput MS. The authors found that approximately 10% of MHC class I antigenic peptides originate from noncoding genomic sequences or exonic out-of-frame translation[113]. More recently, new techniques such as ribosome profiling have moved forward our knowledge about proteome. Ribosome profiling has revealed that ribosomes can be detected in many regions of the transcriptome previously thought to be noncoding including 5' UTRs and long noncoding RNAs. This opened the door to new studies that have found antigenic peptides synthesized by a cryptic translation pathway[102,103].

## XIV. Types of antigenic peptide sources in the MHC class I pathway

Over the years scientists have classified the sources of endogenous antigenic peptides using the time of degradation of the precursors as criteria. Therefore, they have classified the sources of antigenic peptides into 1. Retirees (stable proteins degraded by the proteasome with a general turn-over of approximately two days). 2. Rapidly degraded polypeptides (RDPs) which are much faster degraded than retirees and are composed of three subcategories: defective ribosomal products (DRIPs), very short-life proteins (SLiPs), and pioneer translation products (PTPs)[102,114].

- DRIPs

Initially, DRIPs were categorized as unstable or immature ribosomal products rapidly degraded after synthesis. They were thought only to be misfolded proteins or prematurely terminated proteins. Then, an increasing number of studies have revealed more exceptions where the peptide translation event has occurred. Therefore, the DRIPs conception has evolved, and now there is more evidence showing that antigenic peptides can derive from alternative mRNAs, ribosomal frameshifting, downstream initiation on bona fide mRNAs, tRNA-amino acid misacylation, or transcription errors[107].

- SLiPS

SLiPs are usually subunits of multiprotein complexes that require binding to a partner to achieve a stable conformation. If they do not find the appropriate partner in a short period they are quickly degraded[107,115]. For example, ubiquitinated short-lived proteins[116].

- PTPs

PTPs are antigenic peptides products derived from pre-spliced mRNA synthesized through pioneer round of translation in the nucleus[104,114,117].

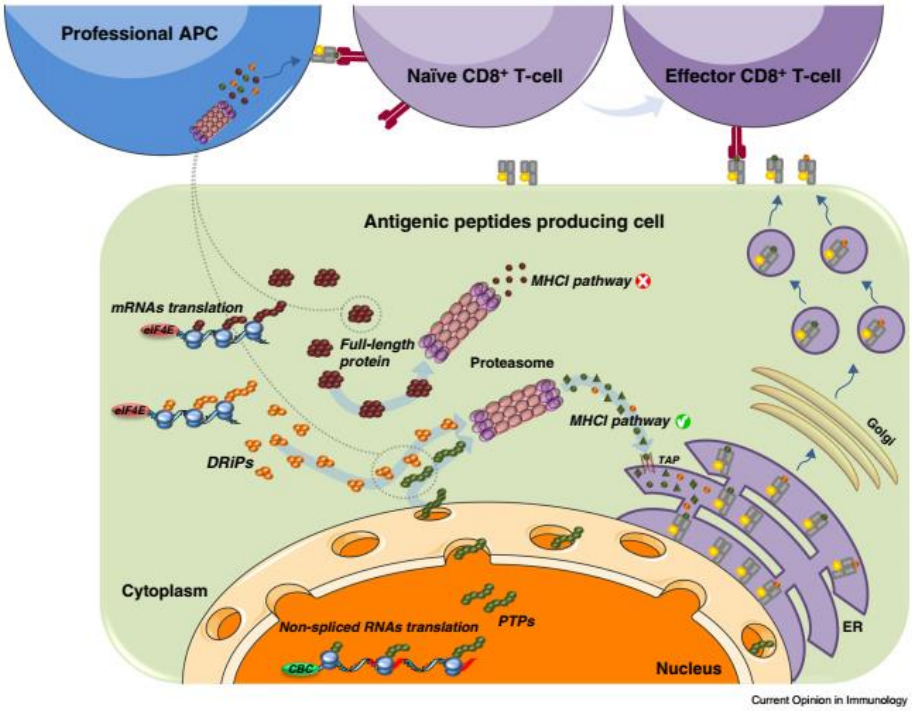


**Figure 1. Major Sources of antigenic peptides for the MHC class I pathway.** Full-length proteins or retirees degraded by the proteasome were thought to be the source of antigenic peptides for the MHC class I pathway. However, new reports have discovered that defective

ribosomal proteins (DRiPs) and pioneer translation products (PTPs) are the major sources. Once PTPs or DRiPs are synthesized in the nucleus or the cytoplasm. They reach the proteasome to be further processed. The peptide products are then translocated to the ER. Within the ER the peptide binds to the MHC class I and is transported to the cell membrane. A previous study by Duvallet et al 2016 has shown that PTPs from tumoral cells are transported to antigen-presenting cells (APC) through exosomes, serving as sources for cross-presentation[107,118,119](Image taken from Apcher et al 2016)[114].

## XV. Alternative mRNA translation as a source of MHC class I antigenic peptides

### XV.A Antigenic peptide synthesis by alternative translation initiation

Shastri N. was one of the first to present proofs of cryptic translation products used for MHC class I antigenic peptides. Using antigen-presenting cells transfected with cDNA constructs coding OVA257-264 (SIINFEKL, SL8) with variations in the translation initiation codons, he found that besides ATG, other codons such as ATT, ACG, CTG, GCG, TGG, and GAT still were able to activate $CD8^+$ T cells in ovalbumin transfected cells. However, he and his team realized that the SIINFEKL peptide generated from alternative codons in the cell was much lower than the concentration of ATG SIINFEKL peptide[120]. They later confirmed these previous findings using a different immune epitope detection system called JAL8/$K^b$. In this publication, they went further, showing that these cryptic antigenic peptides were not a subproduct of replication or transcription errors. Interestingly, they observed that these antigenic peptides could use the CUG coding for leucine as a start codon using High-pressure liquid chromatography (HPLC) analysis[121].

Later, Shastri's team tried to understand the mechanism involved in the translation initiation using CUG as a start codon. In 2004, They tested if their alternative start codon CUG required the standard eukaryotic translation initiation factor 2 (eIF2α). To answer this question, they transfected HeLa cells with the YL8 vector containing an immunogenic peptide bearing CTG or ATG initiation sequences. After, cells were treated with sodium arsenite to induce the phosphorylation of eIF2α and prevent canonical translation. Surprisingly, when they evaluated the antigen presentation of those cells, they realized that $CD8^+$ T cells still were activated. They proposed that eiF2α might not be required for the CUG translation initiation[122]. Later in 2012, Shastri et al. published new information showing that CUG translation indeed was mediated by leucine-tRNA. In this publication, they transfected cos 7 cells with YL8 and blocked

the binding of the met-t-RNA using a synthetic inhibitor. They observed that under these conditions, $CD8^+$ T cells were still activated[123].

Moreover, the work of Shastri not only showed antigenic peptide synthesis from alternative codon initiation. He also revealed that the 3' untranslated region of mRNA could produce antigenic peptides and shape the TCR repertoire in mice[124].

Interestingly, the production of MHC class I antigenic peptides via alternative translation is also reported in viruses. A recent study used SIINFEKL antigenic peptide fused to influenza M1-M2 sequences and evaluated the MHC-I antigen presentation by infected cells upon splicing inhibition. They observed a complete downregulation of mRNA and protein synthesis. Interestingly, $K^b$-SIINFEKL complexes were still highly expressed. This result suggested an alternative non-canonical initiation in the reading frame. Importantly, in the same study, they inserted synonymous changes in CUG codons in the M1-M2 sequences upstream of SIINFEKL and treated cells with splicing inhibitors. They found a significant reduction of MHC-I antigen presentation compared to the non-mutated M1-M2 sequence fused to SIINFEKL[102].

### XV.B Antigenic peptides derived from intron sequences

Antigenic peptides have also been identified to originate from intron sequences. A study carried out in 1995 observed that $CD8^+$ T cells recognized a human melanoma antigen that is also expressed in normal cells. They performed a PCR comparing the antigenic peptide sequence in normal and melanoma cells. They identified a point mutation that replaced serine with isoleucine at position 5 of the antigenic peptide in both cells. Strikingly, the coding sequence of this antigenic peptide came from a point mutation located in an intronic sequence[125].

### XV.C Antigenic peptides derived from the pioneer round of translation

To control the quality of mRNA production and destroy abnormal mRNA, the cell uses a post-transcriptional mechanism called nonsense-mediated decay (NMD) during ribosomal scanning. Generally, eukaryotic mRNAs have an average of over 7 to 8 splicing-generated exon-exon junctions. NMD is triggered when a premature termination codon (PTC) is found in 50 to 55 nucleotides upstream of an exon-exon junctions[126].

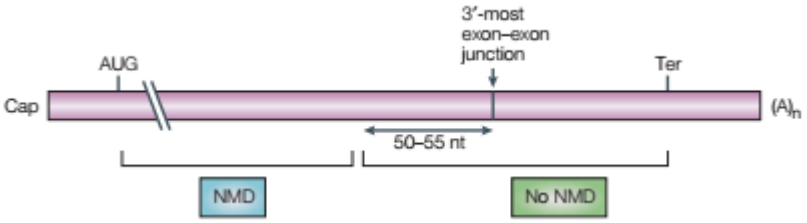


**Figure 2. Nonsense-mediated decay mechanism.** NMD is triggered when a stop codon is located more than 50-55 nucleotides upstream of an exon-exon junction of the mRNA(blue site)[127](Image taken from Maquat et al 2004)[126].

When mRNA is transcribed, the first round of translation occurs, called the “pioneer round of translation”. This translation is triggered when pre-mRNA is bound to cap-binding protein (CBP) heterodimer CBP80-CB20 at the 5’ cap. Then after splicing, the poly-A binding protein (PABP2) is associated with the 3’ poly-A tail and the exon-exon junction complex remains attached to the mRNA. In turn, the exon-exon junction complex recruits the NMD factors, forming the pioneer translation initiation complex. Next, one or more ribosomes translate mRNA during the pioneer round. However, it is unclear if the pioneer round of translation happens in the nucleus or cytoplasm. Since, the CBP80-CB20 complex binds to the cap soon after transcription and during splicing, which is a nuclear process. The pioneer translation mechanism ends with the exchange of the pioneer translation initiation complex with the eIF4E at the 5’ cap and PABP1 at the 3’ poly (A) tail leading to the canonical translation or it ends with the finding of PTC leading to NMD[126].

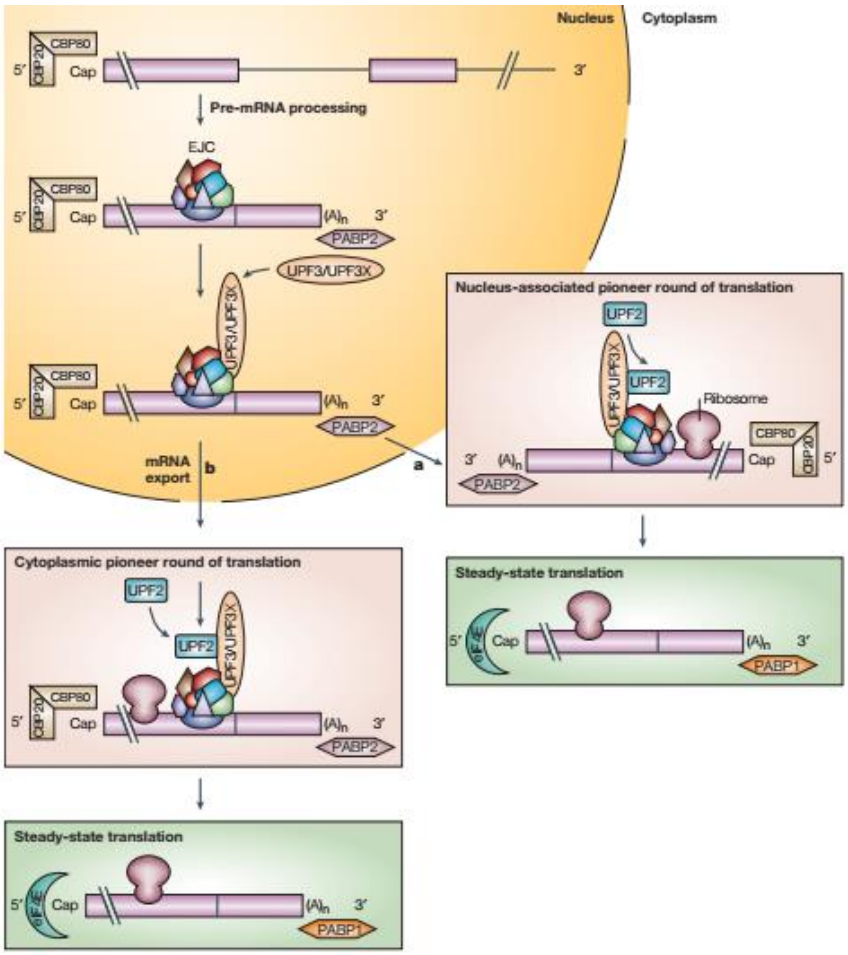


**Figure 3. Pre-mRNA splicing, pioneer round of translation, and steady-state translation.** Pre-mRNA binds to the CBP80 and CBP20 at the 5' cap; Once spliced the 3' poly(A) binds PABP2 and the exon junction complex (EJC) remains upstream of the exon-exon junction. The EJC attracts the UPF3X, which in turn recruits UPF2. This complex is subjected to a pioneer round of translation either in the nucleus or in the cytoplasm. Then, depending on the mRNA, steady-state translation or NMD begins[128]. (Image taken from Maquat et al 2004)[126].

To evaluate the implication of the pioneer round of translation in the generation of antigenic peptides, Fahraeus's team has engineered a construct in which the OVA257-264 (SIINFEKL, SL8) peptide sequence was inserted in the β-globin gene. The SL8 sequence was located in exon 1 of the β-globin gene, just before a PTC located 53 nucleotides upstream of the exon junction complex in exon 2. Evaluating RNA levels, they observed that β-globin RNA was degraded efficiently, indicating the NMD induction. Interestingly, the SL8 immune epitope presentation was very efficient, almost like the presentation levels of the same construct that lacked PTC. In this same experiment, they also used the β-globin construct bearing the PTC at 53 nucleotides upstream of the exon junction complex in exon 2, but having the SL8 after the PTC. They observed no SL8 antigen peptide presentation. Together these results

demonstrated that the production of antigenic peptides can be associated with the pioneer round of translation that precedes the NMD process. Moreover, to understand better how these antigenic peptides translation occurs, they assessed the role of some initiation factors. Using inhibitors targeting eiF4E association to the mRNA cap structure and also to the eiF4G that is necessary for the binding of eiF4E and the CBP heterodimer that initiate ribosomal quality control scanning. They showed that eiF4E inhibition did not affect antigen presentation, while eiF4G inhibition decreased significantly. This result suggested that antigenic peptide synthesis is governed by a different translation mechanism. They named these antigenic peptides as pioneer translation products (PTPs)[104].

Fahraeus's team has continued the research using these peptides, demonstrating that PTPs are synthesized in the early steps of the mRNA maturation and before introns are spliced out. The innovative idea of introducing an immune epitope sequence in the introns, allowed them to probe the possibility of immune peptides derived from pre-spliced mRNAs. Interestingly, they demonstrated that PTPs are synthesized in the nucleus. In this work, they employed the ability of puromycin to be incorporated in the nascent peptide sequence translated by the ribosome. Next, they transfected cells with a β-globin construct carrying an HA tag in the intron sequence. Using antibodies against puromycin and HA they observed the colocalization in the nucleus[119].

### XV.D Immunoribosomes

Ribosomes are complex and highly conserved machinery. It consists of four ribosomal RNA (rRNA) species and 80 ribosomal proteins (RPs)[129]. The eukaryotic 80S ribosome consists of a small 40S subunit and a large 60S subunit. The 40S subunit is composed of the 18S rRNA and 33 different RPs designated with the letter S for the small subunit followed by their number. In contrast, the 60S subunit consists of 25S, 5,8S, and 5S rRNA together with 47 RPs designated by the letter L for the large subunit followed by the number [130]. The ribosomal subunits are assembled in the nucleolus, where the new modified and coded rRNA bounds to the RPs. Those have been translocated from the cytoplasm to the nucleus after their synthesis. Once they are assembled, the two ribosomal subunits are then translocated to the cytoplasm, where they associate and carry out protein synthesis forming polysomes[131]. Structural studies on ribosomes claimed that rRNA is responsible for the ribosomal structure, the location of the tRNA over the mRNA, and their catalytic activity. Thus, rRNA is located in the core of the

ribosome, and RPs are located on the surface[131]. The classical view of RPs claims that their functionality is to stabilize the RNA inside the ribosome[132]. However, it is intriguing that the translation machinery is composed of RPs with high heterogeneity. This poses intriguing questions if there is a functional reason for the RPs diversity. A new hypothesis suggests that the mRNA 40s subunits binding and scanning is influenced by RPs composition. Interestingly, other studies suggest that its importance is linked to the differences in RPs over different tissues or during embryonic development. Some others have identified differences in RP composition and the number of ribosomes bound to each mRNA. According to some studies, RPs seem to be non-essential in mammalian[102].

More recent evidence[133] suggests that RPs can regulate MHC class I peptide generation. Wei and colleagues knocked down each of the 80 RPs and identified RPs that regulates MHC class I antigenic peptide generation, but did not alter source protein expression. The knock down was carried out in cells infected with a recombinant influenza A virus expressing SIINFEKL fused to the neuraminidase or in steady-state cells. They screened all RPs and selected the ones with the highest effects on MHC class I expression or viral/peptide MHC-I complex generation, without affecting the overall translation. They found five possible candidates. Then, they evaluated the effect on the transcriptome by microarray and selected only 3 RPs with a higher resemblance to the scramble control cells. They discovered that in infected cells, depleting RPL6 decreases ubiquitin-dependent viral peptide presentation, while the RPL28 depletion increases both ubiquitin-dependent and -independent peptide presentation. In uninfected cells, depletion of RPS28 increased peptide supply. Even though it is the first evidence revealing the potential RPs specialization related to antigen peptides production, it still unknown if the heterogenicity of the RPs is associated with the different variants in the alternative translation mechanism responsible for antigen peptide production[133].

### XV.D Nuclear Translation

The first studies of nuclear translation were reported in 1954. Allfrey and colleagues observed that nuclei isolated from the thymus (primary lymphoid organs from the immune system) incorporated the radiolabeled $C^{14}$-alanine into nuclear proteins. It was also shown that ribonuclease treatment did not affect the uptake of $C^{14}$-alanine on isolated thymus nuclei[134].

A cutting-edge paper of 2001, using the lysyl-tRNA tagged with biotin has found that biotin immunolabeling was observed mostly in the cytoplasm but also in the nucleus. Surprisingly, electron microscopy evaluated Immune gold labeling of biotin-lysine-tRNA and Br-RNA. They observed both signals associated inside the nucleus. Moreover, RPL7 Immune gold labeling was also found together with biotin inside the nucleus. These results suggested that coupled transcription and translation can occur within the nucleus[135,136].

Two studies have tried to determine whether antigenic peptides can be synthesized in the nucleus by nuclear translation. Both studies have employed similar strategies to block the mRNA export from the nucleus. The first study used the RNA polymerase inhibitor called DRB on cells infected with the influenza A neuraminidase fused to SIINFEKL. They observed that indeed the neuraminidase mRNA was accumulated in the nucleus after DRB treatment. Inhibiting neuraminidase protein translation, but surprisingly $K^b$-SIINFEKL presentation was detectable [137]. Likewise, another work in 2013 used the human immunodeficient virus (HIV) RRE-REV machinery, which is used by HIV to promote the nuclear export of transcripts and efficiently translate viral particles. Generally, in infected cells host ribosomes synthesize REV proteins. These proteins would enter the nucleus and bind the RRE segment in the newly translated HIV pre-mRNA. Then, the mRNA-REV complexes interact with nuclear transporters and trigger the export of the unspliced HIV RNA. This system was used[117] to address the hypothesis that RRE-REV machinery would induce an export of unspliced RNA, inhibiting the nuclear translation of antigenic peptides. Indeed, when they measured the antigen presentation in cells expressing the SL8 peptide overexpressing REV protein, they observed a progressive decrease in antigen presentation[117].

Furthermore, a new improved methodology has been used to visualize nuclear translation sites. Brogna and colleagues detected ribosomal subunits at the transcription sites of *Drosophila salivary* chromosomes, using chromosomal immunostaining and in situ hybridization[138]. Another study used the ribopuromycylation method (RPM), which is based on the visualization of the puromycin entrance in the immobilized ribosome induced by the antibiotic treatment. They observed RPM signals in the nucleoplasm and nucleolus[139]. Then, with another approach, Al-Jubran and colleagues fused halves of fluorescent proteins to RPs. When RPs were closed, a strong fluorescence appeared. They observed that S18 and L18 RPs signal was

located in the cytoplasm, but also clearly in the nucleolus of cultured cells and fly tissues[140].

Also, imaging evidence was obtained by Apcher et al[117] who visualized HA-tagged signals in the nucleus from cells transfected with β-Globin bearing HA-tag sequence in the intron 1. They further confirmed this observation with the visualization of the interaction between puromycin or RPS6 with HA through proximity ligation assay (PLA) in the nucleus.

Even though nuclear translation remains controversial, over the years new studies have agglomerated novel evidence demonstrating that nuclear translation and synthesis of antigenic peptides for the MHC class I pathway. Although, it remains uncovered the translation factors and cellular machinery engaged in nuclear translation.

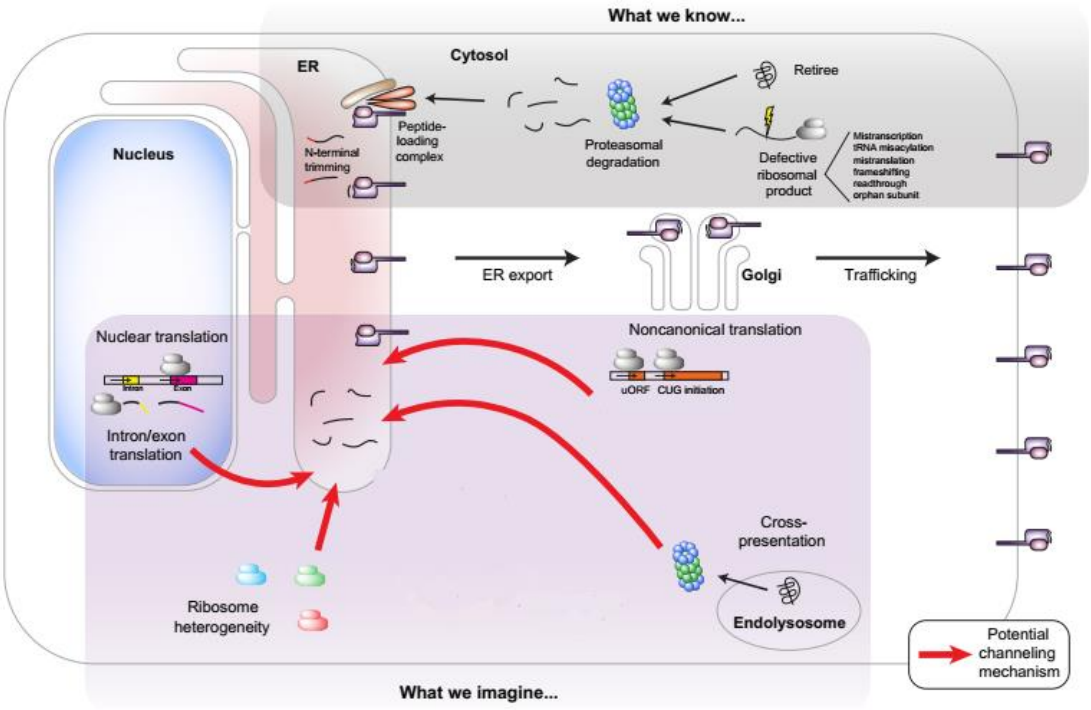


**Figure 4. The classical vs new perspectives for the MHC class I pathway.** A growing body of studies has demonstrated different approaches and theories that explain the selectivity and rapid MHC class I antigen presentation. Antigenic peptides from pre-spliced mRNA (PTPs), DRIPs, and non-canonical translation, could be associated with specialized ribosomes responsible for these newly synthesized peptides used for MHC-I molecule[102,107,114](Image adapted from Yewdell et al 2019)[103].

# XIV. Aim of my Ph.D. study – PART 2

Previous studies have demonstrated that some MHC class I antigenic peptides can be originated from pre-spliced mRNA, these peptides are called PTPs. In this Ph.D., we attempted to provide more evidence using different approaches to support these novel findings and elucidate the riboproteome responsible for PTPs synthesis with a first preliminary approach.

# XV. Material and methods – PART 2

*Plasmids*

The human/murine pCDNA3-β-Globin SL8-Exon1 and human/murine pCDNA3-β-Globin SL8-Intron1 constructs[104,117], and the GFP was obtained as described previously [141]. The murine pCDNA3-β-Globin SL8 Intron2 was a gift from Dr. Rodrigo Martins.

The SL8-GFP was prepared as follows. The SL8 insert was made by annealing the Forward: oligo 5' GGATCCATGTTCAGGGTGAGTCTGATGGGCACCTCCAGTATAA TCAACTTTGAAAAACTGTGGGTTTCCTTCCCCTGGCTATTCTGCGAATTC 3' containing BamHI and EcoRI sites and the Reverse: oligo 5' GAATTCGCAGAATAG CCAGGGGAAGGAAACCCACAGTTTTTCAAAGTTGATTATACTGGAGGTGCCCAT CAGACTCACCCTGAACATGGATCC 3'. containing BamHI and EcoRI. The fragment was cloned into the 5'UTR digested pCDNA3-GFP construct.

*Cell culture and Transfection*

H1299 cells (Human non-small cell lung carcinoma) were cultured in RPMI-1640, supplemented with 10% fetal bovine serum (FBS), 2mM L-glutamine, and 1% Penicillin- Streptomycin. HEK 293 cells (Human embryonic kidney) were cultured in DMEM supplemented with 10% fetal bovine serum (FBS), 2mM L-glutamine, and 1% Penicillin- Streptomycin. For antigen presentation experiments, cells were cultured in 6 wells plates ($8x10^4$ cells/well) at 37˚C with 5% $CO_2$. The day after seeding, transfections were performed using 3 µl of Gene Juice reagent according to the manufacturer's protocol (Merck Bioscience). Cells were co-transfected with 0.5 µg of murine MHC class I molecule Kb and 1 µg of β-Globin SL8-Exon1, β-Globin SL8-Intron1, and β-Globin SL8 Intron 2 cDNA. In all antigen presentation assays, 1 µg of an OVA cDNA was used as positive control and the same quantity for the empty vector (E.V) as a negative control. For microscopy experiments, cells were cultured in 24 wells plates ($3x10^4$ cells/well) at 37˚C with 5% $CO_2$. The day after seeding, transfections were performed as mentioned before. Cells were transfected with 0,5 µg of murine β-Globin, SL8-GFP, GFP, and E.V constructs. For polysome fractionation, HEK 293 cells were cultured in a 10 cm dish ($1x10^6$ cells/well) at 37˚C with 5% $CO_2$. The day after seeding, transfections were performed as mentioned before. Cells were transfected with 2 µg of the murine β-Globin construct.

*Antigen Presentation assay: OT1 CD8+ T cells proliferation*

To determine the levels of antigen presentation, we used CD8+ T cells that express specific receptors to the OVA epitope, SIINFEKL, recognized by H-2 Kb. These CD8+ T cells were purified from OT1 transgenic mice expressing a transgenic TCR specific for SIINFEKL-Kb. Spleen and lymph nodes from OT1 transgenic mice were passed through a 70 µm cell strainer and red blood cells were lysed with ACK buffer treatment for 5 minutes. After several washes with PBS-FBS 5%, CD8+ T cells were negatively selected using a CD8+ T cell isolation kit (MACS Miltenyi Biotec) according to the manufacturer's instructions.

Two days after transfection, H1299 cells used as presenting cells were briefly washed with PBS, trypsinized, resuspended in splenocytes medium (RPMI-1640), supplemented with 10% (FBS), 4mM L-glutamine, 1% Penicillin-Streptomycin, 0.05 mM 2-Mercaptoethanol, and 5 mM HEPES) and seeded in 48 wells plates ($1.25x10^5$) cells per well with OT1-$CD8^+$ T cells ($5x10^5$). Antigen presentation was measured through the IL-2 release by activated CD8+ T-cell using ELISA.

*Quantification of IL-2 release by ELISA*

The day after co-culture, the release of IL-2 in the supernatant was quantified by ELISA using the Mouse IL-2 ELISA MAXTM Standard kit (Biolegend). This ELISA procedure is based on the sandwich method, which uses an anti-IL2 capture antibody and a detection antibody. Immunocomplexes were revealed by a colorimetric enzyme-substrate reaction using Avidin-HRP and TMB substrate. Finally, absorbance levels were quantified in a plate spectrophotometer (Fluo StarOptima) at 450 nm.

*Proximal Ligation Assay (PLA)*

H1299 cells were grown over sterile 22x22mm coverslips, transfected with murine β-Globin, SL8-GFP, GFP, and E.V constructs, and treated with [30 uM] Isoginkgetin (Merck) for 22 hours. The cells were fixed in 4% paraformaldehyde for 20 min before being permeabilized in PBS and 3% BSA containing 0,1% saponin. Primary antibodies- Rabbit FRVSLMGTS**SIIN** and Goat **FEKL**WVSFPWLFC (Eurogentec) were incubated in the same buffer overnight. After the cells were washed, PLA probes were added, followed by hybridization, ligation, and amplification according to the manufacturer's protocol (Duolink, Thermo Fisher). Then, we performed immunofluorescence using mouse anti-β Globin and Anti-mouse Alexa488. Coverslips were mounted on slides using slow fade diamond antifade mounting medium

(Thermofisher) with Hoescht. Slides were analyzed by confocal microscopy. PLA dots were quantified in H1299 cells with or without β-Globin immunofluorescence signal by a custom-made automated script in FIJI.

*Polysome Fractionation*

Five–fifty percent wt/vol linear sucrose gradients were freshly cast on SW41 ultracentrifuge tubes (Beckmann) using the Gradient master (BioComp instruments) following the manufacturer's instructions. H1299 or HEK 293 cells were transfected and treated on the same day with Isoginkgetin at [30µM] or [10µM] respectively. Twenty-two hours post-treatment, cells (with 80% confluency) were treated with cycloheximide 100 µg/ml for 5 min at 37 °C and then washed twice with 1× PBS (Dulbecco modified PBS, GIBCO) containing cycloheximide 100 µg/ml. Cells were then scraped, lysed with polysome lysis buffer (100mM KCL, 50mM HEPES KOH, 5mM MgCl2, 0.1% NP-40, 1 mM DTT, cycloheximide 100 µg/ml, pH 7.4) and spin at 2348xg for 10 minutes at 4°C. Lysates were then loaded on a sucrose gradient and centrifuged at 222228×g for 2 h at 4 °C in an SW41 rotor. Samples were fractionated using a Foxy R1 fraction collector (Teledyne ISCO) at 0.5 min intervals [80]. RNA purifications from fractions were performed using ethanol precipitation combined with RNeasy Mini Kit (Qiagen). RT and qRT-PCR were performed as described above using primers described in (**Annexes table 1**). The relative distribution of target mRNA was calculated using fraction 1 as reference according to Panda et al.[142].

*Statistics*

Data were analyzed by two-tailed unpaired Student's t-test or One sample T-test using GraphPad Prism 6 for Windows (GraphPad Software). Data shown are mean ± sd. of minimum three independent experiments. *P < 0.0332; **P < 0.0021; ***P < 0.0002; ****P < 0.0001; 0,1234 ns, not significant.

# XVI. Results - PART 2

Antigenic peptides for MHC class I are produced from pre-spliced mRNA

Previous studies in the lab have shown that antigenic peptides for the MHC class I pathway are synthesized mainly during the initial ribosomal scanning of pre-spliced mRNAs[104,143]. To study these unique antigenic peptides Apcher S. et al. employed the sequence from the β-globin gene and introduced the highly immunogenic SIINFEKL (SL8) peptide in either intron or exons.

In this Ph.D. study, we have used these same constructs of β-Globin containing chimeras half-murine and half-human (carrying the SL8 peptide in the exon 1 or intron 1) used by S. Apcher and an alternative construct composed of the murine β-Globin gene with the sequence of the SL8 peptide incorporated in the intron 2 (**Fig. 5A**).

Using these constructs, we evaluated the antigen presentation of transfected H1299 cells. Two days after transfection, presenting cells were co-cultured with OT-1 $CD8^+$ T cells and antigen presentation was determined using IL-2 quantification. As previously published data, we observed that the constructs with the SL8 sequences introduced in the intronic regions exhibited a significant IL-2 production by $CD8^+$ T cells compared with the empty vector that produced non. Of note, IL-2 levels were lower compared with SL8 sequences introduced in the exon of the β-globin gene or OVA. (**Fig. 5B**). These results support the idea that antigenic peptides for the MHC class I pathway can come from pre-spliced mRNA and potentially from pioneer translation products (PTPs).

PTPs peptides identification by PLA assay

Previous experiments done in the lab performed intron-derived peptides imaging using β-Globin sequence bearing the HA tag epitope in the intron 1[117]. They observed a specific signal in the nucleus of cells expressing this construct using anti-HA antibodies[117]. Nevertheless, this approach only showed us how PTPs could be visualized, assuming that their behavior would be similar to the HA-tagged intron. To visualize PTPs directly, we used polyclonal antibodies against the SIINFEKL peptide and flanking sequences from the murine β-Globin intron 2. Hence, immune peptides are rare and rapidly degraded we used proximity ligation assay (PLA). An assay that is based on the strong fluorescent signal emitted from a fluorescent oligos chain reaction between two antibodies in close proximity.

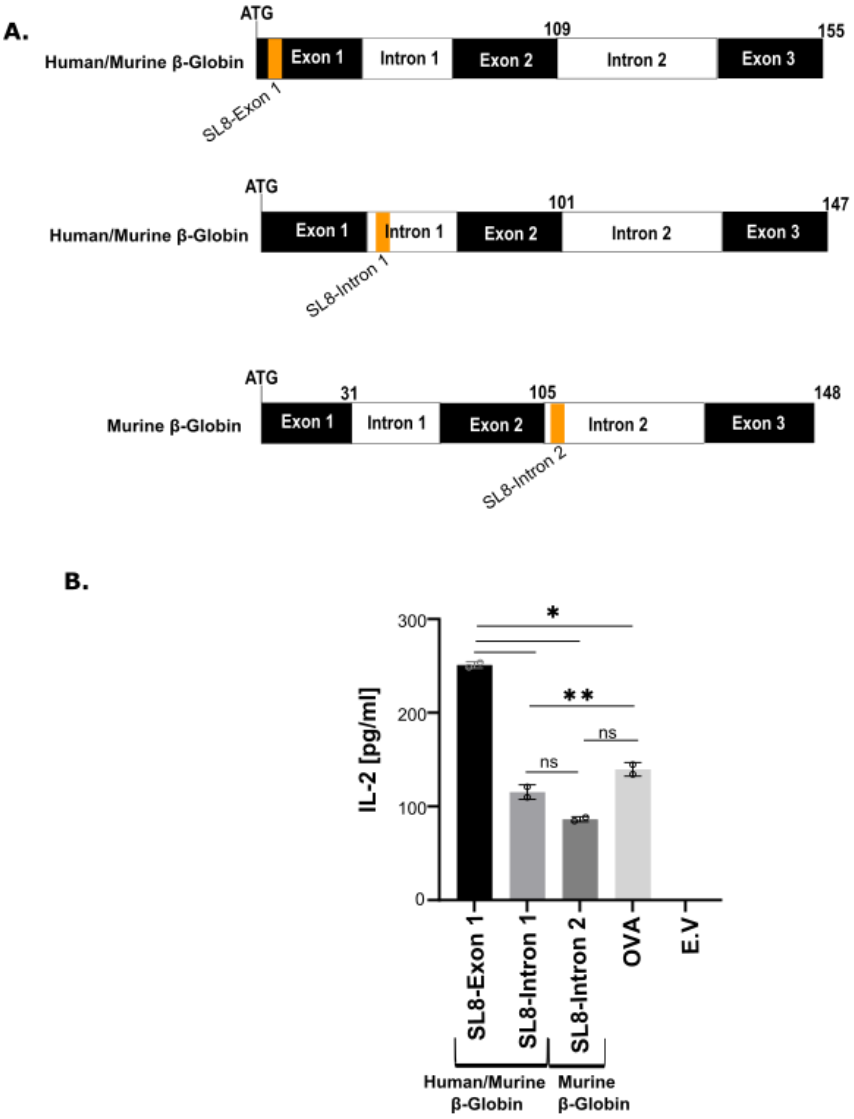


**Figure 5.** *Antigenic peptides for MHC class I are produced from non-spliced mRNA*. **A.** Cartoons illustrate Human/Murine or fully Murine β-Globin constructs. The exonic and intronic regions are depicted in A. SIINFEKL (SL8) peptide was introduced in Exon 1 or Intron 1 of Human/Murine β-Globin gene sequence or intron 2 of Murine β-Globin gene sequence. **B.** H1299 cells co-expressing MHC-I (Kb) and the SL8-containing constructs were co-cultured for 3 days with OT-1 CD8+ T cells. Culture media was collected and IL-2 concentration was measured with an ELISA Kit. Significant values were calculated using the multiple paired groups T-test. *P < 0.0332; **P < 0.0021; 0,1234 ns, not significant.

For the PLA experiments, we employed an antibody targeting FRVSLMGTS**SIIN** and another antibody against the **FEKL**WVSFPWLFC sequence from the *β*-globin gene construct (**Fig. 6A**). Transfected H1299 cells with the construct mentioned before were treated with the splicing inhibitor, Isoginkgetin, for 22 hours. Then cells were fixed and labelled with anti-β Globin and submitted to PLA assay. As expected, all the

transfected cells were positive for β-globin (in green). Equally, we could observe that the Isoginkgetin treatment partially impaired the synthesis of β-globin. Therefore, the cells treated with DMSO showed a higher green fluorescent signal corresponding to β-globin proteins when compared to Isoginkgetin-treated cells. (**Fig. 6B, on the top).** Importantly, PLA signals (white dots) were increased under Isoginkgetin treatment when compared with DMSO (**Fig. 6B, on the top**). Graphs represent the quantification of PLA dots comparing samples with or without treatment in transfected (green positive) or non-transfected cells (green negative) (**Fig. 6B, on the bottom**). The Quantification showed that Isoginkgetin treatment significantly increased PLA dots compared to DMSO treatment, whereas non-transfected cells did not show any difference (**Fig. 6B, on the bottom**). In parallel, other control constructs were used to show the specificity of the PLA assay (**Fig. 6C**). The use of the antibodies specific to the SL8 intronic sequence in PLA assay allows us to identify PTPs peptides in the nuclear and cytoplasmic compartments.

<u>The pre-spliced mRNA SL8 from the intron sequence is found in the light polysomes</u>

To study the translation machinery in charge of the PTPs synthesis and better understand how this translation happens. We used the polysome fractionation approach. This technique allowed us to determine the localization of mRNAs in the different ribosomal conformations. H1299 cells were transfected with β-Globin carrying the SL8 peptide sequence in the intron 2. The day after, cells were treated or not with Isoginkgetin for 22 hours and then with Cycloheximide for 10 min. Next cells were lysed and fractionated through a sucrose gradient. Polysome fractionation showed a standard RNA polysome profile, displaying initially free RNA, the 40s and 60s subunits, the 80s monosomes, light polysomes, and then the heavy polysomes. (**Fig.7A**). In total, we obtained 23 different fractions that were pooled by pairs from fractions 8 to 23 (**Fig.7A**). Next, RNA was purified from each fraction pooled and RT-qPCR analysis was performed using different pairs of primers. To quantify the β-Globin pre-spliced mRNA levels in the samples, we used a pair of primers binding to the exon 2-SL8 sequences, the exon 2-Neo sequences, the Neo sequences, and the SL8 sequences.

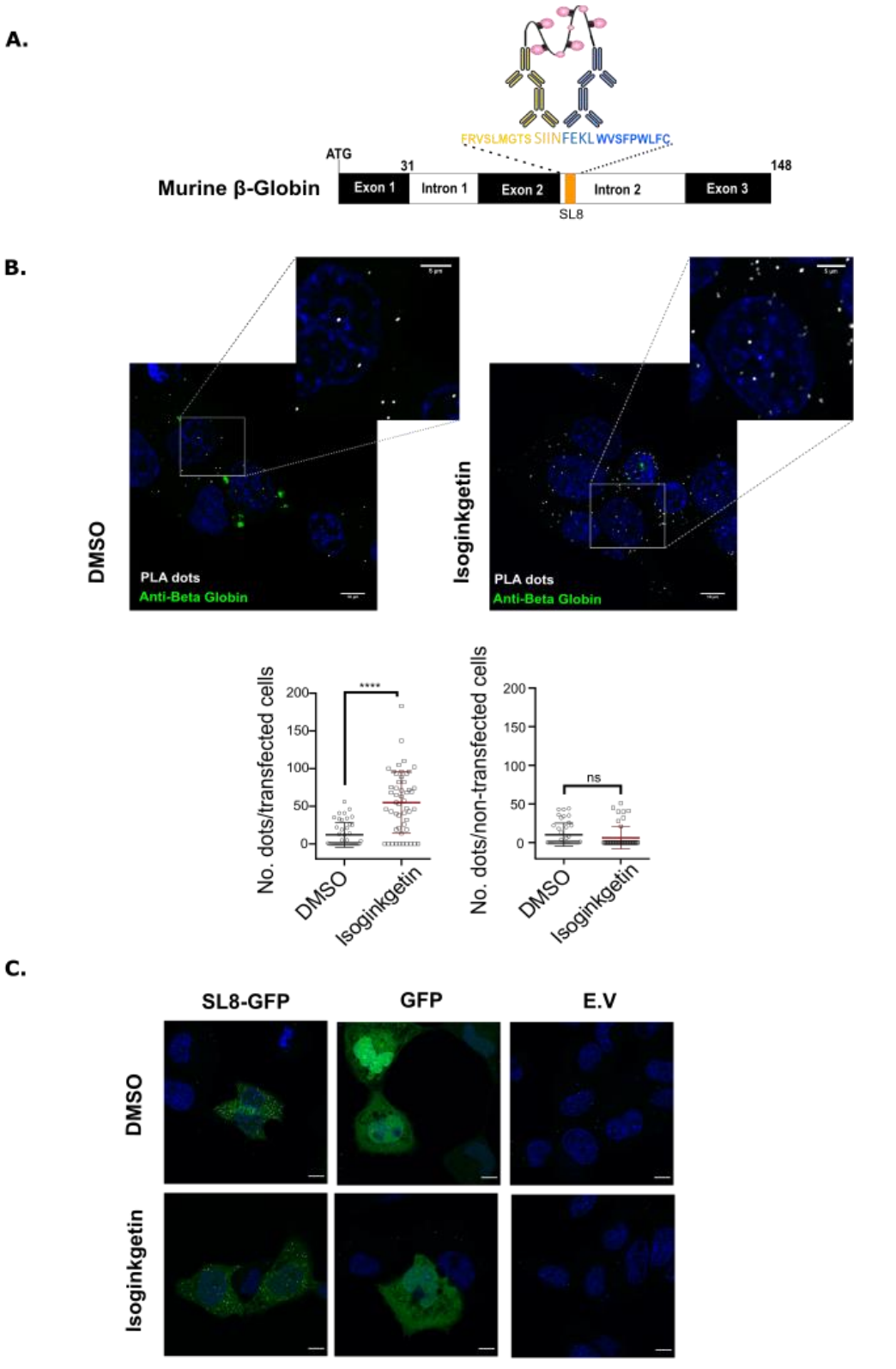


**Figure 6.** *Identification and location of PTPs from murine β-globin gene construct.* **A.** Cartoon illustrating the location of SIINFEKL (SL8) in the intron 2 of murine β-globin gene construct. PLA allows the identification of two primary antibodies in close proximity. We used primary antibodies targeting the SIIN and the FEKL sequence from the β-globin gene construct containing the SL8 sequence insert. The primary antibodies will be in turn recognized, by

secondary PLA-labelled antibodies emitting then a bright specific signal. **B.** PTPs observation by PLA assay in H1299 cells expressing murine β-globin gene constructs, which were treated with the spliced inhibitor, Isoginkgetin, at 30 uM for 22 hours. Images show PLA dots in white and β-Globin immunofluorescence signal in green. A selected area is zoomed in for better appreciation. Graphs (Bottom side) represent the quantification of PLA dots in transfected or non-transfected cells. Significant values were calculated using the multiple paired groups T-test. ****P < 0.0001; 0,1234 ns, not significant. **C.** PLA assay performed in H1299 cells expressing GFP control constructs containing the SL8 peptide sequence or GFP alone or, empty vector (E.V). The white scale bars are equivalent to 10. Of note, this result was done in collaboration with Ewa Sroka Ph.D. student at Gdansk University.

For spliced mRNA quantification, we used primers binding to exon 1-exon 2, exon 2, and actin gene sequence. The primers localization in the construct's sequences is shown in (**Fig.7B**). We demonstrated that the pairs of primers used amplified correctly the pre-spliced or spliced targeted sequences of the β-Globin, showing its correct synthesis (**Fig.7C**). Analysis of the relative mRNA levels in the different fractions showed that pre-spliced β-Globin mRNA was mainly found in the monosomes and light polysomes fractions (early fractions) (**Fig.7D**), whereas spliced β-Globin mRNA was mainly found in the heavy polysome fractions (last fractions) (**Fig7E**). Importantly, we observed that upon splicing inhibition (Isoginkgetin treatment) pre-spliced β-Globin mRNA levels carrying the SL8 sequence were increased in the light polysome fractions (fractions 3 and 4) compared with DMSO (**Fig7F**). On the other hand, splicing inhibition decreased spliced β-Globin mRNA levels in the heavy polysome fractions compared with DMSO (**Fig7F**). Taking together, these results showed that the immune peptide sequence in the pre-mRNA is found in the light polysomes. This suggests that this immunogenic peptide could be synthesized by a specialized ribosome that differs from the machinery used in the canonical translation.

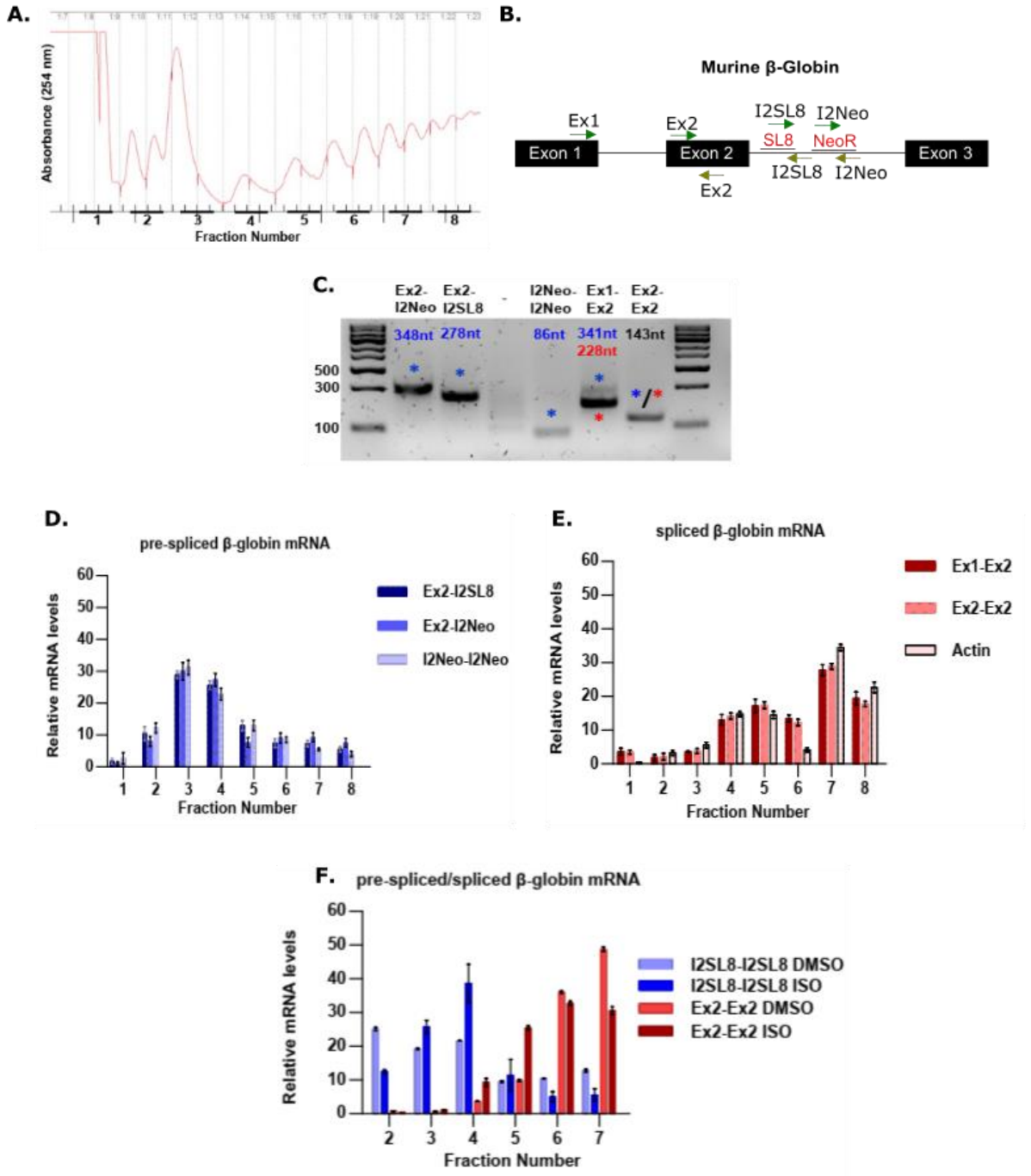


**Figure 7.** *The pre-spliced RNA SL8 from the intron sequence is found in the light polysomes*. **A.** Cells expressing murine β-Globin bearing the SL8 in the intron 2 were lysed and fractionated through sucrose gradients. Global RNA polysome profile generated by density gradient fractionation is shown. **B.** Primers used targeting pre-spliced mRNA and spliced mRNA of β-Globin sequences are indicated. **C.** Fractions 3 to 8 were pooled and RT-qPCR was performed using indicated primers. RT-qPCR products obtained were visualized in agarose gel. Pre-spliced mRNA product size is illustrated in blue, while spliced-mRNA product size is in red. Ex2f and Ex2r products are visualized in both colors because those primers do not distinguish between pre-spliced-mRNA and spliced mRNA **D and E.** RT-qPCR analysis targeting pre-spliced mRNA and spliced mRNA sequences using different primers (B.) in eight collected

gradient fractions. The relative distribution of target RNAs is shown as % and was calculated using fraction 1 as reference. **F.** RT-qPCR analysis of polysome gradient fraction from cells treated with [10 μM] Isoginkgetin or DMSO for 22 hours. Of note, this result was done in collaboration with Ewa Sroka Ph.D. student at Gdansk University.

# XVII. Discussion and Perspectives-PART 2

A large number of studies suggest alternative sources of antigenic peptides for the MHC-I pathway, including translation of pre-spliced mRNA[143,144]. During my studies, we have obtained some results that demonstrate, with two different approaches, the existence of these PTPs and show preliminary results that can provide some clues to identifying the riboproteome in charge of the PTPs translation.

Initially, we have shown that the immune SL8 peptide derived from the intron 2 of the murine β-Globin was presented to OT-1 $CD8^+$ T cells. We obtained a similar response as Apcher and colleagues regarding the antigen presentation levels[143].

Importantly, for the first time, we have been able to directly image the SL8 immune peptide synthesized from an intron sequence through PLA assay. We observed an intron-derived peptide increased following treatment with splicing inhibitors. Labeling cells with an anti-β-Globin antibody was used to demonstrate that the anti-SL8 antibodies used were specific by identifying the cells that were transfected. Considering that SL8 intron-derived immune peptide is translated with an alternative translation mechanism, while the β-Globin protein is translated with the canonical machinery. The SL8 intron-derived immune peptide might be detected on cells not labeled with anti-β-Globin. Therefore, an assay combining Fluorescence in situ hybridization (FISH) assay against β-Globin RNA and PLA assay targeting the SL8 immune peptide derived from the intron would be necessary to corroborate our findings. In addition, SL8 PLA positive labeling was detected in the nucleus as in the cytoplasm. Opposite to the previously reported study by the group, they observed the HA peptide from the intron sequence located in the nucleus. The localization difference could be explained by the fact that Apcher and colleagues used elongation inhibitors, visualizing the nascent HA peptide from the ribosome, whereas, with the splicing inhibitor, we did not control translation.

Furthermore, Apcher et al. 2013 found that the HA tag coded from an intron sequence interacted with the RPS6 within the nucleus[143]. A very interesting RP because RPS6 interacts with the chromatin in primary hepatocytes and phosphorylates within the nucleus in response to hormones[145].

To elucidate the complete riboproteome involved in the synthesis of antigenic peptides from pre-spliced mRNA. We used polysome fractionation that allowed us to visualize

the ribosome assembling process. In this preliminary experiment, we have shown that the splicing inhibition induces the increase of the pre-spliced mRNA in the light polysomes fraction, suggesting that specialized riboproteome synthesize specific peptides.

Next, we thought to continue exploiting polysome fractionation assay to identify these specific RPs found in the light polysomal fraction upon Isoginkgetin treatment compared with other fractions using Mass-spectrometry (MS) analysis. This part of the project is still in progress, although I would like to mention what we have done and the perspectives of this study.

We again used cells coding for the SL8 in the intron 2 of the β-Globin gene and treated them with or without Isoginkgetin. Then, polysome fractionation was performed and proteins were precipitated from three representative fractions to be analyzed by MS: the monosomes, the light, and the heavy polysome fractions. Identified peptides were selected in each sample according to a high false discovery rate, and identified peptides to be more than 2 unique peptides that mapped the identified protein. Samples showed 59% to 14% common hits between replicates and these common hits were compared between fractions to select unique RPs hits in light polysomes fractions from Isoginkgetin treated samples. We still do not have a conclusive result, but we have found potential RPs to be responsible for the synthesis of immune peptide SL8 from pre-splice mRNA. We identified four RPs RPL11, RPL30, RPSA, and RPLP0. RPL11 and RPL30 are both from the large subunit 60s[146], whereas RPSA and RPL0 are accessory proteins for translation[147,148]. Then we looked for the association of these genes with autoimmune diseases or diseases with an interesting immune response using the Disgenet database. We found that RPSA is a gene associated with a chronic inflammatory condition associated with T cells response (Chron disease and Behcet syndrome) and with autoimmune diseases such as Lupus Erythematosus and autoimmune thyroid disease. RPL0 is also interesting because is a gene associated with Lupus Erythematosus and inflammatory Bowel disease. We will confirm these preliminary findings with more samples and evaluate the association between these RPs with the synthesis of the SL8 immune peptide from the β-Globin pre-spliced mRNA. For this purpose, the next step would be to downregulate RPs identified in presenting cells coding SL8 in the intron 2 of the β-Globin gene and evaluate $CD8^+$ T cells proliferation.

# XVIII. Concluding Remarks – PART 2

So far, a significant amount of research has shown evidence for intron and nuclear translation. However, translation of introns and nuclear translation are two controversial topics that have so far been neglected in the molecular field. The scientific community argues that the nucleus has a low abundance of many translation factors and nascent ribosomes found in the nucleus are likely inactive[149,150].

Nevertheless, our study provides additional support for intron translation theory. i) We have shown that MHC class I antigenic peptides are derived from intron sequences. ii) we have visualized intron-derived peptides and iii) identified pre-spliced mRNA antigenic peptide sequence in the light polysome.

These data open the possibility that there are unique RPs in charge of the antigenic peptide translation. In the team, we believed that the highly conserved features and the RPs heterogenicity in ribosomes support the idea that there is specialized ribosomal machinery synthesizing antigenic peptides for the MHC class I pathway.

# XIX. Aknowledgements

I would like to thank my Ph.D supervisor Dr. Robin Fahraeus. I would like to thank you for your vote of confidence, your support, and allowing me work in your team. Your guidance and advice helped me to shape my Ph.D. study, when I felt the results were going nowhere. Thank you for the time and effort spent.

To my lab colleagues, who were always open to help, even we worked in different subjects and everyone was busy in their work and also thank you for all the good times spent that made the lab a more cheerful place. Thank you all.

I would like to thank Chrys for your support. I have learned techniques watching you and all the discussions that helped me to shape my Ph.D. study. To Laurance and Irene for your work made in the maintenance of the lab. I would like to thank Ewa for being by my sight all these four years, sharing many moments in this Ph.D. rolling coaster. To Kat for give to me positive thoughts and a more practical side of life. To Norman for your help and small discussions.

I would like to thank people that were in the lab before. Thank you, Alice, for your advice and wake me up more interested in cooking. To Mathilde, for your always good vibes in the lab and of course, helping me with the mice. To Rodrigo, for welcoming to the lab and the scientific discussions. To agata and Iolanda that were for a short time in the lab but we spent good times together.

I would like to thank Alicja for her kindness and for being the bridge with all the Polish administration. I would like to thank the technology facility from the Hopital Saint Louis in particular to Nicklas, Sophie, and Christelle who were support developing new microscopy or cytometry assays.

To my friends from Colombia Laura, March, Camila, Juli, sofi, and linis for all the skype calls and the joy you gave me when we saw each other. To my friends in Paris, Emily, Joe, and Cat for very nice moments.

I would like to thank my family Consuelo, Hector, Ana Maria, and Carlos Mario. Thank you for your support in my decisions, listening to me and help me when I most needed it. This achievement is also yours. And finally, to you Guille that every day you gave me the straight when I didn’t believe in myself. Your love and support were essential to achieve this goal.

# XX. Bibliography


1. D.F.P., L. *Antigen Processing and Presentation*. *Cicatrising Conjunctivitis* vol. 28 (1997).

2. Murphy, K. *Janeway's Immonobiology*. *Garland Science* (2012).

3. Blum, J. S., Wearsch, P. A. & Cresswell, P. Pathways of antigen processing. *Annu. Rev. Immunol.* **31**, 443–473 (2013).

4. Artyomov, M. N., Lis, M., Devadas, S., Davis, M. M. & Chakraborty, A. K. CD4 and CD8 binding to MHC molecules primarily acts to enhance Lck delivery. *Proc. Natl. Acad. Sci. U. S. A.* **107**, 16916–16921 (2010).

5. Kotsias, F., Cebrian, I. & Alloatti, A. Antigen processing and presentation. *Int. Rev. Cell Mol. Biol.* **348**, 69–121 (2019).

6. Neefjes, J., Jongsma, M. L. M., Paul, P. & Bakke, O. Towards a systems understanding of MHC class I and MHC class II antigen presentation. *Nat. Rev. Immunol.* **11**, 823–836 (2011).

7. Kumánovics, A., Takada, T. & Fischer Lindahl, K. Genomic organization of the mammalian Mhc. *Annu. Rev. Immunol.* **21**, 629–657 (2003).

8. Germain, R. N. MHC-dependent antigen processing and peptide presentation: Providing ligands for T lymphocyte activation. *Cell* **76**, 287–299 (1994).

9. Defranco, A. & Lon-, M. R. Book Reviews Infectious and Inflammatory Dis-. **80**, 2007 (2007).

10. Wieczorek, M. *et al.* Major histocompatibility complex (MHC) class I and MHC class II proteins: Conformational plasticity in antigen presentation. *Front. Immunol.* **8**, 1–16 (2017).

11. Bethesda. *AABB Technical Manual*. (2002).

12. Alberts, B. *et al. Molecular Biology of the Cell, 5th edition*. (2008).

13. Kapp, L. D. & Lorsch, J. R. The molecular mechanics of eukaryotic translation. *Annu. Rev. Biochem.* **73**, 657–704 (2004).

14. Merrick, W. C. & Pavitt, G. D. Protein synthesis initiation in eukaryotic cells. *Cold Spring Harb. Perspect. Biol.* **10**, (2018).

15. Goldberg, A. L., Cascio, P., Saric, T. & Rock, K. L. The importance of the proteasome and subsequent proteolytic steps in the generation of antigenic peptides. *Mol. Immunol.* **39**, 147–164 (2002).

16. Murata, S., Takahama, Y., Kasahara, M. & Tanaka, K. The immunoproteasome and thymoproteasome: functions, evolution and human disease. *Nat. Immunol.* **19**, 923–931 (2018).

17. Cascio, P., Call, M., Petre, B. M., Walz, T. & Goldberg, A. L. Properties of the hybrid form of the 26S proteasome containing both 19S and PA28 complexes. *EMBO J.* **21**, 2636–2645 (2002).

18. Stadtmueller, B. M. & Hill, C. P. Proteasome activators. *Mol. Cell* **41**, 8–19 (2011).

19. Rock, K. L., York, I. A., Saric, T. & Goldberg, A. L. Protein degradation and the generation of MHC class I-presented peptides. *Adv. Immunol.* **80**, 1–70 (1999).

20. Vigneron, N., Ferrari, V., Stroobant, V., Habib, J. A. & Van Den Eynde, B. J. Peptide splicing by the proteasome. *J. Biol. Chem.* **292**, 21170–21179 (2017).

21. Lankat-Buttgereit, B. & Tampé, R. The transporter associated with antigen processing: Function and implications in human diseases. *Physiol. Rev.* **82**, 187–204 (2002).

22. Bouvier, M. Accessory proteins and the assembly of human class I MHC molecules: A molecular and structural perspective. *Mol. Immunol.* **39**, 697–706 (2003).

23. Williams, A., Peh, C. A. & Elliott, T. The cell biology of MHC class I antigen presentation. *Tissue Antigens* **59**, 3–17 (2002).

24. Cresswell, P. A personal retrospective on the mechanisms of antigen processing. *Immunogenetics* **71**, 141–160 (2019).

25. Dhatchinamoorthy, K., Colbert, J. D. & Rock, K. L. Cancer Immune Evasion Through Loss of MHC Class I Antigen Presentation. *Front. Immunol.* **12**, (2021).

26. Pillay, C. S., Elliott, E. & Dennison, C. Endolysosomal proteolysis and its regulation. *Biochem. J.* **363**, 417–429 (2002).

27. Neefjes, J. J. & Ploegh, H. L. Intracellular transport of MHC class II molecules. *Immunol. Today* **13**, 179–184 (1992).

28. Doherty, G. J. & McMahon, H. T. Mechanisms of endocytosis. *Annu. Rev. Biochem.* **78**, 857–902 (2009).

29. Villadangos, J. A. & Schnorrer, P. Intrinsic and cooperative antigen-presenting functions of dendritic-cell subsets in vivo. *Nat. Rev. Immunol.* **7**, 543–555 (2007).

30. Segura, E. & Amigorena, S. *Cross-Presentation in Mouse and Human Dendritic Cells*. *Advances in Immunology* vol. 127 (Elsevier Inc., 2015).

31. You, L. *et al.* The crosstalk between autophagic and endo-/exosomal pathways in antigen processing for MHC presentation in anticancer T cell immune responses. *J. Hematol. Oncol.* **10**, 1–9 (2017).

32. Puleston, D. J. & Simon, A. K. Autophagy in the immune system. *Immunology* **141**, 1–8 (2014).

33. Dikic, I. & Elazar, Z. Mechanism and medical implications of mammalian autophagy. *Nat. Rev. Mol. Cell Biol.* **19**, 349–364 (2018).

34. Mehrpour, M., Esclatine, A., Beau, I. & Codogno, P. Overview of macroautophagy regulation in mammalian cells. *Cell Res.* **20**, 748–762 (2010).

35. Mizushima, N. & Komatsu, M. Autophagy: Renovation of cells and tissues. *Cell* **147**, 728–741 (2011).

36. Sahu, R. *et al.* Microautophagy of Cytosolic Proteins by Late Endosomes. *Dev. Cell* **20**, 131–139 (2011).

37. Li, W. & Zhang, L. *Autophagy: Biology and Diseases*. *Advances in Experimental Medicine and Biology* vol. 1206 (2019).

38. Gatica, D., Lahiri, V. & Klionsky, D. J. Cargo recognition and degradation by selective autophagy. *Nat. Cell Biol.* **20**, 233–242 (2018).

39. Kirkin, V. & Rogov, V. V. A Diversity of Selective Autophagy Receptors Determines the Specificity of the Autophagy Pathway. *Mol. Cell* **76**, 268–285

(2019).

40. Mcewan, D. G. Host – pathogen interactions and subversion of autophagy. **0**, 687–697 (2017).

41. Crotzer, V. L. & Blum, J. S. Autophagy and adaptive immunity. *Immunology* **131**, 9–17 (2010).

42. Münz, C. Autophagy proteins influence endocytosis for MHC restricted antigen presentation. *Semin. Cancer Biol.* (2019) doi:10.1016/j.semcancer.2019.03.005.

43. Münz, C. Autophagy proteins in antigen processing for presentation on MHC molecules. *Immunol. Rev.* **272**, 17–27 (2016).

44. Mintern, J. D. *et al.* Differential use of autophagy by primary dendritic cells specialized in cross-presentation. *Autophagy* **11**, 906–917 (2015).

45. Li, Y. *et al.* Efficient Cross-presentation depends on Autophagy in Tumor Cells. *Cancer Res.* **68**, 6889–6895 (2008).

46. Schmid, D., Pypaert, M. & Münz, C. Antigen-Loading Compartments for Major Histocompatibility Complex Class II Molecules Continuously Receive Input from Autophagosomes. *Immunity* **26**, 79–92 (2007).

47. English, L. *et al.* Autophagy enhances the presentation of endogenous viral antigens on MHC class I molecules during HSV-1 infection. *Nat. Immunol.* **10**, 480–487 (2009).

48. Budida, R. *et al.* Herpes simplex virus 1 interferes with autophagy of murine dendritic cells and impairs their ability to stimulate CD8+ T lymphocytes. *Eur. J. Immunol.* **47**, 1819–1834 (2017).

49. Tey, S., Khanna, R. & Dc, W. Autophagy mediates transporter associated with antigen processing-independent presentation of viral epitopes through MHC class I pathway Autophagy mediates transporter associated with antigen processing-independent presentation of viral epitopes through M. *Blood* **120**, 994–1004 (2012).

50. Parekh, V. V. *et al.* Autophagy-related protein Vps34 controls the homeostasis and function of antigen cross-presenting CD8α+ dendritic cells. *Proc. Natl. Acad.*

*Sci. U. S. A.* **114**, E6371–E6380 (2017).

51. Loi, M. *et al.* Macroautophagy Proteins Control MHC Class I Levels on Dendritic Cells and Shape Anti-viral CD8+ T Cell Responses. *Cell Rep.* **15**, 1076–1087 (2016).

52. Chemali, M., Radtke, K. & Desjardins, M. Alternative pathways for MHC class I presentation : a new function for autophagy. 1533–1541 (2011) doi:10.1007/s00018-011-0660-3.

53. Kopito, R. R. Aggresomes, inclusion bodies and protein aggregation. *Trends Cell Biol.* **10**, 524–530 (2000).

54. Yamamoto, A. & Simonsen, A. The elimination of accumulated and aggregated proteins: A role for aggrephagy in neurodegeneration. *Neurobiol. Dis.* **43**, 17–28 (2011).

55. Schaefer, M. H., Wanker, E. E. & Andrade-Navarro, M. A. Evolution and function of CAG/polyglutamine repeats in protein-protein interaction networks. *Nucleic Acids Res.* **40**, 4273–4287 (2012).

56. Zheng-Hong, Q. *Autophagy: biology and diseases*. *Advances in Experimental Medicine and Biology* vol. 1206 (2019).

57. Qin, Z. H. *et al.* Autophagy regulates the processing of amino terminal huntingtin fragments. *Hum. Mol. Genet.* **12**, 3231–3244 (2003).

58. Young, L. S., Yap, L. F. & Murray, P. G. Epstein-Barr virus: More than 50 years old and still providing surprises. *Nat. Rev. Cancer* **16**, 789–802 (2016).

59. Munz, C. *Epstein-Barr virus volume 1*. *Springer* vol. 6 (2015).

60. Farrel, P. Epstein Barr Virus and Cancer. *Annu. Rev. Pathol. Mech. Dis.* **2**, p1 (2018).

61. Cesarman, E. Gammaherpesviruses and Lymphoproliferative Disorders. *Annu. Rev. Pathol. Mech. Dis.* **9**, 349–372 (2014).

62. Frappier, L. The Epstein-Barr Virus EBNA1 Protein. *Scientifica (Cairo).* **2012**, 1–15 (2012).

63. Blake, N. *et al.* Human CD8+ T cell responses to EBV EBNA1: HLA class I

presentation of the (Gly-Ala)-containing protein requires exogenous processing. *Immunity* **7**, 791–802 (1997).

64. Leviskaya, J. *et al.* Inhibition of antigen processing by the internal repeat region of the Epstein Barr virus nuclear antigen-1. *Nature* **375**, 685–688 (1995).

65. Munz, C. *Epstein Barr Virus Volume 2*. *Springer* vol. 6 (2015).

66. Levitskaya, J., Sharipo, A., Leonchiks, A., Ciechanover, A. & Masucci, M. G. Inhibition of ubiquitin/proteasome-dependent protein degradation by the Gly-Ala repeat domain of the Epstein-Barr virus nuclear antigen 1. *Proc. Natl. Acad. Sci. U. S. A.* **94**, 12616–12621 (1997).

67. Daskalogianni, C. *et al.* Gly-Ala repeats induce position- and substrate-specific regulation of 26 S proteasome-dependent partial processing. *J. Biol. Chem.* **283**, 30090–30100 (2008).

68. Yin, Y., Manoury, B. & Fåhraeus, R. Self-inhibition of synthesis and antigen presentation by Epstein-Barr virus-encoded EBNA1. *Science (80-. ).* **301**, 1371–1374 (2003).

69. Apcher, S. *et al.* mRNA Translation Regulation by the Gly-Ala Repeat of Epstein-Barr Virus Nuclear Antigen 1. *J. Virol.* **83**, 1289–1298 (2009).

70. Apcher, S., Daskalogianni, C., Manoury, B. & Fåhraeus, R. Epstein barr virus-encoded EBNA1 interference with MHC class I antigen presentation reveals a close correlation between mRNA translation initiation and antigen presentation. *PLoS Pathog.* **6**, 1–14 (2010).

71. Zheng, A. J. L. *et al.* The different activities of RNA G-quadruplex structures are controlled by flanking sequences. *Life Sci. Alliance* **5**, 1–15 (2022).

72. Martins, R. P. *et al.* Nuclear processing of nascent transcripts determines synthesis of full-length proteins and antigenic peptides. *Nucleic Acids Res.* **47**, 3086–3100 (2019).

73. Martins, R. P. *et al.* In cellulo protein-mRNA interaction assay to determine the action of G-quadruplex-binding molecules. *Molecules* **23**, (2018).

74. Tellam, J. *et al.* Endogenous presentation of CD8+ T cell epitopes from Epstein-

Barr virus-encoded nuclear antigen 1. *J. Exp. Med.* **199**, 1421–1431 (2004).

75. Murat, P. *et al.* G-quadruplexes regulate Epstein-Barr virus-encoded nuclear antigen 1 mRNA translation. *Nat. Chem. Biol.* **10**, 358–364 (2014).

76. Lista, M. J. *et al.* Nucleolin directly mediates Epstein-Barr virus immune evasion through binding to G-quadruplexes of EBNA1 mRNA. *Nat. Commun.* **8**, (2017).

77. Luka, J., Lindahl, T. & Klein, G. Purification of the Epstein-Barr virus-determined nuclear antigen from Epstein-Barr virus-transformed human lymphoid cell lines. *J. Virol.* **27**, 604–611 (1978).

78. Hennessy, K. & Kieff, E. One of two Epstein-Barr virus nuclear antigens contains a glycine- alanine copolymer domain. *Proc Natl Acad Sci U S A* **80**, 5665–5669 (1983).

79. Paludan, C. *et al.* Endogenous MHC class II processing of a viral nuclear antigen after autophagy. *Science (80-. ).* **307**, 593–596 (2005).

80. Gnanasundram, S. V. *et al.* PI3Kδ activates E2F1 synthesis in response to mRNA translation stress. *Nat. Commun.* **8**, (2017).

81. Daskalogianni, C. *et al.* Gly-Ala repeats induce position- and substrate-specific regulation of 26 S proteasome-dependent partial processing. *J. Biol. Chem.* **283**, 30090–30100 (2008).

82. Axe, E. L. *et al.* Autophagosome formation from membrane compartments enriched in phosphatidylinositol 3-phosphate and dynamically connected to the endoplasmic reticulum. *J. Cell Biol.* **182**, 685–701 (2008).

83. Mizushima, N., Yoshimorim, T. & Levine, B. Methods in mammalian autopahgy reasearch. *Cell* **140**, 2–3 (2010).

84. Lee, H. K. *et al.* In Vivo Requirement for Atg5 in Antigen Presentation by Dendritic Cells. *Immunity* **32**, 227–239 (2010).

85. Tabe, L. *et al.* Segregation of mutant ovalbumins and ovalbumin-globin fusion proteins in Xenopus oocytes. Identification of an ovalbumin signal sequence. *J. Mol. Biol.* **180**, 645–666 (1984).

86. Tabachnick-Cherny, S. *et al.* Polyglutamine-Related Aggregates Can Serve as

a Potent Antigen Source for Cross-Presentation by Dendritic Cells. *J. Immunol.* **205**, 2583–2594 (2020).

87. Suhr, S. T. *et al.* Identities of sequestered proteins in aggregates from cells with induced polyglutamine expression. *J. Cell Biol.* **153**, 283–294 (2001).

88. Ashkenazi, A. *et al.* Europe PMC Funders Group Polyglutamine tracts regulate beclin 1-dependent autophagy. *Nature* **545**, 108–111 (2017).

89. Bloom, J., Amador, V., Bartolini, F., DeMartino, G. & Pagano, M. Proteasome-mediated degradation of p21 via N-terminal ubiquitinylation. *Cell* **115**, 71–82 (2003).

90. Dick, L. R. *et al.* Proteolytic processing of ovalbumin and beta-galactosidase by the proteasome to a yield antigenic peptides. *J. Immunol.* **152**, 3884–94 (1994).

91. Rock, K. L. *et al.* Inhibitors of the proteasome block the degradation of most cell proteins and the generation of peptides presented on MHC class I molecules. *Cell* **78**, 761–771 (1994).

92. Michalek, M. T., P., G. E., Gramm, C., Goldberg, A. L. & Rock, K. L. A role for the ubiquitin-dependent proteolytic pathway in MHC class I-restricted antigen presentation. *Nature* **359**, 167–169 (1993).

93. Pamer, E. & Cresswell, P. MECHANISMS OF MHC CLASS I – RESTRICTED ANTIGEN. (1998).

94. Rammensee, H.-G., Kirsten, F. & Rotzschke, O. Peptides naturally presented by MHC class I molecule. *Annu. Rev. Immunol.* **11**, 213–44 (1993).

95. Liu, J. N. *et al.* The role of autophagy in allergic inflammation: A new target for severe asthma. *Exp. Mol. Med.* **48**, e243-10 (2016).

96. Shen, L., Sigal, L. J., Boes, M. & Rock, K. L. Important role of cathepsin S in generating peptides for TAP-independent MHC class I crosspresentation in vivo. *Immunity* **21**, 155–165 (2004).

97. Wilson, J. B. *et al.* EBNA1: Oncogenic activity, immune evasion and biochemical functions provide targets for novel therapeutic strategies against epstein-barr virus-associated cancers. *Cancers (Basel).* **10**, 1–29 (2018).

98. Du, H. *et al.* A multifaceted role of progranulin in regulating amyloid-beta dynamics and responses. *Life Sci. Alliance* **4**, 1–22 (2021).

99. Yang, J., Wise, L. & Fukuchi, K. I. TLR4 Cross-Talk With NLRP3 Inflammasome and Complement Signaling Pathways in Alzheimer's Disease. *Front. Immunol.* **11**, 1–16 (2020).

100. Shaid, S., Brandts, C. H., Serve, H. & Dikic, I. Ubiquitination and selective autophagy. *Cell Death Differ.* **20**, 21–30 (2013).

101. Nishida, Y. *et al.* Discovery of Atg5/Atg7-independent alternative macroautophagy. *Nature* **461**, 654–658 (2009).

102. Wei, J. & Yewdell, J. W. Immunoribosomes: Where's there's fire, there's fire. *Mol. Immunol.* **113**, 38–42 (2019).

103. Yewdell, J. W., Dersh, D. & Fåhraeus, R. Peptide Channeling: The Key to MHC Class I Immunosurveillance? *Trends Cell Biol.* **29**, 929–939 (2019).

104. Apcher, S. *et al.* Major source of antigenic peptides for the MHC class I pathway is produced during the pioneer round of mRNA translation. *Proc. Natl. Acad. Sci.* **108**, 11572–11577 (2011).

105. Lev, A. *et al.* Compartmentalized MHC class I antigen processing enhances immunosurveillance by circumventing the law of mass action. *Proc. Natl. Acad. Sci. U. S. A.* **107**, 6964–6969 (2010).

106. Granados, D. P., Laumont, C. M., Thibault, P. & Perreault, C. The nature of self for T cells-a systems-level perspective. *Curr. Opin. Immunol.* **34**, 1–8 (2015).

107. Anton, L. C. & Yewdell, J. W. Translating DRiPs: MHC class I immunosurveillance of pathogens and tumors. *J. Leukoc. Biol.* **95**, 551–562 (2014).

108. Milner, E., Barnea, E., Beer, I. & Admon, A. The turnover kinetics of major histocompatibility complex peptides of human cancer cells. *Mol. Cell. Proteomics* **5**, 357–365 (2006).

109. Hanada, K. I., Yewdell, J. W. & Yang, J. C. Immune recognition of a human renal cancer antigen through post-translational protein splicing. *Nature* **427**, 252–256

(2004).

110. Vigneron, N. *et al.* An Antigenic Peptide Produced by Peptide Splicing in the Proteasome. *Science (80-. ).* **304**, 587–590 (2004).

111. Admon, A. Are there indeed spliced peptides in the immunopeptidome? *Mol. Cell. Proteomics* **20**, 100099 (2020).

112. Croft, N. P. *et al.* Kinetics of Antigen Expression and Epitope Presentation during Virus Infection. *PLoS Pathog.* **9**, (2013).

113. Laumont, C. M. *et al.* Global proteogenomic analysis of human MHC class I-associated peptides derived from non-canonical reading frames. *Nat. Commun.* **7**, 1–12 (2016).

114. Apcher, S., Prado Martins, R. & Fåhraeus, R. The source of MHC class I presented peptides and its implications. *Curr. Opin. Immunol.* **40**, 117–122 (2016).

115. Yewdell, J. W., Reits, E. & Neefjes, J. Making sense of mass destruction: quantitating MHC class I antigen presentation. *Nat. Rev. Immunol.* **3**, 952–961 (2003).

116. Ye, W. *et al.* Cross-presentation of viral antigens in dribbles leads to efficient activation of virus-specific human memory T cells. *J. Transl. Med.* **12**, 1–12 (2014).

117. Apcher, S. *et al.* Translation of pre-spliced RNAs in the nuclear compartment generates peptides for the MHC class i pathway. *Proc. Natl. Acad. Sci. U. S. A.* **110**, 17951–17956 (2013).

118. Apcher, S., Daskalogianni, C. & Fåhraeus, R. Pioneer translation products as an alternative source for MHC-I antigenic peptides. *Mol. Immunol.* **68**, 68–71 (2015).

119. Duvallet, E. *et al.* Exosome-driven transfer of tumor-associated Pioneer Translation Products (TA-PTPs) for the MHC class I cross-presentation pathway. *Oncoimmunology* **5**, (2016).

120. Shastri, N., Nguyen, V. & Gonzalez, F. Major histocompatibility class I molecules

can present cryptic translation products to T-cells. *J. Biol. Chem.* **270**, 1088–1091 (1995).

121. Malarkannan, S., Horng, T., Shih, P. P., Schwab, S. & Shastri, N. Presentation of out-of-frame peptide/MHC class I complexes by a novel translation initiation mechanism. *Immunity* **10**, 681–690 (1999).

122. Schwab, S. R., Shugart, J. A., Horng, T., Malarkannan, S. & Shastri, N. Unanticipated antigens: Translation initiation at CUG with leucine. *PLoS Biol.* **2**, (2004).

123. Starck, S. R. *et al.* Leucine-tRNA initiates at CUG start codons for protein synthesis and presentation by MHC class I. *Science (80-. ).* **336**, 1719–1723 (2012).

124. Schwab, S. R., Li, K. C., Kang, C. & Shastri, N. Constitutive display of cryptic translation products by MHC class I molecules. *Science (80-. ).* **301**, 1367–1371 (2003).

125. Coulie, P. G. *et al.* A mutated intron sequence codes for an antigenic peptide recognized by cytolytic T lymphocytes on a human melanoma. *Proc. Natl. Acad. Sci. U. S. A.* **92**, 7976–7980 (1995).

126. Maquat, L. E. Nonsense-mediated mRNA decay: Splicing, translation and mRNP dynamics. *Nat. Rev. Mol. Cell Biol.* **5**, 89–99 (2004).

127. Chang, Y. F., Imam, J. S. & Wilkinson, M. F. The Nonsense-mediated decay RNA surveillance pathway. *Annu. Rev. Biochem.* **76**, 51–74 (2007).

128. Maquat, L. E., Hwang, J., Sato, H. & Tang, Y. CBP80-promoted mRNP rearrangements during the pioneer round of translation, nonsense-mediated mRNA decay, and thereafter. *Cold Spring Harb. Symp. Quant. Biol.* **75**, 127–134 (2010).

129. Zhou, X., Liao, W. J., Liao, J. M., Liao, P. & Lu, H. Ribosomal proteins: Functions beyond the ribosome. *J. Mol. Cell Biol.* **7**, 92–104 (2015).

130. Baßler, J. & Hurt, E. Eukaryotic Ribosome Assembly. *Annu. Rev. Biochem.* **88**, 281–306 (2019).

131. Moore, P. & Steitz, T. The ribosome revealed. *Trends Biochem. Sci.* **30**, 279–281 (2005).

132. Noller, H. F. RNA structure: Reading the ribosome. *Science (80-. ).* **309**, 1508–1514 (2005).

133. Wei, J. *et al.* Ribosomal Proteins Regulate MHC Class I Peptide Generation for Immunosurveillance. *Mol. Cell* **73**, 1162-1173.e5 (2019).

134. Allfrey, V. G. AMINO ACID INCORPORATION BY ISOLATED THYMUS NUCLEI. I. THE ROLE OF DESOXYRIBONUCLEIC ACID IN PROTEIN SYNTHESIS. *PNAS* **40**, 1–5 (1954).

135. Iborra, F. J., Jackson, D. A. & Cook, P. R. Coupled transcription and translation within nuclei of mammalian cells. *Science (80-. ).* **293**, 1139–1142 (2001).

136. Iborra, F. J., Jackson, D. A. & Cook, P. R. The case for nuclear translation. *J. Cell Sci.* **117**, 5713–5720 (2004).

137. Dolan, B. P., Knowlton, J. J., David, A., Bennink, J. R. & Yewdell, J. W. RNA Polymerase II Inhibitors Dissociate Antigenic Peptide Generation from Normal Viral Protein Synthesis: A Role for Nuclear Translation in Defective Ribosomal Product Synthesis? *J. Immunol.* **185**, 6728–6733 (2010).

138. Brogna, S., Sato, T. A. & Rosbash, M. Ribosome components are associated with sites of transcription. *Mol. Cell* **10**, 93–104 (2002).

139. David, A. *et al.* Nuclear translation visualized by ribosome-bound nascent chain puromycylation. *J. Cell Biol.* **197**, 45–57 (2012).

140. Al-Jubran, K. *et al.* Visualization of the joining of ribosomal subunits reveals the presence of 80S ribosomes in the nucleus. *Rna* **19**, 1669–1683 (2013).

141. López, I. *et al.* P53-mediated suppression of BiP triggers BIK-induced apoptosis during prolonged endoplasmic reticulum stress. *Cell Death Differ.* **24**, 1717–1729 (2017).

142. Panda, A., Martindale, J. & Gorospe, M. Polysome Fractionation to Analyze mRNA Distribution Profiles. *Bio-Protocol* **7**, 1–11 (2017).

143. Apcher, S. *et al.* Translation of pre-spliced RNAs in the nuclear compartment

generates peptides for the MHC class I pathway. *Proc. Natl. Acad. Sci.* **110**, 17951–17956 (2013).

144. Apcher, S. *et al.* Major source of antigenic peptides for the MHC class I pathway is produced during the pioneer round of mRNA translation. *Proc. Natl. Acad. Sci. U. S. A.* **108**, 11572–11577 (2011).

145. Meyuhas, O. Chapter 1 Physiological Roles of Ribosomal Protein S6: One of Its Kind. *Int. Rev. Cell Mol. Biol.* **268**, 1–37 (2008).

146. Wilson, D. N. & Nierhaus, K. H. Ribosomal proteins in the spotlight. *Crit. Rev. Biochem. Mol. Biol.* **40**, 243–267 (2005).

147. Juri, M., Barroso, J. A., Levin, M. J. & Aguilar, C. F. Preliminary Structural Studies of the Hydrophobic Ribosomal P0 Protein from Trypanosoma cruzi , A Part of the P0 / P1 / P2 Complex. 521–525 (2005).

148. Malygin, A. A., Babaylova, E. S., Loktev, V. B. & Karpova, G. G. Biochimie A region in the C-terminal domain of ribosomal protein SA required for binding of SA to the human 40S ribosomal subunit. *Biochimie* **93**, 612–617 (2011).

149. Nathanson, L., Xia, T. & Deutscher, M. P. Nuclear protein synthesis : A re-evaluation. *file///E/Articles/Ribosome nucleous&intron Transl. (2003).pdf* 9–13 (2003) doi:10.1261/rna.2990203.RNA.

150. Dahlberg, J. E., Lund, E. & Goodwin, E. B. Nuclear translation : What is the evidence ? 1–8 (2003) doi:10.1261/rna.2121703.IS.

# XXI. Annexes

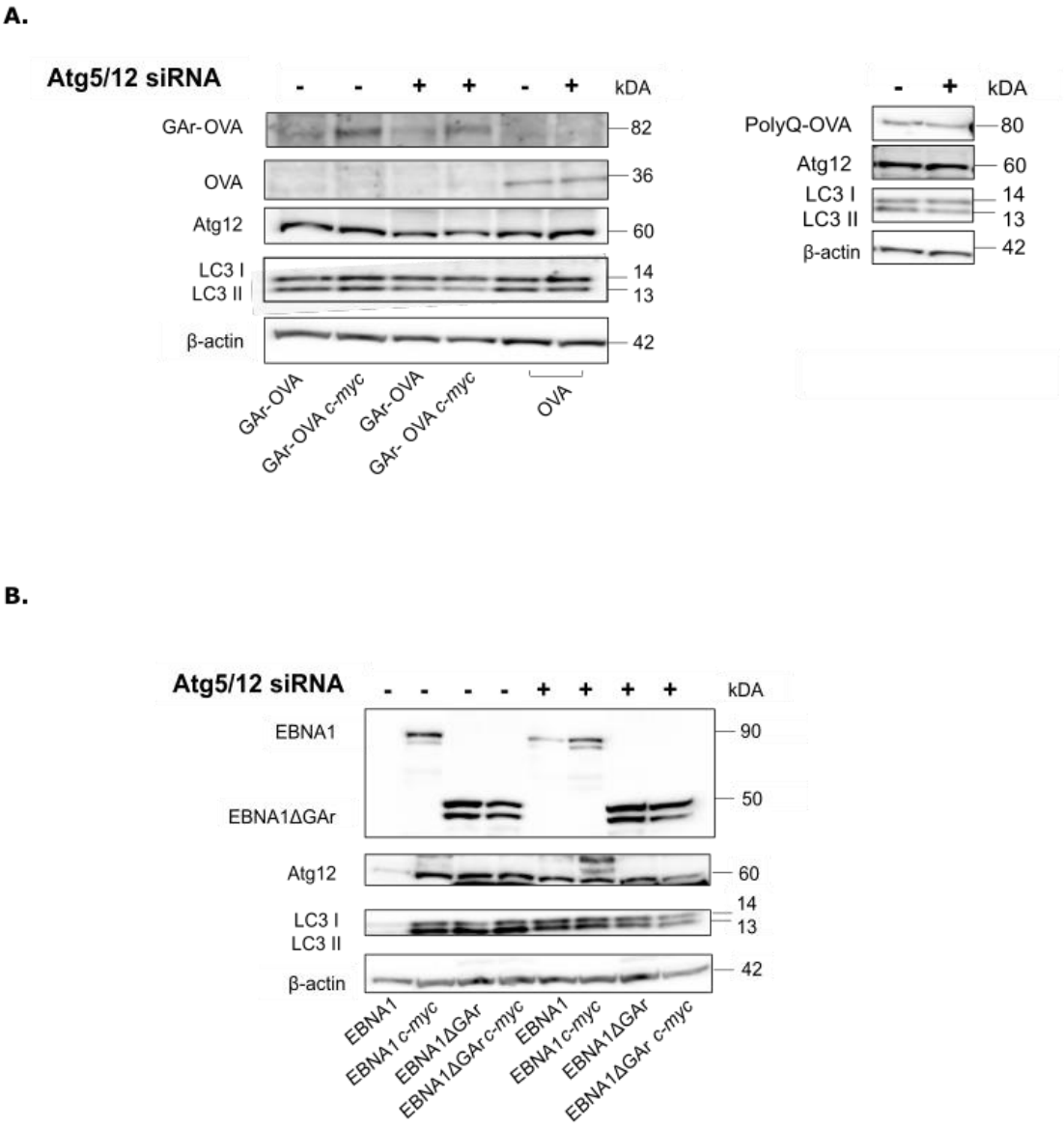


**Supplementary Figure 1.** *Autophagy inhibition downregulates Atg5/12 protein levels and decreased LC3 II-I ratio of the presenting cells after co-culture*. Western Blot showing the effect of autophagy inhibition in protein levels of **A.**GAr-OVA, OVA and PolyQ-OVA with, or without the *c-myc* in the 5' UTR **B.** EBNA1 and EBNA1ΔGAr with, or without, the *c-myc* in the 5' UTR .One representative experiment out of three is shown.

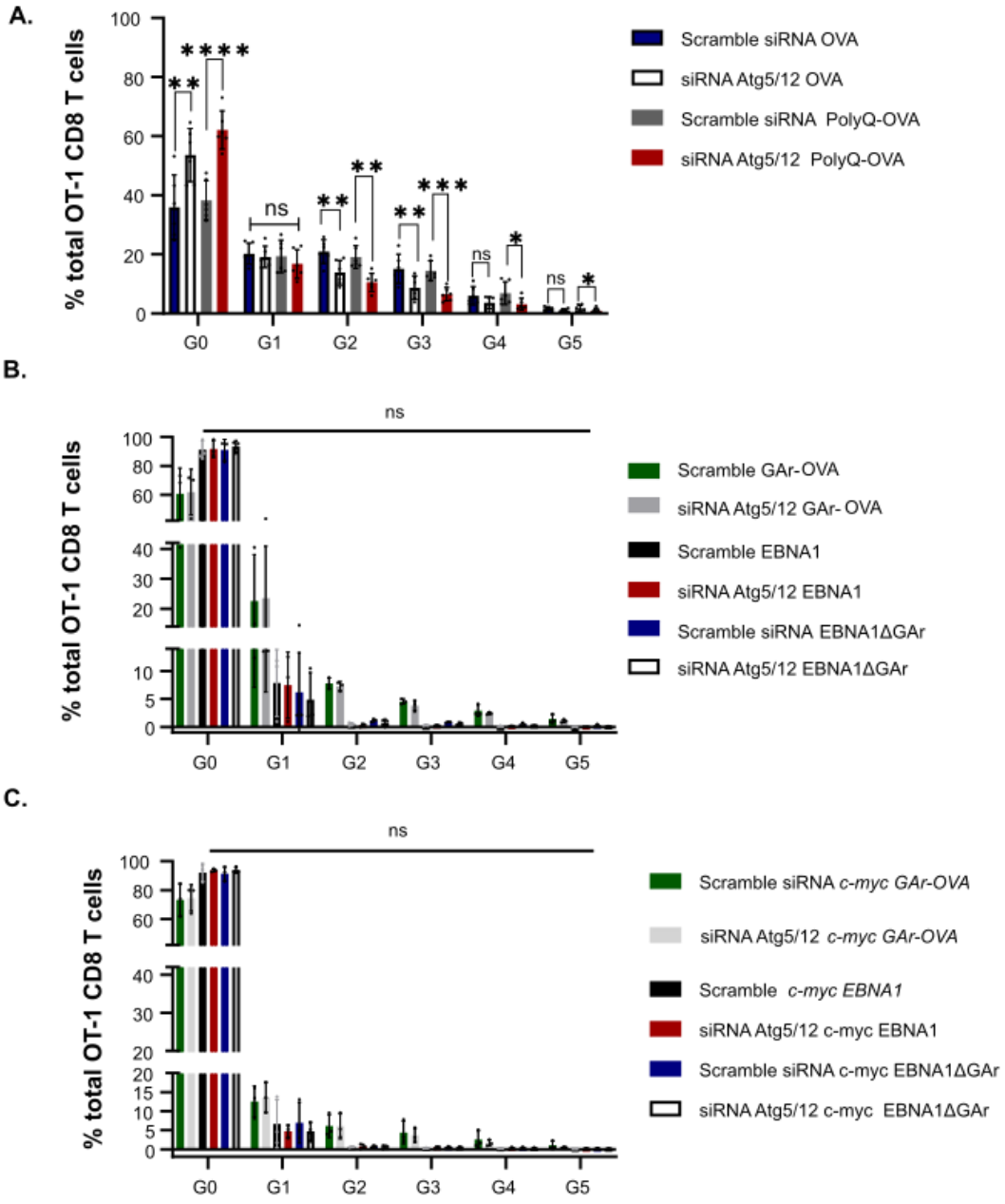


**Supplementary Figure 2.** *Evaluation of autophagy dependence in antigen presentation assays.* Co-culture of H1299 presenting cells with different endogenous antigenic substrates and OT-1 CD8+ T cells labeled with Cell-trace violet. The levels of OT-1 CD8+ T cells proliferation were analyzed by flow Cytometry. Percentage of total OT1 CD8+ T cells was calculated using the number of cells in each generation generated by the modeling of the Proliferation tool in Flow Jo software. The graphs show the percentage of cells from each generation compared with percentage of non-divided cells (generation 0). **A.** Presentation of antigenic derive peptides from OVA and PolyQ-OVA **B.** Presentation of antigenic derive peptides from GAr-OVA, EBNA1 and EBNA1ΔGAr **C.** Presentation of antigenic derive peptides from same constructs as B., but fused with the *c-myc* in the 5' UTR. Graphs represent 6 or 3 independent experiments. Significant values were calculated using Multiple paired T test grouped. *P < 0.0332; **P < 0.0021; ***P < 0.0002; ****P < 0.0001; 0,1234 ns, no significant.

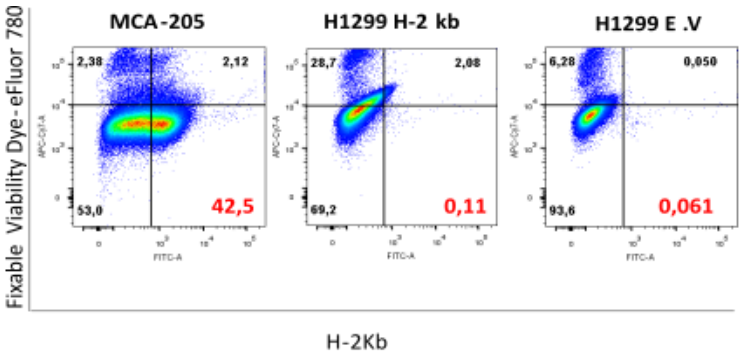


**Supplementary Figure 3.** Antigen presentation measured from presenting cells. Directly H-2Kb was measured by cytometry in murine MCA cells, human H1299 cells expressing H-2kb and human H1299 cells expressing E.V.

**Table 1.** Primers used in β-Globin polysome fractionation (Results Part2,Figure 7)

| Primers qPCR | Sequence (5'-3') |
|---|---|
| I2Neo Forward | CTCGAGCTCGCGAAAGCTAGC |
| I2Neo Reverse | CCTCGAGATCTAGATATCGATGAATTG |
| I2SL8 Forward | GGGCACCTCCAGTATAATCAACT |
| I2SL8 Reverse | CTTTCGCGAGCTCGAGTTTC |
| Ex1 Forward | GGTGAACGCCGATGAAGTTG |
| Ex2 Reverse | GCCATGGGCCTTCACTTTGG |
| Ex2 Forward | GCTGGTTGTCTACCCTTGGA |
| Actin Forward | TCACCCACACTGTGCCCATCTACGA |
| Actin Reverse | TGAGGTAGTCAGTCAGGTCCCG |

Cellular Immunology 374 (2022) 104484

Contents lists available at ScienceDirect

Cellular Immunology

journal homepage: www.elsevier.com/locate/ycimm

# Substrate-specific presentation of MHC class I-restricted antigens via autophagy pathway

Maria C. Tovar Fernandez [a,b], Ewa M. Sroka [a,b,1], Mathilde Lavigne [a,1], Aikaterini Thermou [a,b], Chrysoula Daskalogianni [a,b], Bénédicte Manoury [c], Rodrigo Prado Martins [a,d], Robin Fahraeus [a,b,e,f,*]

[a] Inserm UMRS1131, Institut de Génétique Moléculaire, Université Paris 7, Hôpital St. Louis, F-75010 Paris, France
[b] ICCVS, University of Gdańsk, Science, ul. Wita Stwosza 63, 80-308 Gdańsk, Poland
[c] Institut Necker Enfants Malades, INSERM U1151-CNRS UMR 8253, Université de Paris, Faculté de Médecine Necker, France
[d] ISP, INRAE, Université de Tours, UMR1282, Tours, Nouzilly, France
[e] Department of Medical Biosciences, Building 6M, Umeå University, 901 85 Umeå, Sweden
[f] RECAMO, Masaryk Memorial Cancer Institute, Zluty kopec 7, 65653 Brno, Czech Republic

ARTICLE INFO

*Keywords:*
MHC class I restricted antigen presentation
Autophagy
Protein aggregates
EBV-encoded EBNA1

ABSTRACT

The accumulation of protein aggregates is toxic and linked to different diseases such as neurodegenerative disorders, but the role of the immune system to target and destroy aggregate-carrying cells is still relatively unknown. Here we show a substrate-specific presentation of antigenic peptides to the direct MHC class I pathway via autophagy. We observed no difference in presentation of peptides derived from the viral EBNA1 protein following suppression of autophagy by knocking down Atg5 and Atg12. However, the same knock down treatment suppressed the presentation from ovalbumin. Fusing the aggregate-prone poly-glutamine (PolyQ) to the ovalbumin had no effect on antigen presentation via autophagy. Interestingly, fusing the EBNA1-derived gly-ala repeat (GAr) sequence to ovalbumin rendered the presentation Atg5/12 independent. We also demonstrate that the relative levels of protein expression did not affect autophagy-mediated antigen presentation. These data suggest a substrate-dependent presentation of antigenic peptides for the MHC class I pathway via autophagy and indicate that the GAr of the EBNA1 illustrates a novel virus-mediated mechanism for immune evasion of autophagy-dependent antigen presentation.

## 1. Introduction

The cellular CD8$^+$ T cell immune response is based on the recognition of antigenic peptides presented on the surface of host cells on the major histocompatibility complex (MHC) class I molecules. The presentation of antigenic peptides via the direct MHC class I pathway involves the degradation of the substrate by the proteasome, transport into the endoplasmic reticulum and further processing by peptidases and loading onto the MHC I molecules [1,2]. On the other hand, exogenous antigens endocytosed by professional presenting cells, such as dendritic cells or macrophages, are translocated to endosomal compartments and presented to the MHC I pathway via the so-called cross presentation pathway [1]. It was thought early on that peptides for the MHC I & II pathways were derived from processing of full length proteins but studies have since discovered a more complex origin of MHC-I antigenic peptides, including peptides derived from the 3′ untranslated sequences (UTRs) of mRNAs [3] and from introns [4–6], supporting a model in which non-canonical translation can provide antigenic peptide substrates.

The latent Epstein-Barr (EBV) and Kaposi's sarcoma viruses both target mRNA translation to evade the MHC-I pathway [7,8]. The EBV-encoded EBNA1 uses a glycine-alanine repeat (GAr) consisting of small non-polar amino acids that is prone to cause aggregates [9,10]. The GAr suppresses translation of any mRNA to which it is fused and this has been shown to minimize the presentation of antigenic peptides for the direct MHC class I pathway [7]. It consists of a stretch of up to 250 single glycine residues separated by one, two or three alanines. Inserting a single serine in every eight residue renders the GAr non-functional

* Corresponding author.
*E-mail address:* robin.fahraeus@inserm.fr (R. Fahraeus).
[1] These authors contributed equally.

https://doi.org/10.1016/j.cellimm.2022.104484
Received 17 October 2021; Received in revised form 28 January 2022; Accepted 29 January 2022
Available online 17 February 2022

[11]. EBNA1 has been reported to be presented to the class II pathway via autophagy [12] but whether, or not, peptides for the class I pathway can be generated from processing of full length proteins via autophagy remains an open question. A cross-presentation study reported MHC I molecules on endolysosomal compartments [13] and it was suggested that endogenous human cytomegalovirus latency-associated protein (pUL138) can be presented to $CD8^+$ T cells through autophagy [14].

The poly glutamine (PolyQ) is well known to cause aggregates to which it is fused and is implicated in various neurodegenerative diseases such as Huntington disease (HD), dentatorubral pallidoluysian atrophy (DRPLA), spinobulbar muscular atrophy (SBMA) and six spinocerebellar ataxias (SCA) [15].

Autophagy is a key degradative process of endogenous cytoplasmic proteins [16,17]. It was first defined as non-specific degradation process, but it was later revealed that autophagy has selectivity for specific cargos including, but not exclusively, aggregated proteins tagged with ubiquitin chains that are recognized by autophagy receptors bound to the autophagosomes membrane protein LC3 (Light chain 3) [18–20]. There are different autophagy such as microautophagy, chaperon mediated autophagy and macroautophagy [21]. In this study, we focused on the macroautophagy pathway that has been implicated in presenting EBNA1 to the class II pathway [12]. It involves the recruitment of ATG proteins, such as Atg5 and 12, to specific phagophore assembly sites (PAS) that elongates and traps a portion of the cytosol until it is sealed in the double membrane autophagosome vesicle. After trapping the engulfed cytosolic cargo, autophagosomes fuse to the lysosome to clear the cargo and the autophagic body [20]. It was recently proposed that the trafficking route of autophagosomes carrying cytoplasmic molecules fuse with endosomes carrying MHC class II molecules and thereby facilitate presentation of endogenous antigens on MHC II molecules [22].

In this study we have used the EBNA1 protein that is known to be processed by the autophagy pathway as well as protein aggregates caused by the poly-glutamine (PolyQ) repeat to address if autophagy is a source of peptide substrates for the MHC class I pathway.

## 2. Material and methods

### 2.1. Plasmids

The pCDNA3-EBNA1, pCDNA3-EBNA1ΔGAr, pCDNA3-Ovalbumin (OVA), pCDNA3-GAr-OVA and pCDNA3-*c-myc* GAr-OVA constructs were obtained as described previously [23].

*c-myc* EBNA1 and *c-myc* EBNA1ΔGAr were generated by amplification of full-length human *c-myc* by polymerase chain reaction (PCR), using a 5′ sense primer containing a *Hin*dIII site 5′ AAT**AAGCTT**CCACTGCTTACTGGCTTATCG 3′ and a 3′ antisense primer 5′ TAA**AAGCTT**CGGCCGTTACTAGTGGATCC 3′ containing another *Hin*dIII site. The fragment was cloned into the 5′UTR digested pCDNA3-EBNA1 and EBNA1ΔGAr constructs.

The OVA Poly 125 glutamine (Q) construct was made by digestion of OVA construct with *Eco*RI and *Xba*I enzyme and introducing 125 glutamine repetition sequence contained in a vector already mentioned previously [24].

### 2.2. Cell culture and transfection

H1299 cells (Human non-small cell lung carcinoma) were cultured in RPMI-1640, supplemented with 10% fetal bovine serum (FBS), 2 mM L-glutamine and 1% Penicillin- Streptomycin and mouse cell atlas (MCA-205) were cultured in RPMI-1640, supplemented with 10% fetal bovine serum (FBS), 2 mM L-glutamine, 1% non-essential amino acids, 1% sodium pyruvate and 1% Penicillin-Streptomycin. For antigen presentation experiments, cells were cultured in 6 wells plates ($8x10^4$ cells/well) at 37 °C with 5% $CO_2$. The day after seeding and Atg5/12 siRNA induction, transfections were performed using 3 μl of Gene Juice reagent according to the manufacture's protocol (Merck Bioscence). Cells were co-transfected with 0.5 μg of murine MHC class I molecule Kb and 1 μg of EBNA1, EBNA1ΔGAr, GAr-OVA and PolyQ-OVA cDNA carrying the SIINFEKL (SL8) epitope coding sequences in its open reading frame (ORF). In all antigen presentation assays, 1 μg of an OVA cDNA was used as positive control and the same quantity for the empty vector as negative control.

### 2.3. siRNA against Atg5/12

The day after seeding, cells were transfected with Human siRNAs or Murine siRNAs at 20 pM using Jet Prime reagent (Polyplus) following the manufacturer's instructions. The knock down of these proteins was evaluated by Real time PCR (qRT-PCR) and Western Blot at the end of 72 h incubation and 120 h.

Human siRNAs used were: two siRNAs against Atg12 (SI02655289 and SI04335513, Qiagen) and three siRNAs against Atg5 (SI02655310, SI02633946 and SI00069251, Qiagen).

Murine siRNAs used were: two siRNAs against Atg12 (SI00900319|S0 and SI00900333|S0, Qiagen) and three siRNAs against Atg5 (SI02696806|S0, SI02720186|S0 and SI02745435|S0, Qiagen).

### 2.4. Chloroquine treatment

The day after seeding, cells were treated with Chloroquine at [30 μM] during 36 h. The autophagy inhibition was evaluated by Western Blot assessing LC3-II accumulation.

### 2.5. Antigen presentation assay: OT1 $CD8^+$ T cells proliferation

To determine the levels of antigen presentation, we used $CD8^+$ T cells that express specific receptors to the OVA epitope, SIINFEKL, recognized by H-2 Kb. These $CD8^+$ T cells were purified from OT1 transgenic mice expressing a transgenic TCR specific for SIINFEKL-Kb. Spleen and lymph nodes from OT1 transgenic mice were passed through a 70 μm cell strainer and red blood cells were lysed with ACK buffer treatment during 5 min. After several washes with PBS-FBS 5%, $CD8^+$ T cells were negatively selected using a $CD8^+$ T cell isolation kit (MACS Miltenyi Biotec) according to manufacturer's instructions. Afterwards, the $CD8^+$ T cells were stained with CellTrace™ Violet at 5 μM during 10 min (Thermo Fisher Scientific, USA) according to the manufacturer's protocol.

Two days after transfection, H1299 cells used as presenting cells were briefly washed with PBS, trypsinized, resuspended in splenocytes medium (RPMI-1640), supplemented with 10% (FBS), 4 mM L-glutamine, 1% Penicillin-Streptomycin, 0.05 mM 2-Mercaptoethanol and 5 mM HEPES) and seeded in 48 wells plates ($1.25x10^5$) cells per well. Then, $5x10^5$ CellTrace™ labelled *T*-cells were added per well and the co-cultures were incubated at 37 °C with 5% $CO_2$. The levels of antigen presentation were deduced from the percentage of *T*-cell proliferation verified by flow cytometry.

### 2.6. Flow cytometry analysis: OT1 $CD8^+$ T cells proliferation

After 3 days, cells were harvested, stained with anti-mouse CD45.2-PE-Cy7 (BD Pharmingen), fixable viability dye eFluor® 506 (eBioscience, USA) and analyzed on a CANTO II flow cytometer (BD Biosciences, USA). Cells were gated for live CD45.2 + cells ($4x10^5$ events collected) and data was analyzed using FlowJo software version 8 (Tree Star). The percentage of live $CD8^+$ T cells in each generation was calculated using FlowJo proliferation platform and this value was considered for statistical analysis.

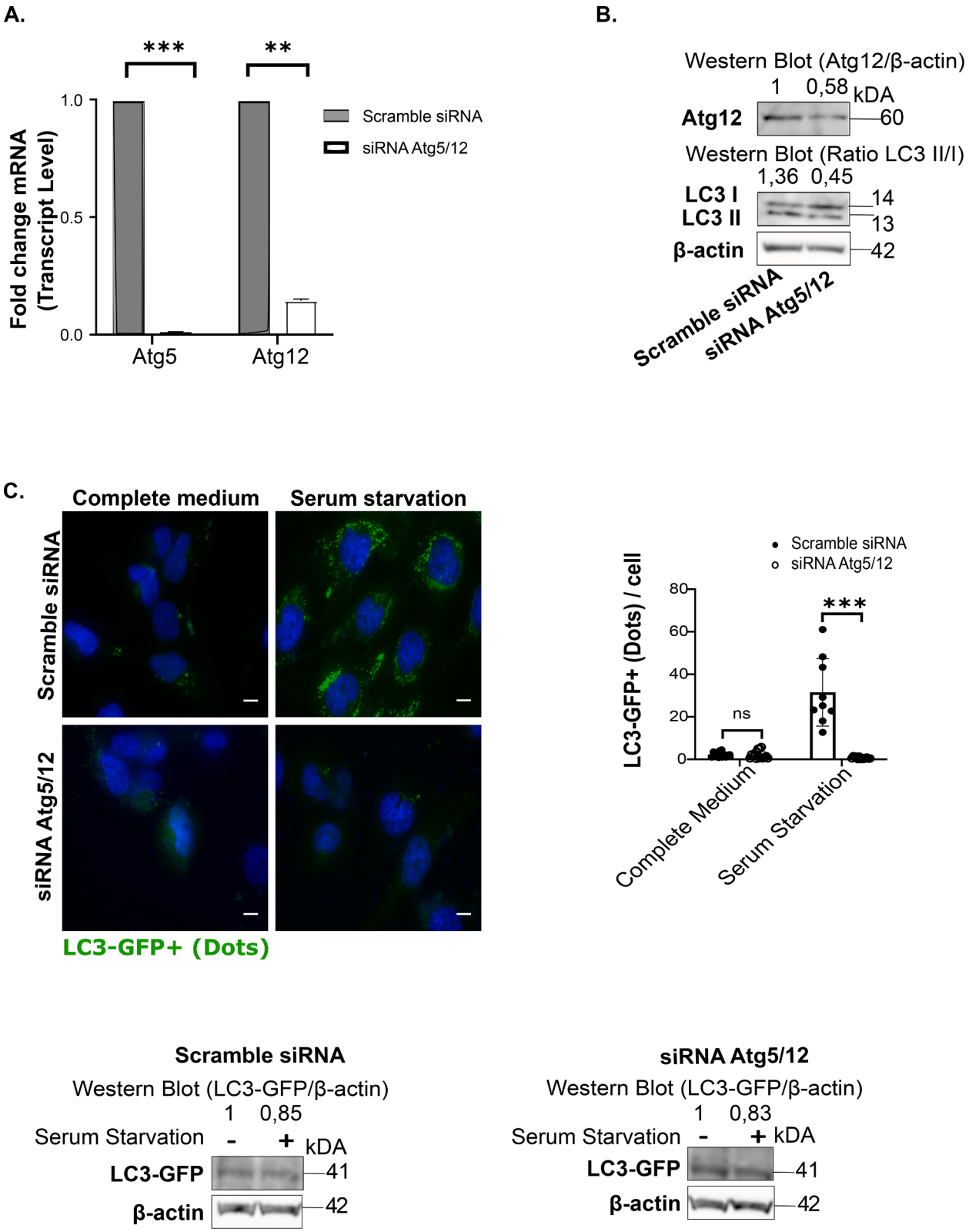


**Fig. 1.** *Autophagy Inhibition.* **A.** The *Atg5/12* mRNA levels were confirmed using RT-qPCR seventy-two hours following transfection of [20 pM] human siRNA against Atg5/12 or scramble siRNA **B.** Western Blots show the expression of Atg12, LC3 I and LC3 II. Values above the bands show the densitometry analysis normalized against β-actin and the fold change compared with the scramble siRNA. Autophagy suppression was estimated by the ratio between LC3 II and LC3 I **C.** H1299 cells were transfected with a plasmid encoding LC3-GFP 24 h after treatment with siRNAs as in A and B. 48 h later, cells were treated without serum during two hours and then fixed. One of 10 fields is shown from one of three similar experiments. LC3-GFP fluorescence was observed as green dots, indicating autophagosomes formation. Number of GFP dots was calculated (top right graph). LC3-GFP expression was determined by Western Blot (bottom panels). Values above the bands show the densitometry analysis of bands normalized with β-actin and the fold change comparing the complete medium with the serum starvation treatment. Significant values were calculated using Multiple paired T test grouped. ***P $<$ 0.0002; **P $<$ 0.0021; 0,1234 ns, not significant. White scale bars denote 10 μm.

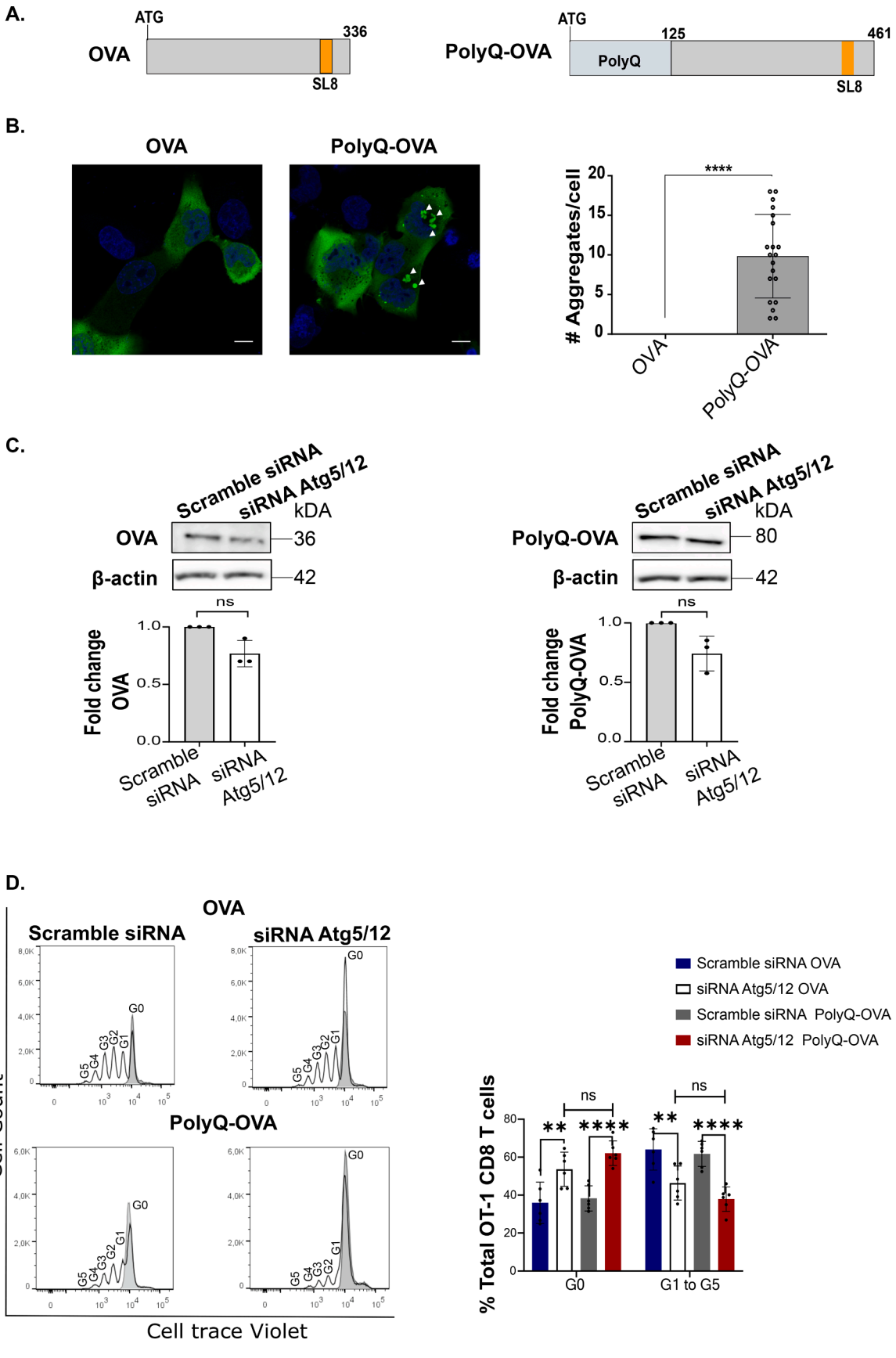


(caption on next page)

**Fig. 2.** *Autophagy affects antigen presentation of Ovalbumin and Ovalbumin fused to the poly glutamine peptide* **A.** Cartoon illustrating chicken ovalbumin (OVA) sequence with the location of the immune peptide SL8 and the glutamine repeat (PolyQ) **B.** Representative immunofluorescence image of OVA and PolyQ-OVA. White arrows heads indicate aggregation pattern. The graph shows the average number of aggregates observed **C.** Western Blot showing the effect of 72 h Atg5/12 human siRNA transfection on OVA and PolyQ-OVA expression. The graphs below show the densitometry analysis, normalized against β-actin and expressed in fold change compared with the scramble siRNA **D.** H1299 were transfected with human siRNA Atg5/12 [20 pM] or scrambled siRNA. 24 h later they were transfected with murine MHC-I (kb) and indicated constructs. After 48 h they were incubated with OT-1 $CD8^+$ T cells labeled with cell-trace violet for another 72 h. OT-1 $CD8^+$ T cell proliferation was analyzed by flow cytometry. Higher rate of proliferation indicates more antigen presentation. Open peaks in the histogram represent the proliferating populations and grey peaks denote unstimulated population (Empty Vector transfected cells) (left graph). The graph shows the sum of percentage of cells from generation 1 to 5 compared with percentage of non-dividing cells (generation 0) from 6 independent experiments (right graph). Significant values were calculated using Multiple paired T test grouped. *P < 0.0332; **P < 0.0021; ***P < 0.0002; ****P < 0.0001; 0.1234 ns, not significant. White scale bars denote 10 μm.

### 2.7. Antigen presentation assay: direct measurement in the presenting cells

H1299 cells co-expressing murine MHC I Kb and the constructs mentioned above were submitted to Chloroquine treatment. Then, cells were harvested and stained with APC anti-mouse H-2 Kb bound to SIINFEKL Antibody (Biolegend) and Fixable viability 506 (eBioscience, USA). These cells were analyzed on a CANTO II flow cytometer (BD Biosciences, USA) and were gated for live cells. Data was analyzed using FlowJo software version 8 (Tree Star).

### 2.8. Direct measurement of MHC I Kb and HLA-ABC

MCA-205 and H1299 cells were submitted to murine or human Atg5/12 siRNA transfection. Then, cells were harvested and stained. MCA-205 cells with anti-mouse H-2Kb Antibody (Biolegend) and FITC anti-mouse IgG2a Antibody (Biolegend); H1299 cells with HLA-ABC FITC antibody (Invitrogen). Both cell types were also stained with Fixable viability 780 (eBioscience, USA). These cells were analyzed on a CANTO II flow cytometer (BD Biosciences, USA) and were gated for live cells. Data was analyzed using FlowJo software version 8 (Tree Star).

### 2.9. RNA extraction, RT-PCR and qRT-PCR

At 72 h post siRNA Atg5/12 transfection, H1299 cells were washed with PBS and RNA was purified using the RNeasy Plus Mini Kit (Qiagen) following the manufacturer's protocol. cDNA synthesis was carried out using M-MLV reverse transcriptase and oligo(dT) primers (Invitrogen). For qRT-PCR, the StepOne (Applied BioSystems) real-time PCR system was used, and the reactions were performed with the Perfecta SYBR green Fast mix ROX (Quanta) using specific primer pairs for human Atg5 (Forward: 5′ GCTGCAGATGGACAGTTGCA 3′and Reverse: 3′ TGTTCACTCAGCCACTGCAG 5′), human Atg12 (Forward: 5′ ATGACTAGCCGGGAACACCA 3′ and Reverse : 3′ CACGCCTGAGACTTGCAGTA 5′), murine Atg5 (Forward: 5′TGTGCTTCGAGATGTGTGGTT 3′and Reverse: 3′ GGTCCCCTTTGCACACTTACA 5′) and murine Atg12 (Forward: 5′GCCATCTCACCAGCCCAATA 3′ and Reverse: 3′CATGC CTGGGATTTGCAGT 5′).

### 2.10. LC3-GFP induction

To confirm the blockage of autophagosomes formation by Atg5 and Atg12 siRNA, we performed epifluorescence microscopy. For this, we seeded $1.5 \times 10^4$ H1299 cells in a 24 well plate over a sterile 22x22mm cover slip. Then, cells were transfected with 20 pM of siRNA against Atg5/12 and 0.1 μg of a LC3-GFP construct at 24 and 48 h after seeding, respectively. After 72 h of culture, cells were treated with a starvation buffer described elsewhere [25] (140 mM NaCl, 1 mM CaCl2, 1 mM MgCl2, 5 mM glucose, and 20 mM Hepes, pH 7.4) during 2 h and complete RPMI-1640 medium was used for the negative control cells. Images were taken at 63x using the Axio Imager D2 microscope. All images were analyzed in Fiji software and the number of green dots was calculated as previously described [26].

### 2.11. Western Blot

Cells were trypsinised and the obtained pellets were resuspended with 50 μl of lysis buffer (20 mM HEPES KOH, 50 mM β-Glycerol phosphate, 1 mM EDTA, 1 mM EGTA, 0.5 mM Na3VO4, 100 mM KCL, 10% Glycerol and 1% Triton x-100, protease inhibitor cocktail Roche). Total lysates were obtained after mechanic hitting and freezing at −80 °C for at least 2 h. After, samples were centrifuged at 13 000 RCF during 10 min at 4 °C and supernatants were collected. Samples were quantified using Bradford Reagent (BioRad) and 50 μg of protein were separated on 4–12% SDS-PAGE gels (Thermo Fisher Scientific) and transferred to nitrocellulose blotting membranes (Pall Corporation). After saturation of membranes with TBS- 0.5% Tween containing 5% non-fat milk, membranes were overnight incubated with anti-EBNA1 (16216–1-AP Abnova), anti-Atg12 (R&D systems), anti-chicken egg albumin (C6534 Sigma), anti-LC3B (L75443 Sigma), anti-GFP (11814460001 Roche) and anti-actin (AC-15 Sigma) antibodies. After washing with TBS-Tween, bound antibodies were detected using a rabbit anti-mouse (Dako) or a mouse anti-rabbit (Dako) secondary antibody conjugated to horseradish peroxidase (1:1000; 1 h at room temperature). Immunocomplexes were then revealed with ECL (Thermo scientific) and imaged using a MyECL Imager (Thermo scientific).

### 2.12. Immunofluorescence

H1299 cells were seeded as described for LC3-GFP induction experiments and transfected with 0.8 μg of EBNA1, EBNA1ΔGAr, GAr-OVA, EBNA1 *c-myc*, EBNA1ΔGAr *c-myc*, GAr-OVA *c-myc*, OVA, PolyQ-OVA or empty vector. Samples were fixed with 4% paraformaldehyde and permeabilized with 0.4% Triton x-100 0.05% CHAPS PBS. Afterwards, cells were blocked with 3% Bovine serum albumin (BSA) Saponin 0.1% PBS during 1 h and then incubated with mouse anti-EBNA1 (16216–1-AP Abnova) or rabbit anti-egg albumin (C6534 Sigma) during 1 h at room temperature. After two washes with PBS, samples were incubated with an anti-mouse Alexa 488 or anti-rabbbit Alexa 647 antibodies during 1 h at room temperature. Next, samples were washed with PBS, stained with DAPI and mounted with a fluorescence mounting media (Dako). Samples were examined in a LSM 800 confocal laser microscope (Carl Zeiss MicroImaging GmbH, Jena, Germany) and images were treated using the Fiji software.

### 2.13. Statistics

Data were analyzed by two-tailed unpaired Student's *t*-test or One sample *T*-test using GraphPad Prism 6 for Windows (GraphPad Software). Data shown are mean ± sd. of minimum three independent experiments. *P < 0.0332; **P < 0.0021; ***P < 0.0002; ****P < 0.0001; 0.1234 ns, not significant.

## 3. Results

### 3.1. Knocking down Atg5 & Atg12 blocks autophagy in H1299 cells.

In order to evaluate the role of autophagy in antigen presentation to the MHC class I pathway we knocked down the expression of Atg5 and

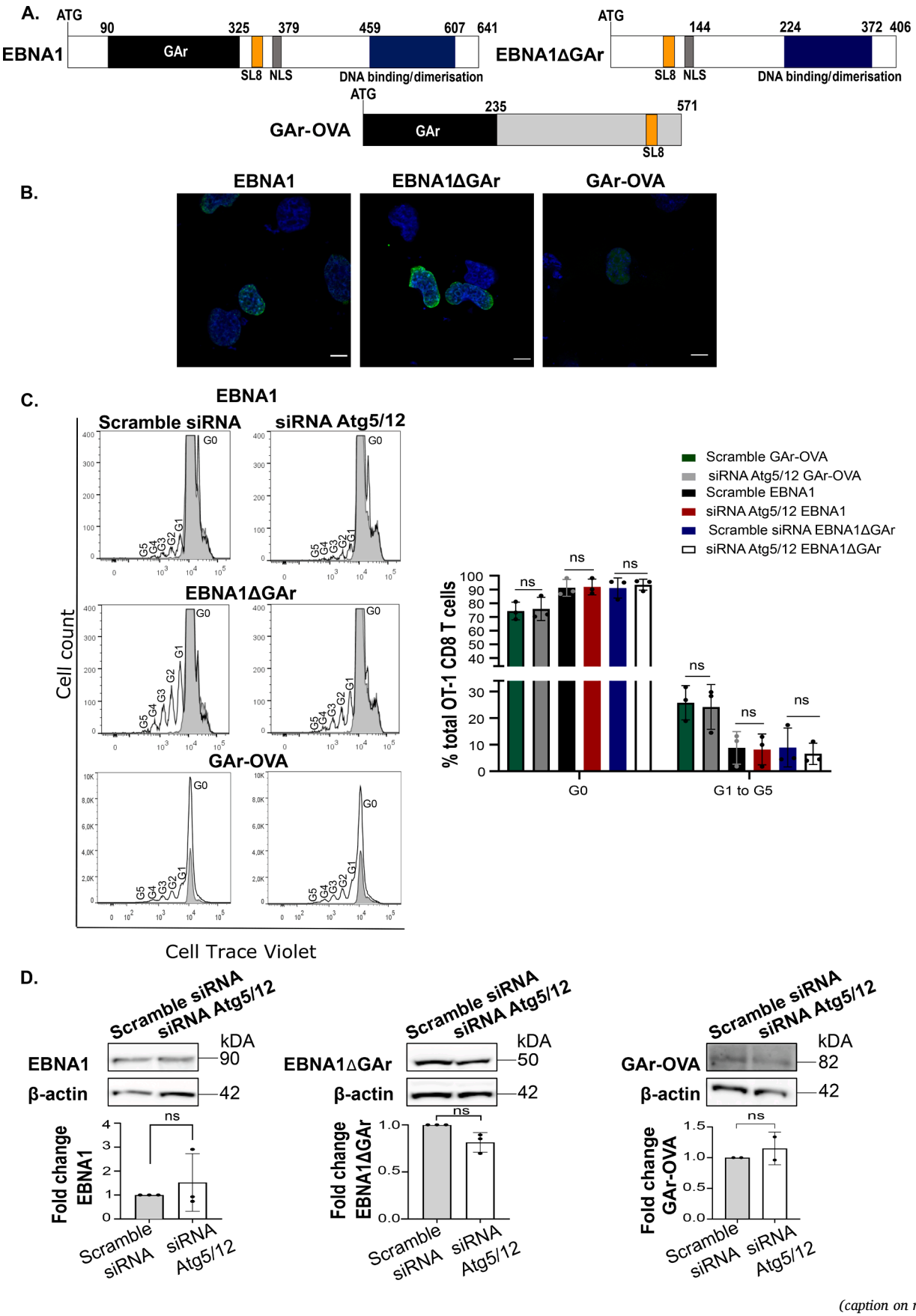


(caption on next page)

**Fig. 3.** *Fusion of the EBNA1-derived gly-ala repeat (GAr) sequence suppresses Atg5/12-dependent antigen presentation.* **A.** Cartoon illustrating different EBNA1 constructs with, or without, the GAr (EBNA1ΔGAr) and GAr fused to Ovalbumin. The location of the nuclear localization signal (NLS), the DNA binding/dimerization sequence in EBNA1 and the SL8 epitope are indicated. **B.** Representative immunofluorescence image of EBNA1, EBNA1ΔGAr and GAr-OVA. **C.** H1299 cells co-expressing murine MHC-I (Kb) and the indicated constructs were transfected with human siRNA Atg5/12 [20 pM] or scramble siRNA during 72 h like in Fig. 2D. The graph shows the percentage of cells from generation 1 to 5 compared with percentage of non-divided cells (generation 0) from 3 independent experiments (right graph) **D.** Western Blots show one out of three representative experiments on the effect of autophagy inhibition on EBNA1, EBNA1ΔGAr and GAr-OVA protein expression levels. The graphs show densitometry analysis normalized against β-actin and expressed in fold change compared with the scramble siRNA. Significant values were calculated using Multiple paired T test grouped. Not significant ns: 0.1234. White scale bars denote 10 μm.

Atg12 using specific siRNAs. These proteins are crucial in the conjugation system that allows the formation of autophagosomes and their downregulation is reported to block the macroautophagy pathway (from here on simply referred to as autophagy) [12,27,28]. The efficiency of siRNA treatments was confirmed by the downregulation of Atg5/12 at both mRNA (Fig. 1**A**) and protein levels (Fig. 1**B, upper lane**). siRNA treatments resulted in a decrease of LC3 II-I ratio (Fig. 1**B, middle lane**) and suppressed autophagy flux following serum deprivation (Fig. 1**C, upper part**) Of note, LC3-GFP protein levels did not change under serum starvation (Fig. 1**C, bottom part**). Together, these data show that the siRNA against Atg5/12 interfere with the autophagy pathway in H1299 cells.

### *3.2. Preventing autophagy reduces MHC class I antigen presentation independently of protein aggregate formation.*

Autophagy can degrade harmful cytosolic protein, including aggregates, [18–20] and we tested the capacity of this pathway to process protein substrates for the MHC-I pathway. We used a chicken OVA construct whose secretion was blocked by the deletion of the first 50 amino acids [29]. This construct enabled us to study the antigen presentation via the MHC-I pathway using $CD8^+$ T cells from OT-1 mice that specifically recognize the OVA-derived SL8 antigenic peptide in the context of the murine Kb MHC class I molecule. We also used a polyglutamine repetition (PolyQ), well known to cause aggregates and to be processed by autophagy [30–33] that we fused to OVA (Fig. 2**A**). We used a GFP construct to estimate transfection efficiency of approximately 30% to 50% of cells (Suppl. Fig. 1). Immunohistochemistry assays using anti-OVA antibodies showed that PolyQ-OVA forms approximately 10 aggregates per cell (white arrow heads) while OVA was uniformly stained throughout the cells and no visible aggregate detected (Fig. 2**B**). Expression of the reporter constructs were not significantly affected by siRNA against ATG5/12 (Fig. 2**C and** suppl. Fig. 2). We did not detect an accumulation of PolyQ-OVA upon ATG5/12 knock down, presumably due to the fact that the PolyQ-OVA is not present only in the aggregate conformation (Fig. 2**B**) due to the limited time (24 h) of expression. To test the role of autophagy on the processing of antigenic peptide substrates for the MHC class I pathway, we co-expressed the indicated SL8-carrying constructs together with the Kb MHC cDNA in human H1299 cells. Transfected cells were subject to autophagy inhibition through Atg5/12 siRNA treatment and antigen presentation was evaluated by co-culture with OT1 $CD8^+$ *T*-cells. The relative level of antigen presentation was estimated by OT1 $CD8^+$ *T*-cells proliferation using flow cytometry. For every assay we confirmed suppression of autophagy by in parallel estimating the LC3 I/II ratio (Fig. 1B and data not shown). We observed that under Atg5/12 knock down, OVA and PolyQ-OVA showed a higher percentage of cells in the non-proliferating OT1 $CD8^+$ T cell population (G0) and a corresponding decrease in the proliferating population (G1 to G5), indicating a reduction of antigen presentation (Fig. 2**D**). The percentage of OT1 $CD8^+$ T cells in each generation is shown in (Suppl. Fig. 3**A**). Despite being uniformly expressed and showing no apparent formation of aggregates, it was surprising to see that knocking down Atg5/12 affected the presentation of antigenic peptides from OVA as much as from PolyQ-OVA.

### *3.3. MHC class I-restricted presentation of peptides derived from EBNA1 is not affected by suppressing autophagy.*

The Epstein-Barr virus-encoded EBNA1 has been reported as an aggregate prone protein and this feature has been attributed to the long repeat of non-polar gly-ala residues (GAr) [9,10]. Since EBNA1-derived antigenic peptides are processed for the MHC class II pathway via autophagy [12] and autophagy is associated to the clearance of proteins, including aggregates [18–20], we wanted to know if EBNA1-derived peptides can also be presented for the MHC class I pathway through autophagy. We inserted the antigenic SL8 peptide into the EBNA1 open reading frame (ORF), or in an EBNA1 depleted of the GAr-domain (EBNA1ΔGAr). We also used a construct carrying the GAr-domain fused to OVA cDNA (GAr-OVA) (Fig. 3**A**). To test if EBNA1 shows the same aggregation pattern observed for PolyQ-OVA, we performed immunohistochemistry assays. However, we observed no obvious aggregates of EBNA1, EBNA1ΔGAr or GAr-OVA and no differences in subcellular localisation with, or without, the GAr (Fig. 3**B**). The GAr mediates suppression of antigenic peptides for the MHC class I pathway by inhibiting *EBNA1* mRNA translation *in cis* [7]. In agreement with this, we observed a low percentage of $CD8^+$ T cell proliferation in response to SL8 derived from EBNA1 and GAr-OVA, as compared to EBNAΔGAr (Fig. 3**C**) and OVA (Fig. 2**D**). Importantly, we observed no significant difference between percentages of OT-1 $CD8^+$ T cells in the undivided (G0) or in the proliferating populations (G1 to G5), for any of the tested conditions following Atg5/12 siRNA treatment (Fig. 3**C** and suppl. Fig. 3B). We also showed that Atg5/12 knock down had no significant effect on EBNA1, EBNA1ΔGAr and GAr-OVA expression (Fig. 3**D** and suppl. Fig. 2). In addition, we observed no effect on antigen presentation of EBNA1, EBNA1ΔGAr or GAr-OVA following treatment with the autophagy inhibitor drug Chloroquine (Suppl. Fig. 4). These results support the idea that the autophagy pathway does not provide EBNA1-derived antigenic peptides for the class I pathway and that the fusion of the GAr prevents OVA from being presented via autophagy.

### *3.4. The level of protein expression does not determine MHC class I restricted antigen presentation via the autophagy pathway.*

The above results were surprising considering that OVA alone, or OVA fused to the PolyQ, present antigenic peptides in an Atg5/12-dependent fashion, while this antigen presentation pathway is prevented by the fusion of the GAr. We next set out to test if the effect of the GAr on antigen presentation is associated with its effect on suppressing mRNA translation *in cis*. For this we fused the *c-myc* 5′UTR to the 5′ of the EBNA1, EBNAΔGAr and GAr-OVA (Fig. 4**A**). The presence of the *c-myc* sequence overcomes the translation inhibitory capacity of the GAr and restores protein synthesis without altering the coding sequence [23]. Western blots and Immunofluorescence showed that the insertion of the *c-myc* sequence resulted in the expected increase in expression of EBNA1 and GAr-OVA but not EBNAΔGAr (Fig. 4**B** and **suppl. Fig.5A)**, and did not affect the subcellular localization (Fig. 4**C**). Atg5/12 knock down did not affect the expression of either construct (Fig. 4**D and** suppl. Fig. 2). When we compared antigen presentation we observed the expected increase in presentation from the *c-myc*-carrying GAr-OVA construct, as compared to GAr-OVA alone (**Suppl. Fig.5B**). Importantly, there was no significant difference in antigen presentation between *c-myc* carrying constructs following Atg5/12 knock down.

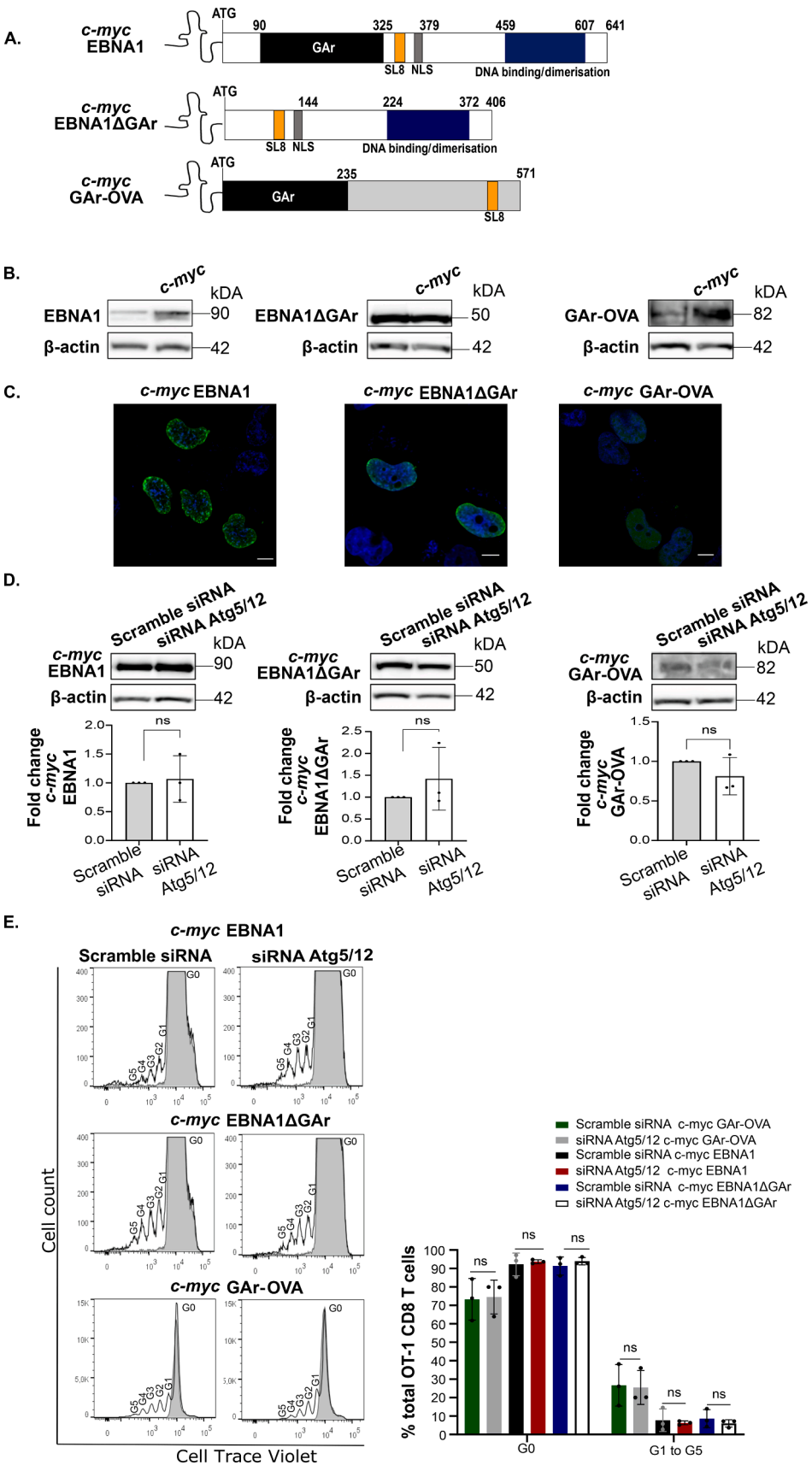


**Fig. 4.** *Protein levels do not change autophagy-dependent antigen presentation.* **A.** Cartoon illustrating the location of *c-myc* 5′ UTR RNA sequence inserted in the 5′UTR of EBNA1, EBNA1ΔGAr and GAr-OVA **B.** The *c-myc* fused to the 5′ UTR of EBNA1, EBNA1ΔGAr and GAr-OVA constructs overcomes GAr-mediated mRNA translation suppression. Western blots show the differences in protein expression levels **C.** Representative immunofluorescence of EBNA1, EBNA1ΔGAr and GAr-OVA constructs carrying the *c-myc*. **D.** Western Blot showing the effect of autophagy inhibition on protein levels of the indicated constructs. The graphs show densitometry analysis, normalized against β-actin for all targeted proteins and expressed in fold change compared with the scramble siRNA. **E.** H1299 cells co-expressing murine MHC-I (Kb) and the indicated constructs following human siRNA Atg5/12 [20 pM] or scramble siRNA treatment during 72 h. The antigen presentation was estimated as described in Figs. 2 and 3. The graph shows the percentage of cells from generation 1 to 5 compared with percentage of non-divided cells (generation 0) from 3 independent experiments (right graph). Significant values were calculated using Multiple paired T test grouped. Not significant ns: 0.1234. White scale bars denote 10 μm.

(Fig. 4**E and** suppl. Fig. 3C). These results show that the levels of protein expression do not affect autophagy-dependent presentation of antigenic peptides derived from EBNA1 or from GAr-Ova for the MHC class I pathway.

## 4. Discussion

Alternative sources of peptides for the MHC class I pathway have been proposed but if, and to what extent, peptides derived from the processing of peptide substrates via the autophagy pathway can be presented to the class I pathway is poorly investigated. The PolyQ sequence is linked to several neurodegenerative diseases, including Huntington's disease, and is well known to cause aggregates of proteins to which it is fused [15,34]. The GAr is a disordered domain derived from the EBNA1, a viral protein expressed in all Epstein-Barr virus (EBV)-infected cells [35], and known to cause aggregates [9,10]. EBV needs to ensure that EBNA1-expressing cells are not detected and destroyed by the immune system and it has previously been shown that EBNA1 uses a mechanism based on minimizing EBNA1 synthesis to evade MHC class I pathway and $CD8^+$ T cell recognition. At the same time, EBNA1′s low turnover rate ensures that a sufficient amount of EBNA1 is expressed to support the virus [36]. The inhibition of synthesis and stability are both mediated by the GAr sequence [7]. However, although autophagy has been shown to contribute to the processing of EBNA1 for the MHC class II pathway [12], our data suggest that this mechanism is not involved in the production of EBNA1-derived substrates for the MHC class I pathway. This raises the possibility that EBNA1 has evolved a mechanism to specifically evade autophagy-mediated class I- but not class II-restricted antigen presentation. In line with the notion of an active EBNA1–mediated mechanism to evade class I-restricted antigen presentation, we observed that when the GAr is fused to OVA it prevents OVA from being presented via autophagy. This suggests that evasion of autophagy-mediated MHC class I-restricted antigen presentation is another mechanisms employed by viruses to remain undetected by the immune system.

Although the fusion of the PolyQ sequence to the OVA led to the formation of aggregates, it did not alter Atg5/12-dependent change in MHC class I-restricted antigen presentation, suggesting that aggregates alone is not the key to antigen presentation via autophagy. This is supported by the observation that OVA alone, nor EBNA1, results in any obvious aggregate formation, at least which could be detected by the methods used here. Nevertheless, it is interesting that the disordered gly-ala domain that is known to affect protein folding and unfolding, [24] prevents presentation to the class I pathway via synthesis and autophagy suppression. If this reflects a more general mechanism to evade the class I pathway, or if it is restricted to the GAr, remains to be seen. The reporter constructs we used carries the PolyQ and the GAr sequences in the *N*-termini of the OVA reporter constructs and even though the GAr is located inside the EBNA1 protein, it is possible that the location of the GAr and the PolyQ can affect how substrates are presented to the class I pathway via autophagy.

By inserting *c-myc* 5′ UTR upstream of GAr-carrying constructs we could override its translation inhibitory capacity and show that protein expression levels have little effect on GAr-mediated evasion of antigen presentation via autophagy. This points towards a more selective mechanism for how peptide substrates are presented to the class I pathway by autophagy and has interesting implications for understanding not only the cell biological aspects of how proteins are processed by autophagy, but also in terms of disease etiology. Animal studies have suggested that the inflammasome plays a role in Alzheimer disease, indicating that the immune response can play a role in the etiology of neurological disease associated with protein aggregates [37,38]. It is an interesting possibility that there could be a selective autophagy-dependent processing of cellular disease-associated substrates for the MHC I and II pathways. Further studies using more substrates and deeper analysis of autophagy pathways shall confirm, or not, this possibility. The implication of autophagy in the clearence of intracellular protein aggregates associated with poluglutamine disorders such as Hungtington disease (HD) is known [15] and Qin and colleagues showed that autophagy inhibition reduced cell viability and increased Huntingtin protein aggregation [34].

It is unlikely that the knock down of Atg5/12 affects the MHC class I pathway *per se* as the effect we observed are substrate-specific and secondly, that the addition of synthetic SL8 peptide to the Kb class I molecules did not show any difference during Atg5/12 knock down (**Supplementary Fig. 6A**) and neither in the membrane location of endogenous MHC-I Kb molecules in murine MCA-205 cells or HLA-ABC molecules in human H1299 cells (**Supplementary Fig. 6B**).

In line with our results, Liu and colleagues implicated OVA as being a substrate for autophagy and showed that mice immunized with OVA caused an allergy reaction and induced activation of autophagy accompanied by a relative increase of LC3 II compared to LC3 I in eosinophils cells from lung tissues [39]. Our study shows autophagy-dependent presentation of OVA for the direct class I pathway but other studies have associated autophagy with cross-presentation via uptake of substrates by dendritic cells. For example, polyQ fused to OVA was shown to be presented to the MHC class I pathway following injection into mice [30].

Taken together, this study shows a substrate-specific presention of peptides via autophagy that is selective for the MHC class I pathway. it has interesting implications for viral immune evasion and for inflammatory reactions associated with disease in which cellular proteins are processed by autophagy.

## Acknowledgements

This work was partially supported by Inserm, European Regional Development Fund (ENOCH, CZ.02.1.01/0.0/0.0/16_019/0000868), MH CZ – DRO (MMCI, 00209805), Cancerforskningsfonden Norr, Cancerfonden (160598), Vetenskapsradet and by the International Centre for Cancer Vaccine Science within the International Research Agendas program of the for Polish Science co-financed by the European Union under the European Regional Development Fund.

## Appendix A. Supplementary material

Supplementary data to this article can be found online at https://doi.org/10.1016/j.cellimm.2022.104484.

## References

[1] J. Neefjes, M.L.M. Jongsma, P. Paul, O. Bakke, Towards a systems understanding of MHC class I and MHC class II antigen presentation, Nat. Rev. Immunol. 11 (12) (2011) 823–836, https://doi.org/10.1038/nri3084.

[2] J.W. Yewdell, D. Dersh, R. Fåhraeus, Peptide channeling: the key to MHC class I immunosurveillance? Trends Cell Biol. 29 (12) (2019) 929–939, https://doi.org/10.1016/j.tcb.2019.09.004.

[3] J. Wei, R.J. Kishton, M. Angel, C.S. Conn, N. Dalla-Venezia, V. Marcel, A. Vincent, F. Catez, S. Ferré, L. Ayadi, V. Marchand, D. Dersh, J.S. Gibbs, I.P. Ivanov, N. Fridlyand, Y. Couté, J.-J. Diaz, S.-B. Qian, L.M. Staudt, N.P. Restifo, J. W. Yewdell, Ribosomal proteins regulate MHC class I peptide generation for immunosurveillance, Mol. Cell. 73 (6) (2019) 1162–1173.e5, https://doi.org/10.1016/j.molcel.2018.12.020.

[4] S. Apcher, C. Daskalogianni, F. Lejeune, B. Manoury, G. Imhoos, L. Heslop, R. Fahraeus, Major source of antigenic peptides for the MHC class I pathway is produced during the pioneer round of mRNA translation, Proc. Natl. Acad. Sci. 108 (28) (2011) 11572–11577, https://doi.org/10.1073/pnas.1104104108.

[5] S. Apcher, G. Millot, C. Daskalogianni, A. Scherl, B. Manoury, R. Fahraeus, Translation of pre-spliced RNAs in the nuclear compartment generates peptides for the MHC class I pathway, Proc. Natl. Acad. Sci. 110 (44) (2013) 17951–17956, https://doi.org/10.1073/pnas.1309956110.

[6] E. Duvallet, M. Boulpicante, T. Yamazaki, C. Daskalogianni, R. Prado Martins, S. Baconnais, B. Manoury, R. Fahraeus, S. Apcher, Exosome-driven transfer of tumor-associated Pioneer Translation Products (TA-PTPs) for the MHC class I cross-presentation pathway, Oncoimmunology. 5 (2016) 1–15, https://doi.org/10.1080/2162402X.2016.1198865.

[7] Y. Yin, Bénédicte Manoury, R. Fåhraeus, Self-inhibition of synthesis and antigen presentation by Epstein-Barr virus-encoded EBNA1, Science 301 (5638) (2003) 1371–1374.
[8] H.J. Kwun, S.R. da Silva, I.M. Shah, N. Blake, P.S. Moore, Y. Chang, Kaposi's sarcoma-associated herpesvirus latency-associated nuclear antigen 1 mimics epstein-barr virus EBNA1 immune evasion through central repeat domain effects on protein processing, J. Virol. 81 (15) (2007) 8225–8235.
[9] J. Luka, T. Lindahl, G. Klein, Purification of the epstein-barr virus-determined nuclear antigen from epstein-barr virus-transformed human lymphoid cell lines, J. Virol. 27 (3) (1978) 604–611, https://doi.org/10.1128/jvi.27.3.604-611.1978.
[10] K. Hennessy, E. Kieff, One of two Epstein-Barr virus nuclear antigens contains a glycine- alanine copolymer domain, Proc. Natl. Acad. Sci. USA 80 (18) (1983) 5665–5669.
[11] S. Apcher, A. Komarova, C. Daskalogianni, Y. Yin, L. Malbert-Colas, R. Fahraeus, mRNA translation regulation by the Gly-Ala repeat of epstein-barr virus nuclear antigen 1, J. Virol. 83 (3) (2009) 1289–1298.
[12] C. Paludan, D. Schmid, M. Landthaler, M. Vockerodt, D. Kube, T. Tuschl, C. Munz, Endogenous MHC class II processing of a viral nuclear antigen after autophagy, Science (80). 307 (2005) 593–596. https://doi.org/10.1126/science.1104904.
[13] C.C. Oliveira, T. van Hall, Importance of TAP-independent processing pathways, Mol. Immunol. 55 (2) (2013) 113–116, https://doi.org/10.1016/j.molimm.2012.10.005.
[14] S.K. Tey, R. Khanna, Autophagy mediates transporter associated with antigen processing- independent presentation of viral epitopes through MHC class I pathway, Blood. 120 (2012) 994–1004, https://doi.org/10.1182/blood-2012-01-402404.
[15] Q. Zheng-Hong, Autophagy: biology and diseases, 2019.
[16] D.G. Mcewan, Host – pathogen interactions and subversion of autophagy, 0 (2017) 687–697.
[17] M. Mehrpour, A. Esclatine, I. Beau, P. Codogno, Overview of macroautophagy regulation in mammalian cells, Cell Res. 20 (7) (2010) 748–762, https://doi.org/10.1038/cr.2010.82.
[18] V. Kirkin, V.V. Rogov, A Diversity of selective autophagy receptors determines the specificity of the autophagy pathway, Mol. Cell. 76 (2) (2019) 268–285, https://doi.org/10.1016/j.molcel.2019.09.005.
[19] D. Gatica, V. Lahiri, D.J. Klionsky, Cargo recognition and degradation by selective autophagy, Nat. Cell Biol. 20 (3) (2018) 233–242, https://doi.org/10.1038/s41556-018-0037-z.
[20] I. Dikic, Z. Elazar, Mechanism and medical implications of mammalian autophagy, Nat. Rev. Mol. Cell Biol. 19 (6) (2018) 349–364, https://doi.org/10.1038/s41580-018-0003-4.
[21] N. Mizushima, M. Komatsu, Autophagy: renovation of cells and tissues, Cell. 147 (4) (2011) 728–741, https://doi.org/10.1016/j.cell.2011.10.026.
[22] V.L. Crotzer, J.S. Blum, Autophagy and adaptive immunity, Immunology 131 (2010) 9–17, https://doi.org/10.1111/j.1365-2567.2010.03321.x.
[23] S. Apcher, C. Daskalogianni, B. Manoury, R. Fåhraeus, B. Sugden, Epstein barr virus-encoded EBNA1 interference with MHC class I antigen presentation reveals a close correlation between mRNA translation initiation and antigen presentation, PLoS Pathog. 6 (10) (2010) e1001151.
[24] C. Daskalogianni, S. Apcher, M.M. Candeias, N. Naski, F. Calvo, R. Fåhraeus, Gly-Ala repeats induce position- and substrate-specific regulation of 26 S proteasome-dependent partial processing, J. Biol. Chem. 283 (44) (2008) 30090–30100, https://doi.org/10.1074/jbc.M803290200.
[25] E.L. Axe, S.A. Walker, M. Manifava, P. Chandra, H.L. Roderick, A. Habermann, G. Griffiths, N.T. Ktistakis, Autophagosome formation from membrane compartments enriched in phosphatidylinositol 3-phosphate and dynamically connected to the endoplasmic reticulum, J. Cell Biol. 182 (2008) 685–701, https://doi.org/10.1083/jcb.200803137.
[26] R. Prado Martins, S. Findakly, C. Daskalogianni, M.-P. Teulade-Fichou, M. Blondel, R. Fåhraeus, In cellulo protein-mRNA interaction assay to determine the action of G-quadruplex-binding molecules, Molecules. 23 (12) (2018) 3124, https://doi.org/10.3390/molecules23123124.
[27] M. Noboru, T. Yoshimorim, B. Levine, Methods in mammalian autophagy researvh, Cell. 140 (2010) 313–326, https://doi.org/10.1016/j.cell.2010.01.028.Methods.
[28] H.K. Lee, L.M. Mattei, B.E. Steinberg, P. Alberts, Y.H. Lee, A. Chervonsky, N. Mizushima, S. Grinstein, A. Iwasaki, In vivo requirement for Atg5 in antigen presentation by dendritic cells, Immunity. 32 (2) (2010) 227–239, https://doi.org/10.1016/j.immuni.2009.12.006.
[29] L. Tabe, P. Krieg, R. Strachan, D. Jackson, E. Wallis, A. Colman, Segregation of mutant ovalbumins and ovalbumin-globin fusion proteins in Xenopus oocytes. Identification of an ovalbumin signal sequence, J. Mol. Biol. 180 (3) (1984) 645–666, https://doi.org/10.1016/0022-2836(84)90031-7.
[30] S. Tabachnick-Cherny, S. Pinto, D. Berko, C. Curato, Y. Wolf, Z. Porat, R. Karmona, B. Tirosh, S. Jung, A. Navon, Polyglutamine-related aggregates can serve as a potent antigen source for cross-presentation by dendritic cells, J. Immunol. 205 (10) (2020) 2583–2594, https://doi.org/10.4049/jimmunol.1901535.
[31] S.T. Suhr, M.C. Senut, J.P. Whitelegge, K.F. Faull, D.B. Cuizon, F.H. Gage, Identities of sequestered proteins in aggregates from cells with induced polyglutamine expression, J. Cell Biol. 153 (2001) 283–294, https://doi.org/10.1083/jcb.153.2.283.
[32] A. Ashkenazi, C.F. Bento, T. Ricketts, M. Vicinanza, F. Siddiqi, M. Pavel, F. Squitieri, M.C. Hardenberg, S. Imarisio, F.M. Menzies, D.C. Rubinsztein, Polyglutamine tracts regulate beclin 1-dependent autophagy, Nature. 545 (7652) (2017) 108–111, https://doi.org/10.1038/nature22078.
[33] A.R. La Spada, J.P. Taylor, Repeat expansion disease: progress and puzzles in disease pathogenesis, Nat. Rev. Genet. 11 (4) (2010) 247–258, https://doi.org/10.1038/nrg2748.
[34] Z.H. Qin, Y. Wang, K.B. Kegel, A. Kazantsev, B.L. Apostol, L.M. Thompson, J. Yoder, N. Aronin, M. DiFiglia, Autophagy regulates the processing of amino terminal huntingtin fragments, Hum. Mol. Genet. 12 (2003) 3231–3244, https://doi.org/10.1093/hmg/ddg346.
[35] C. Münz, Epstein Barr Virus Volume 2: One Herpes Virus: Many Diseases, Springer US, 2015. https://doi.org/10.3109/08820137709055812.
[36] J.B. Wilson, E. Manet, H. Gruffat, P. Busson, M. Blondel, R. Fahraeus, EBNA1: Oncogenic activity, immune evasion and biochemical functions provide targets for novel therapeutic strategies against epstein-barr virus-associated cancers, Cancers (Basel). 10 (2018) 1–29, https://doi.org/10.3390/cancers10040109.
[37] H. Du, M.Y. Wong, T. Zhang, M.N. Santos, C. Hsu, J. Zhang, H. Yu, W. Luo, F. Hu, A multifaceted role of progranulin in regulating amyloid-beta dynamics and responses, Life Sci. Alliance. 4 (2021) 1–22. https://doi.org/10.26508/lsa.202000874.
[38] J. Yang, L. Wise, K.I. Fukuchi, TLR4 cross-talk with NLRP3 inflammasome and complement signaling pathways in Alzheimer's disease, Front. Immunol. 11 (2020) 1–16, https://doi.org/10.3389/fimmu.2020.00724.
[39] J.-N. Liu, D.-H. Suh, H.K.T. Trinh, Y.-J. Chwae, H.-S. Park, Y.S. Shin, The role of autophagy in allergic inflammation: a new target for severe asthma, Exp. Mol. Med. 48 (7) (2016) e243, https://doi.org/10.1038/emm.2016.38.

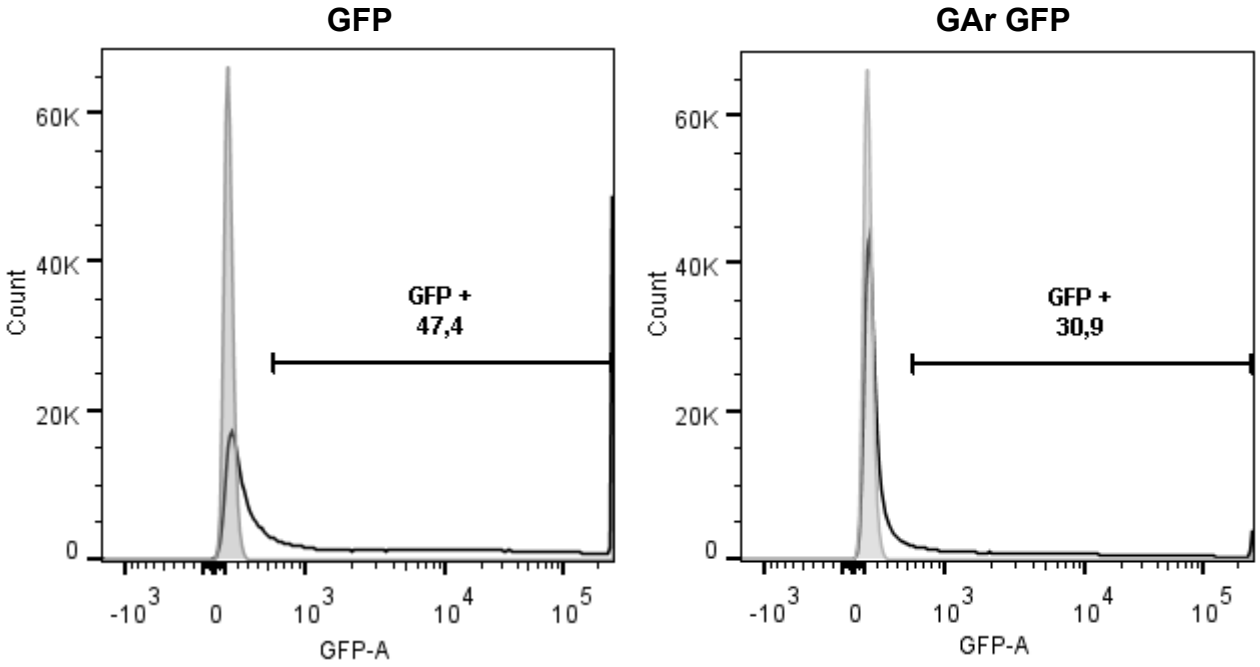


**Supplementary Figure 1.** Q*uantification of transfection efficiency it is around 31 to 50%*. H1299 cells were transfected with 1ug of GFP or GAr GFP cDNA constructs. After 48 hours cells were harvested and quantified by flow Cytometry. Gray histogram shows cells expressing empty vector (not fluorescent cells) and open histograms the corresponding cDNA constructs.

**A.**

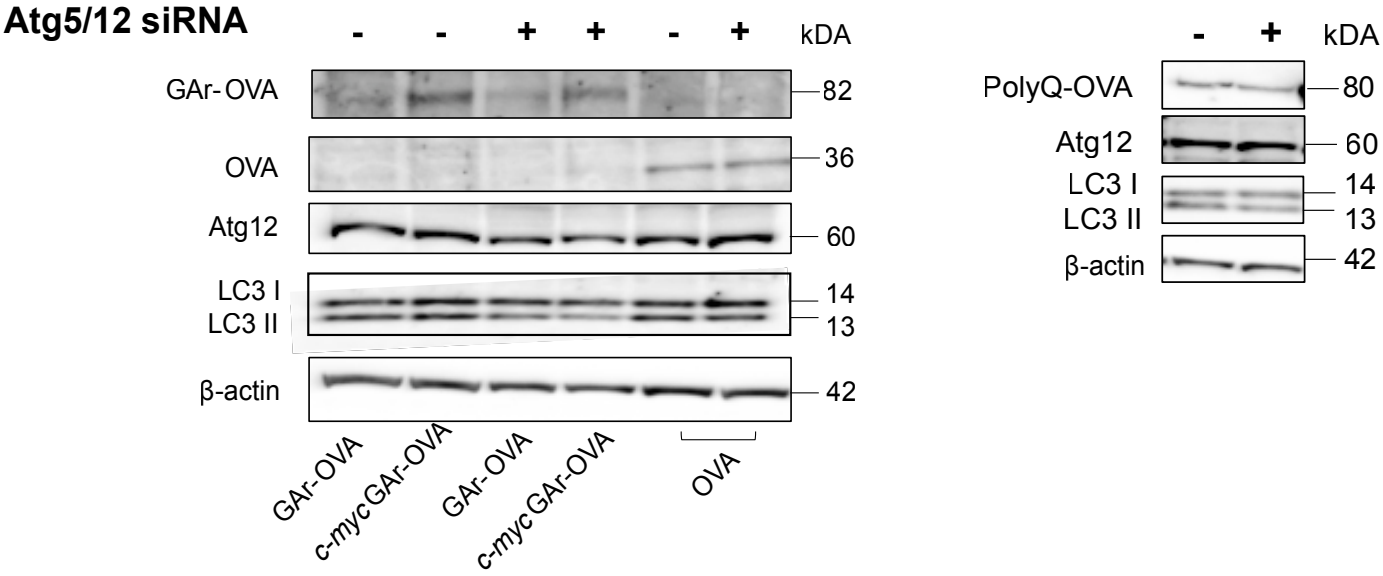


**B.**

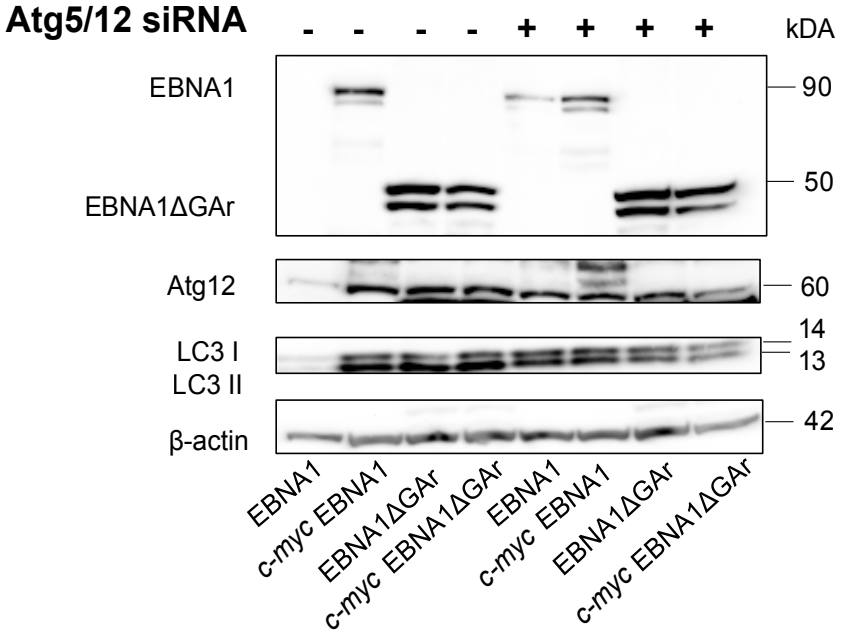


**Supplementary Figure 2.** *Autophagy inhibition downregulates Atg5/12 protein levels and decreased LC3 II-I ratio of the presenting cells after co-culture*. Western Blot showing the effect of autophagy inhibition in protein levels of **A.**GAr-OVA, OVA and PolyQ-OVA with, or without the *c-myc* in the 5' UTR **B.** EBNA1 and EBNA1ΔGAr with, or without, the *c-myc* in the 5' UTR .One representative experiment out of three is shown.

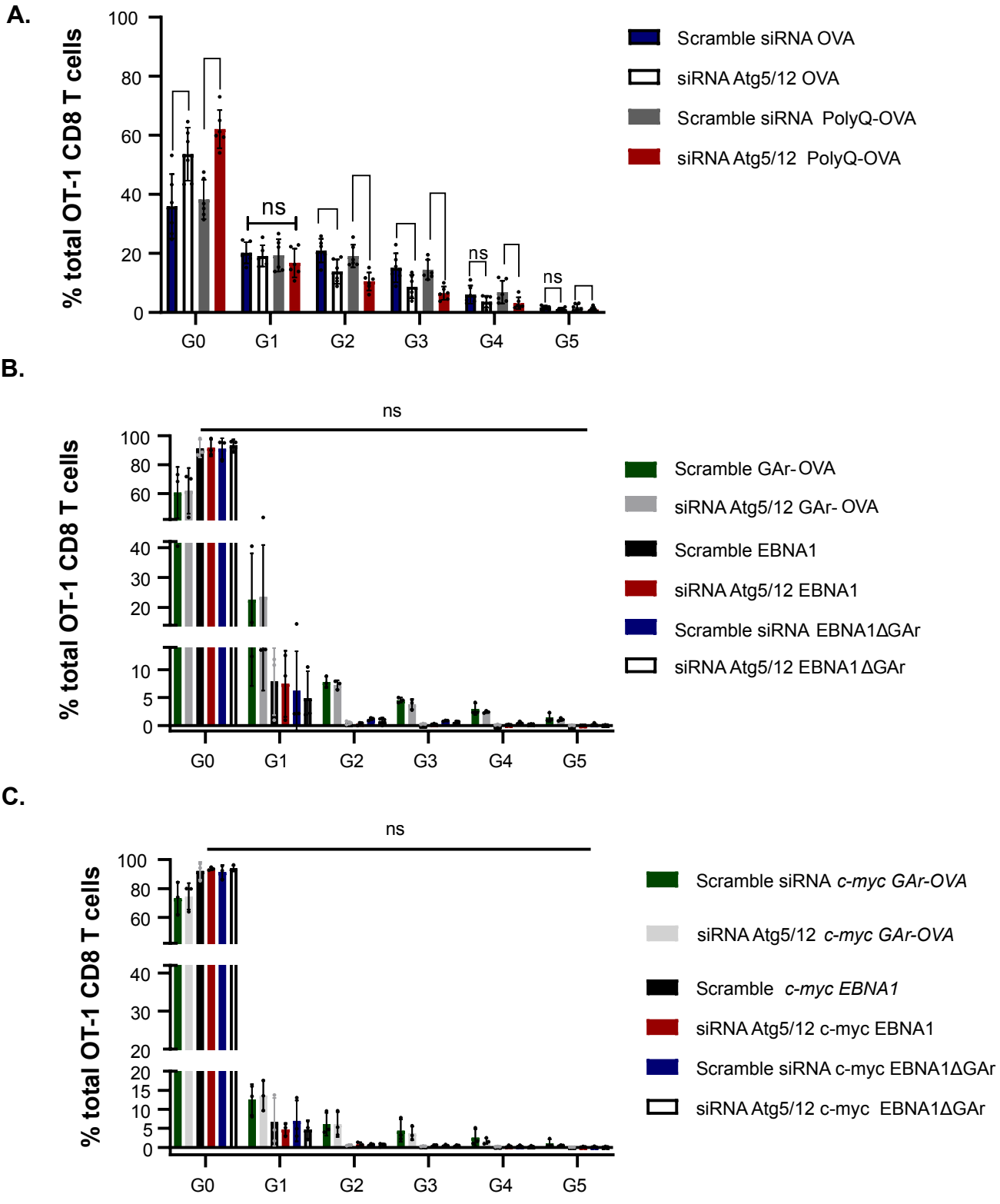


**Supplementary Figure 3.** *Evaluation of autophagy dependence in antigen presentation assays.* Co-culture of H1299 presenting cells with different endogenous antigenic substrates and OT-1 CD8+ T cells labeled with Cell-trace violet. The levels of OT-1 CD8+ T cells proliferation were analyzed by flow Cytometry. Percentage of total OT1 CD8+ T cells was calculated using the number of cells in each generation generated by the modeling of the Proliferation tool in Flow Jo software. The graphs show the percentage of cells from each generation compared with percentage of non-divided cells (generation 0). **A.** Presentation of antigenic derive peptides from OVA and PolyQ-OVA **B.** Presentation of antigenic derive peptides from GAr-OVA, EBNA1 and EBNA1ΔGAr **C.** Presentation of antigenic derive peptides from same constructs as B., but fused with the *c-myc* in the 5' UTR. Graphs represent 6 or 3 independent experiments. Significant values were calculated using Multiple paired T test grouped. *P < 0.0332; **P < 0.0021; ***P < 0.0002; ****P < 0.0001; 0,1234 ns, no significant.

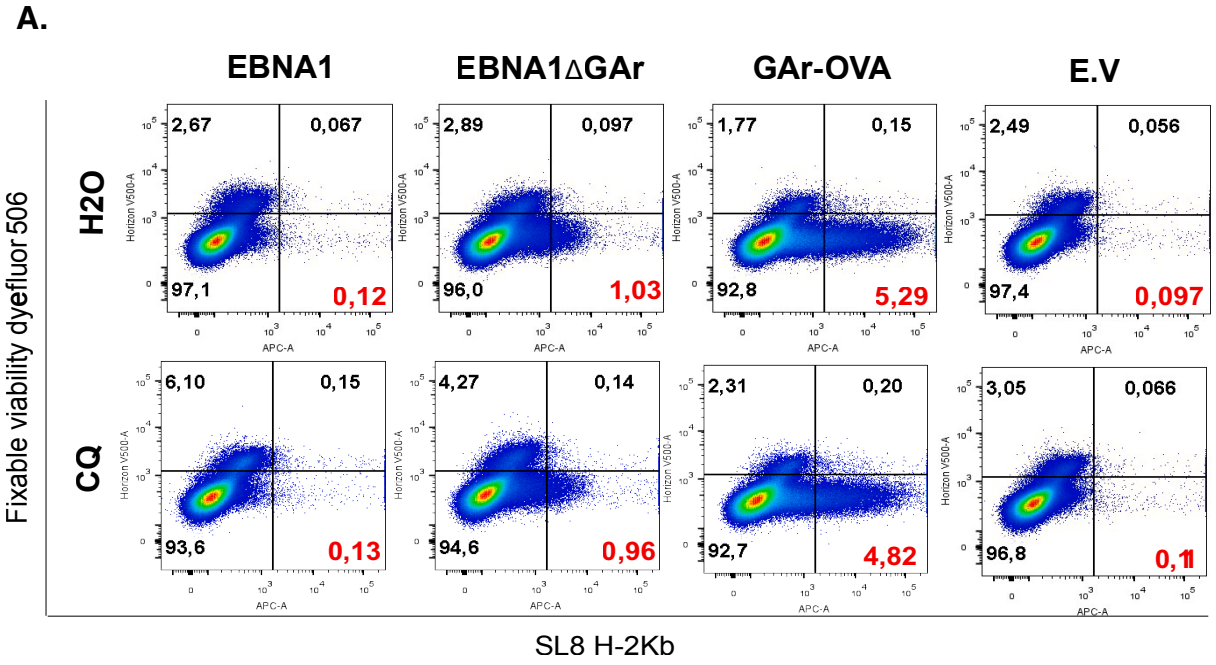


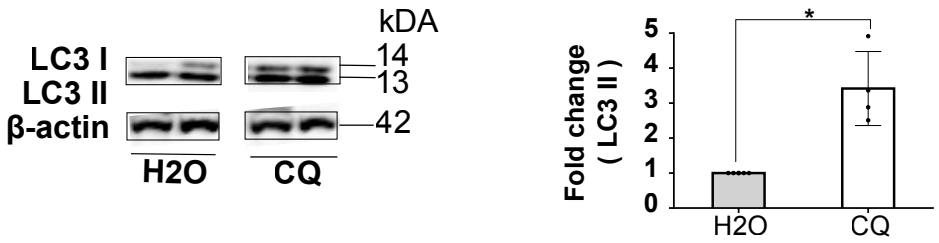


**Supplementary Figure 4** *Autophagy inhibition with Chloroquine (CQ) does not affect antigen presentation of EBNA1 or GAr-OVA derive peptides in MHC-I pathway.* **A.** H1299 cells co-expressing murine MHC-I (Kb), EBNA1, EBNA1ΔGAr, GAr-OVA and E.V were treated with Chloroquine [30 μM] during 36 hours. Then, cells were harvested and labeled with SL8 H-2Kb APC and fixable viability dye 506. Cells having SL8 H-2Kb on the membrane were measured by flow cytometry. **B.** Western Blots shows autophagy inhibition by accumulation of LC3 II, after 36 hours of [30μM] Chloroquine treatment. The graphs below show the densitometry analysis, normalized against β-actin and expressed in fold change compared with water. Significant values were calculated using Multiple paired T test grouped. *P < 0.0332.

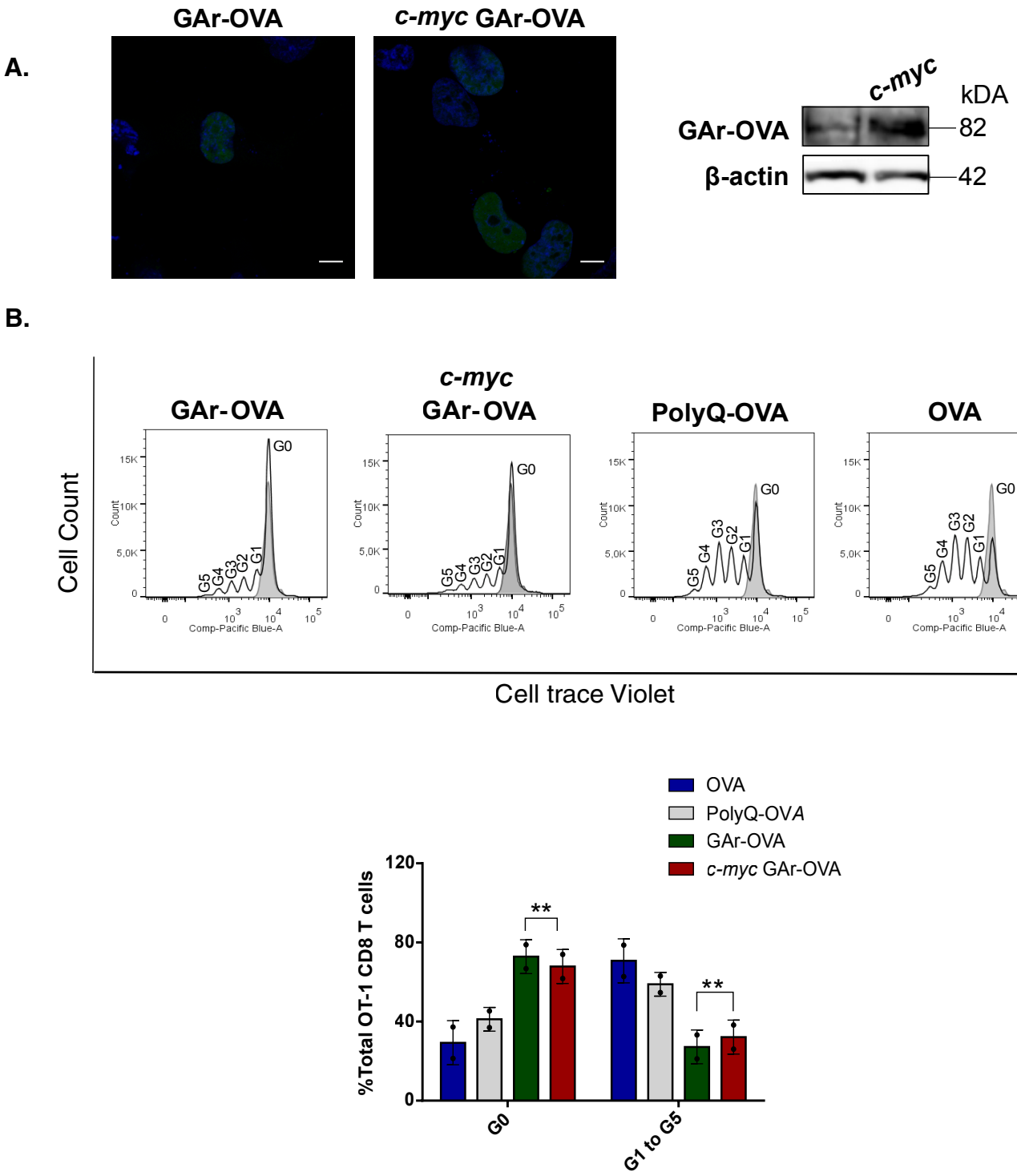


**Supplementary Figure 5** *c-myc sequence increase protein expression of GAr-OVA and antigen presentation of GAr-OVA derive antigenic peptides*. **A.** Immunofluorescence and Western Blot comparing GAr-OVA with their fusion to *c-myc* sequence **B.** H1299 cells co-expressing murine MHC-I (Kb) and the indicated constructs were co-cultured with OT1-CD8 T cells during three days. OT1 CD8 T cells proliferation was measured by flow cytometry. The graph shows the percentage of cells from generation 1 to 5 compared with percentage of non-divided cells (generation 0) from 2 independent experiments (bottom graphs). Significant values were calculated using Multiple paired T test grouped. *P < 0.0332; **P < 0.0021; 0,1234 ns, no significant.

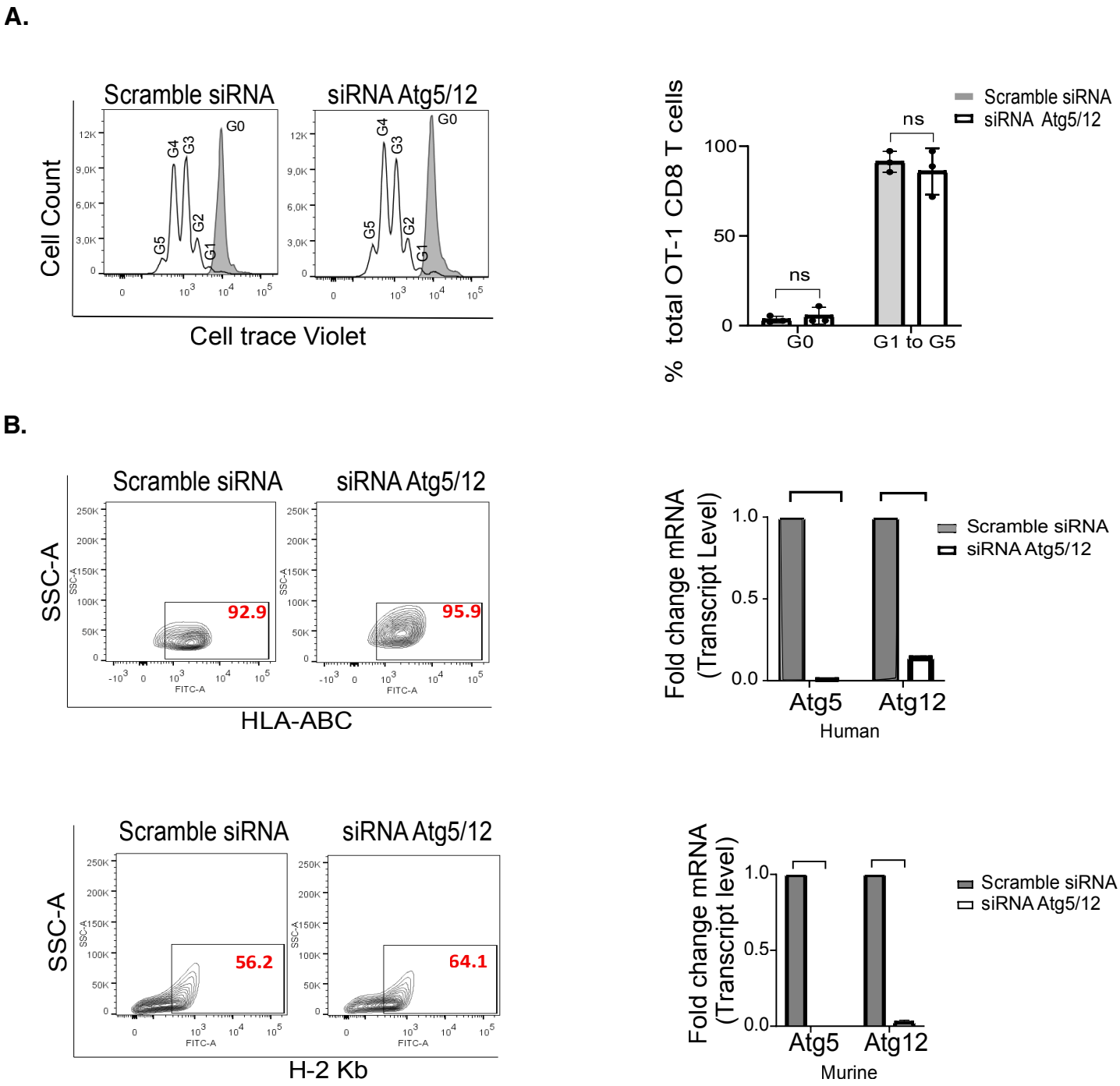


**Supplemental Figure 6**. *Presentation of exogenous SL8 peptide and membrane location of MHC Class I molecule is not affected by Atg5/12 knock down*. **A.** H1299 cells co-expressing murine MHC-I (Kb) were transfected with human siRNA Atg5/12 [20 pM] or scramble siRNA during 72 hours. Next three days, these presenting cells were co-incubated with OT-1 CD8+ T cells labeled with Cell-trace violet and free SL8 peptide [1ug/ml]. The levels of OT-1 CD8+ T cells proliferation were analyzed by Flow Cytometry. Open peaks in the histogram represent the proliferating populations and grey peaks denote unstimulated population (Empty Vector transfected cells). Percentage of total OT1 CD8+ T cells was calculated using the number of cells in each generation generated by the modeling of the Proliferation tool in Flow Jo software. The graph show the sum of percentage of cells from generation 1 to 5 compared with percentage of non-divided cells (generation 0) from 3 independent experiments. **B.** MCA-205 and H1299 cells were transfected with murine/human siRNA Atg5/12 [20 pM] or scramble siRNA respectly during 72 hours. HLA-ABC FITC or H-2 Kb FITC antibody were used to measure MHC class I molecule in alive cells by Flow Cytometry. Murine or human Atg5/12 siRNA knock down was confirmed by qRT-PCR. Significant values were calculated using Multiple paired T test grouped. **P < 0.0021; ***P < 0.0002; ****P < 0.0001; 0,1234 ns, not significant.